Generalising Dynamical 3-Space Theory through comparisons with Modified Newtonian Dynamics and the General Theory of Relativity

Daniel James Kerrigan

School of Chemical and Physical Sciences

College of Science and Engineering

A thesis submitted in fulfillment of the requirements for the degree of Doctor of Philosophy at

Flinders University, South Australia

February 2018

Contents

List of Figures

List of Tables

Abstract

This thesis extends and generalises work on a theory of gravity broadly dubbed Dynamical 3-Space theory with reference to ongoing work in the development of other theories of gravitation. Chapter 1 seeks to first outline current research into theories of gravitation, and notably makes reference to currently unexplained phenomena and relations within cosmology. This first chapter also notes in particular another theory of gravitation, Modified Newtonian Dynamics, due to similarities with previous work in Dynamical 3-Space theory. Chapter 2 serves as a broad introduction to Dynamical 3-Space theory from its Process Physics origin, noting a number of key results and methods used within the theory. This in particular includes discussion of the importance of space itself within the theory, and why the theory has developed in the way it has.

Chapters 3 and 4 serve as original contribution to this work, and it is here that generalisation of the theory begins, with reference to two other theories of gravitation; Modified Newtonian Dynamics and the General Theory of Relativity. Chapter 3 begins with a discussion of work that was originally developed to explain the behaviour of free parameters within Dynamical 3-Space theory, before deconstructing and rebuilding this work with reference to research into Modified Newtonian Dynamics. From here Chapter 3 serves to explore the impacts of this on broader Dynamical 3-Space theory. Chapter 4 seeks to construct a self-consistent description of Dynamical 3-Space theory from comparison with Painlevé-Gullstrand coordinates, first noting the behaviour of these coordinates, and discussing this with relation to Dynamical 3-Space theory, before deriving a number of key results seen in Dynamical 3-Space theory from the use of these coordinates alone. This is then used as a vehicle for first discussing why the theory behaves differently to the General Theory of Relativity, before using this base to generalise Dynamical 3-Space theory overall.

Declaration

I, Daniel James Kerrigan, certify that this thesis titled 'Generalising Dynamical 3-Space Theory through comparisons with Modified Newtonian Dynamics and the General Theory of Relativity', does not incorporate without acknowledgment any material previously submitted for a degree or diploma in any university; and that to the best of my knowledge and belief it does not contain any material previously published or written by another person except where due reference is made in the text.

Signed: *Daniel James Kerrigan*

Date: *07/02/2018*

Acknowledgments

I first came across Prof. Cahill's work during my undergraduate studies when another student referenced a pair of images he had kept up on his wall; the first being an aerial view of the Laser Interferometer Gravitational-Wave Observatory (LIGO), and the second being a box on a record turntable. At the time LIGO had yet to find the gravitational waves that it was created for, although that has all recently changed, but Prof. Cahill had claimed that through his own work a different gravitational wave phenomena could be detected through his far cheaper and indeed cruder apparatus. Even as an undergrad though, Prof. Cahill had taken the time to explain his work to myself and others, and whilst even to this day I'm far from convinced that the supposed direct detection methods of the '3-space' are solid enough for the claims made, other work in the theory regarding gravitation and how this may be described in a flow model did keep my attention. I must give my sincerest thanks to Prof. Cahill for his help and support over these years.

I also thank everyone I have had a chance to work with over the years, and my friends over these years. Having the chance to not only just have a chat, and relate with others about how we were doing over not only our respective projects, but for many careers, was invaluable in working during this time. I also with to acknowledge in particular some friends who have gone on to work outside of Adelaide, notably including Imran, Rhiannon, Toby and Hamish. I also wish to give special thanks to my long time friend and colleague Julius Zieleniecki, although I'd dare say our madness has rubbed off on eachother.

Finally, I also thank my family, my parents Deborah and Michael, my wife Ingrid, and my now 1 year old son Arthur. Whilst the latter has only been a part of my life for a fraction of the project, it is difficult to describe how much support someone whose vocabulary only consists of 'mama', 'dada', 'oma' and 'dooh' can provide in many respects. I'm still not entirely sure how my wife has managed to put up with me, or indeed my work over these years, adjusting to the ever changing methods I have used. From a house plastered in whiteboards, to the 'butcher paper' phase.

Thank you all for helping me through these years.

Nomenclature

Roman Symbols

$\boldsymbol{v}$	3-space velocity
g_0	Acceleration Scale for D3ST
a_0	Acceleration Scale from Modified Newtonian Dynamics
V_{circ}	Circular Velocity
$G_{\mu\nu}$	Curvature Tensor
$\boldsymbol{E}$	Electric Field
$F_{\mu\nu}$	Electromagnetic Tensor
M	Enclosed Mass
$T_{\mu\nu}$	Energy-Stress Tensor
g	Gravitational Acceleration
g_{bar}	Gravitational Acceleration from Baryonic Matter
g_{DM}	Gravitational Acceleration from Effective Dark Matter
g_{obs}	Gravitational Acceleration Observed
$H\left(t\right)$	Hubble Function
H_0	Hubble Constant
$M\left(a,b,z\right)$	Hypergeometric Function
$\boldsymbol{H}$	Magnetic Field
$g_{\mu\nu}$	Metric Tensor

A^{μ}	Four-Potential
p	Pressure
r	Radius, distance from object.
$R_{\mu\nu}$	Ricci Curvature Tesnor
R	Ricci Scalar
$R^{\alpha}_{\mu\nu\sigma}$	Riemann Curvature Tesnor
$R\left(t\right)$	Scale Factor

Greek Symbols

α'	Adjusted Fine Structure Constant, $\alpha' \equiv \frac{\pi^2 \alpha}{2}$
Ω	Density Parameter
ρ_{DM}	Effective Dark Matter Density, $\rho_{\mathrm{DM}} = \frac{1}{32\pi G}\left(\frac{\alpha'}{4} + \delta^2\nabla^2\right)\left(\left(\mathrm{tr}D\right)^2 - \mathrm{tr}\left(D^2\right)\right)$
$\mu\left(x\right)$	Interpolating Function
$\Gamma^{\alpha}_{\mu\nu}$	Levi-Civita Connections
γ	Lorentz Factor, $\gamma^{-2} = 1 - \beta^2$
ρ	Matter Density
$\eta_{\mu\nu}$	Minkowski Metric
Φ	Scalar Gravitational Acceleration
τ	Proper Time
β	Velocity divided by speed of light (c).
$\boldsymbol{\omega}\left(\mathbf{r}, t\right)$	Vorticity Vector Field

Mathematical Symbols

$F_{[\alpha_1\alpha_2\ldots\alpha_n]}$	Anti-Symmetric part of the tensor, $F_{[\alpha_1\alpha_2\ldots\alpha_n]} \equiv \frac{1}{n!}\delta^{\beta_1\beta_2\ldots\beta_n}_{\alpha_1\alpha_2\ldots\alpha_n} F_{\beta_1\beta_2\ldots\beta_n}$
∇	Del Operator
∂^{μ}	Four-Gradient

$\frac{\mathrm{D}}{\mathrm{D}t}$	Material Derivative, $\frac{\mathrm{D}\boldsymbol{A}}{\mathrm{D}t} \equiv \frac{\partial \boldsymbol{A}}{\partial t} + (\boldsymbol{A} \cdot \nabla)\, \boldsymbol{A}$
$F_{,\alpha}$	Partial Derivative, $F_{,\alpha} \equiv \partial_\alpha F$

Abbreviations

AQUAL	A Quadratic Lagrangian
BTFR	Baryonic Tully-Fisher Relation
D3ST	Dynamical 3-Space theory
Dec	Declination
DM	Effective Dark Matter
EG	Entropic Gravity
FLRW	Friedmann–Lemaître–Robertson–Walker metric
GaR	Galilean Relativity
GR	General Theory of Relativity
ΛCDM	Λ–Cold Dark Matter model of the universe
MOND	Modified Newtonian Dynamics
NG	Newtonian Gravity
PG	Painlevé–Gullstrand class of metrics
RA	Right Ascension
SrgA*	Sagittarius A*
SR	Special Theory of Relativity
TeVeS	Tensor-Vector-Scalar Gravity
TFR	Tully-Fisher Relation

Physical Constants

Λ	Cosmological Constant
α	Fine Structure Constant

G	Gravitational Constant
c	Speed of Light

Introduction

At the core of modern theories of gravitation sits an implicit assumption, one that is rarely if ever directly acknowledged, but one that has profound effects on how we model and perceive the universe. The theories themselves have come in many forms, but ultimately always boil down to the same basic idea; a theory of gravitation is about the interaction between masses. This of course would seem obvious. Gravitation is an effect where paths of objects bend towards masses, whether this be modeled as a force as with Newton or through the curvature of spacetime as with Einstein. Yet here in a day and age where two of the most crucial elements of our modern understanding of the universe are broadly dubbed 'dark matter' and 'dark energy', it still remains that no pause for thought was given to the one player in our understanding of gravitation that receives the least attention, the space objects themselves are contained it. Yes, relativistic theories rely on the bending of space, and other theories model how objects move through space, but no dynamics are given to this space. We start our understandings of the universe at a point where space is a mere empty container which holds objects, and work from there. It is not seen as a dynamic, nor emergent part of the system, just a convenient method of describing it. This is analogous to mapping the World without oceans, yet here in an age where we search for our planet Vulcan, the 'dark' elements of our universe, that we still ignore this most crucial part in the dynamics of gravitational theory. It is no wonder then that theories of gravitation still remain incompatible with quantum understandings of reality, for they are treated so differently, as to leave little space

for direct comparison.

This thesis seeks to expand and generalise the work on a theory of gravitation that does attempt to take into account space itself as a dynamic component of reality and gravitation. This theory, dubbed Dynamical 3-Space theory (D3ST), is based on Process Physics, an attempt at modeling space, time and the behaviours that accompany these out of an emergent neural network. Despite this being the base for the logic that goes into the theory however, Process Physics is at this time unable to determine any more than the behaviours required by such a theory, and D3ST itself is largely built through unique generalisations of other formulations of gravitation. Within this though are the dynamics of the space itself, and most notably within its construction is a potential solution to the expansion of the universe without the need for dark matter, nor dark energy. At this time however the theory does lack a number of key components, notably a full description of galactic scale dark matter distributions, as well as a full covariant formulation. To this end this thesis is largely focused within these two broad areas, first seeking to further develop previous work in the theory's description of dark matter, and secondly seeking to develop such a covariant description of the theory.

Within the description of dark matter for D3ST, this thesis expands on previous work on setting free parameters within this theory. This, however, was found to demonstrate that the theory provided an incomplete description through this method, and hence replaces it with newer methods of dealing with these issues within the theory. Comparisons of this with Modified Newtonian Dynamics show striking similarities with the original form of the theory, but also provide a base for discussions of how these methods could be successfully used. Despite the similarities however, the dynamical effects of space itself are not taken into account in constructions of other theories.

The covariant formulation of the theory is broadly based on a class of metrics referred to as the Painlevé–Gullstrand class of metrics. The chapter seeks to

demonstrate firstly how they provide a description for D3ST at a basic level, before demonstrating their relationship with other results in GR, as well as how the myriad of results within D3ST may be derived. This is then used for a direct comparison of how the expansion of the universe is accounted for in D3ST, and hence demonstrates why D3ST allows for an expanding universe without dark matter and dark energy where the standard model fails to.

Chapter 1

Gravity and Relativity

This chapter discusses the development of gravitational theories, and the historical basis for many of the currently commonly held notions about gravitation. Through a discussion of how current theories were developed, an understanding of why we model gravity as we do can be grasped. This chapter seeks to discuss the introduction of ideas within gravitational theories and how this has in turn led to the current position dealing with dark matter and dark energy, while equally going over a number of key results of interest to the rest of this thesis. Some astronomical relations of interest are also noted, as well as competing theories of gravitation for further discussion and later comparison.

1.1 Galilean Relativity and Gravity

Physics before Galileo was strikingly different. Things commonly held now as basic knowledge and assumptions about how objects move, such as Newton's laws of motion and the equivalence principle were not known. Indeed, at some level this makes sense. The World of Aristotle was before the scientific method as we would currently describe it, and his observations were of course a creation of their time. They were, however, persuasive, and would be considered the leading authority on such ideas for the best part of two millennia. Part of the reason for this has been

argued to be the nature of the way that observations were made in Aristotle's time, and equally that his descriptions did work in a heuristic sense [110]. Of course, with complex interactions such as fluid dynamics being involved with falling motion, before such ideas were separated, these descriptions were necessarily intertwined. In this sense, it could be argued that the great success of Galilean physics and what followed would be to allow physics to control variables and begin to create a description free from multiple complex interactions, and hence view each physical relation separately.

It is through this lens that the advancements that were made during Galileo's time should be viewed. Galilean challenges to the Aristotlean view of the World did not simply replace prior work, but rather reframed it in a new and more usable manner, and hence began the process of unraveling these relationships, as has characterised the changes that would follow. The first of Galileo's challenges to Aristotelian physics, Galilean relativity (GaR), is based on the assumption that the laws of motion are the same in all reference frames. Unlike Aristotle who classified motion in two broad ways, natural and forced motion, Galileo defined motion in the same terms for all reference frames. The motions of any object could be classified under the same rules, rather than rules for one, not for the other. By studying the motions of objects, Galileo also noted that objects tended to remain in motion unless otherwise acted on, though this idea would be more directly formulated by Newton. Namely, for an observer O' moving at a velocity $\boldsymbol{u} = u_x\boldsymbol{i} + u_y\boldsymbol{j} + u_z\boldsymbol{k}$ away from O we have the transformation

$$\begin{aligned} t' &= t \\ x' &= x - u_x t \\ y' &= y - u_y t \\ z' &= z - u_z t \end{aligned} \tag{1.1.1}$$

or as a linear transformation

$$\begin{pmatrix} t' \\ x' \\ y' \\ z' \end{pmatrix} = \begin{pmatrix} 1 & 0 & 0 & 0 \\ -u_x & 1 & 0 & 0 \\ -u_y & 0 & 1 & 0 \\ -u_z & 0 & 0 & 1 \end{pmatrix} \begin{pmatrix} t \\ x \\ y \\ z \end{pmatrix} \tag{1.1.2}$$

which can be written more generally as

$$\begin{aligned} \boldsymbol{x}' &= \boldsymbol{L}\boldsymbol{x} \\ x'^i &= L^i_j x^j \end{aligned} \tag{1.1.3}$$

where here $\mathbf{L}$ is non-symmetric as time is not impacted by changes in velocity within GaR. These transformations may also be defined for rotations, and by design Galilean transformations leave the length of these vectors as invariant under these translations and rotations. Of course, from the above, for the same change in observer, the transformation of velocity is

$$\boldsymbol{w}' = \boldsymbol{w} - \boldsymbol{u}. \tag{1.1.4}$$

This formulation of relativity is particularly important as all more general versions of relativity reduce to it under some assumptions, including most notably the Special and General theories of relativity. In this sense, Galilean relativity underpins the modern understanding of motion, and relationship between observers.

Galileo's second challenge to Aristotle came in the form of gravitation. Aristotle had postulated that objects fell due to their particular properties and in a way defined by solely that. Galileo, however, determined the first statement of the equivalence, which represented a direct challenge to this idea. It is of course worth noting that Aristotle, much as Galileo, could only observe this acceleration by observing motion in a medium, and hence making this discovery more subtle than its modern importance would make it seem. Vincenzo Viviani [39], a student of Galileo gave an account of how Galileo explored this. Galileo had dropped two balls of different

densities from the top of the Leaning Tower of Pisa. With both hitting the ground at the same time, it was demonstrated that in fact, unlike previous assertions such as those of Aristotle, the rate at which objects fall was not down to their 'nature', but rather a property of gravitation itself [49]. Whilst it is debated as to whether or not this experiment was actually carried out, or was in fact merely a thought experiment, it is an interesting insight in the early ideas around gravitation. In effect, such understandings are the first statements of the equivalence principle. In a sense, Galilean gravity on Earth can be stated as

$$a = g = \text{const.} \tag{1.1.5}$$

this being independent of the material or 'nature of the object' and approximately uniform across the surface of the Earth. Of course, the surface gravity on Earth does vary, and this has some uses within various fields surveying the surface of the Earth [68, 120, 119], but these changes are subtle and not of key importance to this discussion. This in turn is not only the first statement of the equivalence principle, but also notes the key elements within gravitational theory, and one that is generally brushed past even in the teaching of gravitation. Whilst generally described as a force, and generally as one of the four fundamental forces of nature, gravitation appears as a pure acceleration towards masses, and one that is unrelated to the properties of the object being accelerated. This is included in more modern theories of gravity which involve lensing, though this is generally through the idea of a warped spacetime. Whilst this acceleration is understood and built into all theories that would follow, and indeed a key component within relativistic theories, the force notion of gravitation would remain a key part of gravitational theory for centuries to come, and arguably to this day. Despite it appearing, acting and behaving as an acceleration, the 'force of gravity' still remains a key element even in modern interpretations.

1.2 Newtonian Gravity

The next important step in the development of modern gravitational theory was the observation of planetary motion, which led to the development of Kepler's Laws. It was not until Sir Isaac Newton and his work 'Philosophiæ Naturalis Principia Mathematica' [91] that this was put into its more modern context. His three laws of motion outlined what would become the very basis of classical mechanics, these being

1. An object maintains its current velocity, unless acted upon by a force.

2. The net force on an object is proportional to the magnitude of acceleration it will experience, this being related by the mass of the object.

3. Each action has an equal and opposite reaction.

It was in this manner that Aristotle's understanding of the physical world would give way, at least within physics, to a more modern one, and through this a better understanding of motion could be attained. Of particular interest to gravitation however, and particularly the notion of 'the force of gravitation' is Newton's second law, which may also be stated as an equation as

$$\boldsymbol{F} = m\boldsymbol{a}. \tag{1.2.1}$$

Here $\boldsymbol{F}$ is the force, $\boldsymbol{a}$ is the acceleration of the object. With such an understanding of motion, as well as the sense that objects are 'forced' downward, it is understandable that this particular law would dominate thoughts on how gravity acts. Using the second law, and considering Kepler's Laws

1. All orbits of planets form an ellipse, with the Sun at one of the two foci.

2. A line from the planet to the sun sweeps out equal areas per equal time.

3. The square of the period of a planet's orbit is proportional to the cube of its semimajor axis.

Newton had managed to derive Kepler's Laws from his own description of gravity [91, 37]. This can be stated as Newtonian gravity (NG) in one direction between two objects. Labeling these two objects 'a' and 'b', NG may be written as a force law as

$$F_1(r) = \frac{M_a G M_b}{r^2} \tag{1.2.2}$$

with G being the gravitational constant and r being the distance between the two objects. Defining inertial mass as m, for object 'a', gravitational acceleration may be defined as

$$g(r) = \frac{F_a(r)}{m_a} = \frac{M_a}{m_a}\frac{G M_b}{r^2}. \tag{1.2.3}$$

This as such only leads to the equivalence principle if $M_a = m_a$. This may seem like a simple and reasonable assumption to make, but here exists one of the key reasons that a force formulation of gravitation needed to be considered. Prior to the Eötvös experiment [129, 34], this stood only as an assumption, and there does not exist a clear reason that in such formulation, inertial and gravitational masses need be the same. With this determined however, Newton's force law for gravitation does lead to the equivalence principle, and determines gravitational acceleration towards a mass M as

$$g(r) = \frac{GM}{r^2}. \tag{1.2.4}$$

This is of course identical to 1.1.5 for constant or near constant r, such as the surface of the Earth. The above may also be expressed in terms of vectors as

$$\boldsymbol{g}(\mathbf{r}) = \frac{-GM}{r^2}\hat{r}, \tag{1.2.5}$$

in Gauss' form

$$\nabla \cdot \boldsymbol{g}(\mathbf{r}, t) = -4\pi G\rho(\boldsymbol{r}, t), \tag{1.2.6}$$

or in terms of a scalar potential Φ in Laplace's form

$$\nabla^2\Phi = 4\pi G\rho. \tag{1.2.7}$$

This in essence is the basis of classical gravitational theories. Here the consideration of gravity as a force can be clearly seen, despite its origins and behaviour being that of an acceleration. This is also despite it being demonstrated at multiple steps that gravity was describable as an acceleration alone, without reference to it as a force. Referencing it as a force is a consequence of Newton's second law, though the significance of this will become more apparent in the coming chapters.

Newton's forms of gravitation are also important even to this day not only in the education of gravitational theory, but in that modern theories under certain assumptions reduce to them, much as relativistic formulations reduce to GaR.

1.3 Special Theory of Relativity

With the behaviour of GaR in mind, one question does arise, this being the nature of the speed of light. Present to a student unaware of relativistic principles the problem of an observer and the speed of light, and they will invariably suggest that the speed of light would be the speed of the object added to the initial speed. This is of course a natural consequence of the construction of GaR. This as a sense of thinking, however, is important to remember in the construction of relativistic theories, particularly with a modern understanding of the speed of light.

The construction of the Special Theory of Relativity (SR) is best considered in reference to the World it developed in. Maxwell's 'A treatise on electricity and magnetism' [74] presented for the first time the Maxwell equations in their more modern form, which can be stated as

$$\mu_0 \frac{\partial \boldsymbol{H}}{\partial t} = -\nabla \times \boldsymbol{E} \tag{1.3.1}$$

$$\epsilon_0 \frac{\partial \boldsymbol{E}}{\partial t} = \nabla \times \boldsymbol{H} \tag{1.3.2}$$

$$\nabla \cdot \boldsymbol{H} = 0 \tag{1.3.3}$$

$$\nabla \cdot \boldsymbol{E} = 0 \tag{1.3.4}$$

in the sourceless case. These equations predicted and described light as an electromagnetic wave for the first time, and in doing so began research into the nature and properties of this, as well as research into the understanding of how a wave could exist without a medium. Of course, none of these were new ideas as such; indeed, debates about whether light propagated through an aether medium were contemporary to Newton [92]. With growing interest in magnetism and electricity, the idea of luminiferous aether was commonplace, and by Maxwell's time it was essentially considered a requirement. Of course, understanding of light brought about a greater understanding of the speed of light, and it was expected that the speed of light would only be relative to the aether at rest, as would be expected under GaR. In this sense, measurement of the speed of the Earth moving against this aether as it orbited the sun could be measured within anisotropy of the speed of light, as it seemed natural to assume that the Sun was central and unmoving against this aether rest frame. Hypotheses with reference to the nature of this included Fresnel drag [44], as well as others of similar design. Under Fresnel drag, first order experiments were expected to not pick up any anisotropy of light, as was the result with early experiments; second order experiments were however anticipated to have

detectable results. The Michelson–Morley experiment [81], the first of the famous second order experiments, did determine that null result, and hence demonstrated the isotropy of light and acted as was the beginning of the end for aether theories. This null result was with the finding of 8 km s^{-1} as the speed of Earth, as opposed to the expected result of 30 km s^{-1}. There were attempts to explain how this result could come about with an aether theory, such as by Lorentz [70], which suggested physical contraction of the rods in response to the aether. Such attempts were quickly refuted however, and the two postulates that SR would be constructed from were cemented:

- The laws of physics are the same in all reference frames.
- The speed of light in a vacuum is the same for all observers.

In order for this to work, the concepts of absolute motion and absolute time were discarded, and the world of physics would enter the era of SR, as opposed to GaR. This of course meant that time itself was now relative to the observer, each observer would have their own measure of time, but this item would present its own problems. To compare to GaR, SR can be stated in an analogous sense to equations 1.1.1 and 1.1.2 for a boost of v in the x direction relative to the coordinate frame

$$\begin{aligned} ct' &= \gamma\left(ct - \frac{u}{c}x\right) \\ x' &= \gamma\left(x - ut\right) \\ y' &= y \\ z' &= z \end{aligned} \tag{1.3.5}$$

where

$$\gamma^{-2} = 1 - \frac{u^2}{c^2}. \tag{1.3.6}$$

Defining $\beta = u/c$, and $\beta_i = u_i/c$, this can be written as a linear transformation as

$$\begin{pmatrix} ct' \\ x' \\ y' \\ z' \end{pmatrix} = \mathbf{\Lambda} \begin{pmatrix} ct \\ x \\ y \\ z \end{pmatrix} \tag{1.3.7}$$

with

$$\mathbf{\Lambda} = \begin{pmatrix} \gamma & -\beta_x\gamma & -\beta_y\gamma & -\beta_z\gamma \\ -\beta_x\gamma & 1+\frac{\gamma-1}{\beta^2}\beta_x^2 & \frac{\gamma-1}{\beta^2}\beta_x\beta_y & \frac{\gamma-1}{\beta^2}\beta_x\beta_z \\ -\beta_y\gamma & \frac{\gamma-1}{\beta^2}\beta_y\beta_x & 1+\frac{\gamma-1}{\beta^2}\beta_y^2 & \frac{\gamma-1}{\beta^2}\beta_y\beta_z \\ -\beta_z\gamma & \frac{\gamma-1}{\beta^2}\beta_z\beta_x & \frac{\gamma-1}{\beta^2}\beta_z\beta_y & 1+\frac{\gamma-1}{\beta^2}\beta_z^2 \end{pmatrix}. \tag{1.3.8}$$

This can also be represented as a linear transformation

$$x'^{\mu} = \Lambda^{\mu}_{\nu} x^{\nu} \ . \tag{1.3.9}$$

While of course, the addition of two velocities is no longer a trivial linear sum, and u' as u boosted by w is given by

$$u' = \frac{u+w}{1+uw/c^2}. \tag{1.3.10}$$

or in vector form

$$\boldsymbol{u}' = \frac{1}{1+\boldsymbol{u}\cdot\boldsymbol{w}}\left(\boldsymbol{u}+\boldsymbol{w}+\frac{1}{c^2}\frac{\gamma_{\boldsymbol{w}}}{1+\gamma_{\boldsymbol{w}}}\boldsymbol{w}\times(\boldsymbol{w}\times\boldsymbol{u})\right). \tag{1.3.11}$$

Here $\gamma_{\boldsymbol{u}}$ is the Lorentz factor in $\boldsymbol{u}$. These of course all reduce to Galilean relativity in the case $u \ll c$, as would be expected. This includes the lack of symmetry in 1.1.2; in truth it should be in the form

$$\begin{pmatrix} ct' \\ x' \\ y' \\ z' \end{pmatrix} = \begin{pmatrix} 1 & -\beta_x & -\beta_y & -\beta_z \\ -\beta_x & 1 & 0 & 0 \\ -\beta_y & 0 & 1 & 0 \\ -\beta_z & 0 & 0 & 1 \end{pmatrix} \begin{pmatrix} ct \\ x \\ y \\ z \end{pmatrix} . \tag{1.3.12}$$

Here the reason for the form in 1.1.2 becomes apparent. In this case the transformation is symmetric, yet when calculated, the c terms on the time components give $-\beta_i ct = -u_i t$, while other time components keep their $1/c$ terms, which of course tend to zero in the limiting case of $u \ll c$. The Minkowski metric may be presented in the form

$$\eta = \begin{pmatrix} -1 & 0 & 0 & 0 \\ 0 & 1 & 0 & 0 \\ 0 & 0 & 1 & 0 \\ 0 & 0 & 0 & 1 \end{pmatrix} \tag{1.3.13}$$

this defining the scalar product, and hence length within SR in the form

$$\begin{aligned} \boldsymbol{x} \cdot \boldsymbol{x} &= \eta_{\mu\nu} x^\nu x^\mu \\ &= x_\mu x^\mu \\ &= -c^2 t^2 + x^2 + y^2 + z^2 \end{aligned} . \tag{1.3.14}$$

Here note that a time negative convention for the Minkowski metric has been used and will be used for the remainder of the thesis. Through this, time and space are under SR indivisible, if fundamentally different, this giving rise to spacetime as it is now known as a concept. This has become the prevailing understanding of the relationship between space and time in the modern era, yet within this formulation some sense of the behaviour of time has been lost. This will be discussed in further depth in chapter 2.

Returning to the concept of electromagnetism, the electromagnetic tensor may

be represented in the form

$$F_{\mu\nu} = \partial_\mu A_\nu - \partial_\nu A_\mu \tag{1.3.15}$$

where ∂^μ is the four-gradient and A^μ is the four potential. These may be written in vector form as

$$\partial = \left(-\frac{1}{c}\frac{\partial}{\partial t}, \nabla\right) \tag{1.3.16}$$

that is, it is the standard 3-gradient with the addition of a normalised time term, noting that this is the contravariant form. The electromagnetic four-potential A^μ can be represented as $A^0 = \phi$, that is the electric potential, while A^i is the standard magnetic potential. This is a useful representation of electromagnetism, demonstrating the connected nature of electricity and magnetism in the process. Useful properties of the tensor include $F_{\mu\mu} = 0$, while standard electric and magnetic fields may be recovered as $E_i = cF_{0i} = -cF_{i0}$ and $B_i = -\frac{1}{2}\epsilon_{ijk}F^{jk}$. The Maxwell equations take on a new, more compact form of in this formulation

$$F_{[\alpha\beta,\gamma]} = 0 \tag{1.3.17}$$

$$F^{\alpha\beta}_{\ \ ,\gamma} = 0 \tag{1.3.18}$$

these represent the equivalent formulation of Maxwell's equations in the source-less case in SR. Here $F_{[\alpha_1\alpha_2\ldots\alpha_n]}$ represents the anti-symmetric part of the tensor, that is, $F_{[\alpha_1\alpha_2\ldots\alpha_n]} \equiv \frac{1}{n!}\delta^{\beta_1\beta_2\ldots\beta_n}_{\alpha_1\alpha_2\ldots\alpha_n}F_{\beta_1\beta_2\ldots\beta_n}$, while $F_{,\alpha}$ is the partial derivative in α in the form $F_{,\alpha} \equiv \partial_\alpha F$.

In effect, SR created the basis for understanding of relativistic principles, but it did not tackle some of the more important questions involved in an understanding of these phenomena. It was useful only for frames not experiencing acceleration, yet in

a universe dominated by accelerating frames due to gravitation, this is understandably limited in utility. Of course, SR could be generalised to tackle accelerating reference frames, but even so generalisations of this to better include such phenomena is a natural progression of SR.

1.4 General Theory of Relativity

The General Theory of Relativity (GR) follows on from the ideas of SR, and does so in a way to include gravitational phenomena. The relativity of SR appeared to be valid, but only in the case of inertial reference frames. Of course, gravitational phenomena appear as accelerations, and hence reference frames affected by gravitation are not inertial reference frames. Whilst SR had been generalised to be able to deal with accelerating reference frames, the more complicated examples seen in the study of gravitation require a more complete description. Equally, time within SR is only relative to the observer themselves, which causes issues within NG, where the instantaneous nature of the equations could no longer be modeled. Issues with NG had already manifested by the late 19th, and there was a well known problem with Mercury's orbit, such as with the work by Le Verrier [64]. Much as with their discovery of Neptune, Le Verrier had hypothesised another planet creating perturbations within orbits, this one existing in a closer orbit to the Sun than Mercury, and hence disturbing its orbit. Le Verrier had named this hypothetical planet Vulcan, alluding to its closeness to the Sun. By the time of Einstein however, searches for Vulcan had proved fruitless and it had been all but rejected as a possibility. Einstein in his construction of a General Theory of Relativity would include in scope first accelerated motion of reference frames, and then later equivalence with gravitational acceleration; this being the equivalence principle. From here, Einstein made what would become known as the three classical tests of relativity [40]

1. The perihelion procession of the orbit of Mercury.

2. Bending of light around the Sun.

3. Redshift of light caused by gravity.

All three of these would be found to be the case, and hence GR gained legitimacy within scientific consciousness of the time. Here of course, the same spacetime of SR is present, but here used to describe the universe as a sheetlike structure that could be bent by masses, and hence geodesics within this theory could be bent. In a more modern context, GR can be summarised broadly with the following equations, firstly the Einstein Field Equation with $G_{\mu\nu}$ as the curvature of space, $R_{\mu\nu}$ the Ricci curvature tensor, R the scalar curvature, $g_{\mu\nu}$ the metric tensor, $T_{\mu\nu}$ the energy-stress tensor and Λ a cosmological constant

$$G_{\mu\nu} = R_{\mu\nu} - \left(\frac{1}{2}R - \Lambda\right) g_{\mu\nu} = \frac{8\pi G}{c^4} T_{\mu\nu}. \tag{1.4.1}$$

That is, the curvature of space is proportional to the energy-stress of space. Here the convention used is to include the cosmological constant term within the curvature tensor. The paths of objects are then determined by the geodesic equation in the form

$$\frac{\mathrm{d}^2 x^\lambda}{\mathrm{d}\tau^2} + \Gamma^\lambda_{\mu\nu} \frac{\mathrm{d}x^\mu}{\mathrm{d}t} \frac{\mathrm{d}x^\nu}{\mathrm{d}t} = 0 \tag{1.4.2}$$

where $\Gamma^\lambda_{\alpha\beta}$ represents Levi-Civita connections, and τ proper time, and can be calculated as

$$\Gamma^\alpha_{\beta\gamma} = \frac{1}{2} g^{\alpha\epsilon} \left(g_{\beta\epsilon,\gamma} + g_{\gamma\epsilon,\beta} - g_{\beta\gamma,\epsilon}\right). \tag{1.4.3}$$

The Riemann curvature tensor takes the form

$$R^\rho{}_{\sigma\mu\nu} = \Gamma^\rho_{\nu\sigma,\mu} - \Gamma^\rho_{\mu\sigma,\nu} + \Gamma^\rho_{\mu\lambda}\Gamma^\lambda_{\nu\sigma} - \Gamma^\rho_{\nu\lambda}\Gamma^\lambda_{\mu\sigma} \tag{1.4.4}$$

where here

$$R_{\sigma\nu} \equiv R^{\rho}{}_{\sigma\rho\nu} \tag{1.4.5}$$

and finally the scalar curvature

$$R \equiv R^{\sigma}{}_{\sigma}. \tag{1.4.6}$$

These together generate the turning of vectors from curvature of the manifold. The metric tensor takes the place of the Minkowski metric, and hence lengths are determined in GR as

$$\begin{aligned} \boldsymbol{x} \cdot \boldsymbol{x} &= x^{\mu} g_{\mu\nu} x^{\nu} \\ &= x^{\mu} x_{\mu} \end{aligned} \tag{1.4.7}$$

and determined by the curvature by the above. Of course, the above does reduce to NG in the weak field case, this known as the weak field approximation. In a weak field the metric tensor may be linearised as a linear sum of the Minkowski Metric and another small metric h_{ab} of the form [85, 121]

$$g_{\mu\nu} = \eta_{\mu\nu} + h_{\mu\nu} \tag{1.4.8}$$

where h_{mn} must be of negligible contribution. In the Newtonian limit the energy-stress tensor reduces to only $T_{00} = c^2\rho$, with $T_{\mu\nu} = 0$ for all $\mu \neq 0$, $\nu \neq 0$; that is, the only component is a matter density. Equally, in the case of a slowly moving x^{μ}, all components of equation 1.4.2 that are not a derivative of time will be dwarfed by the time coordinates, reducing the equation to

$$\frac{\mathrm{d}^2 x^{\lambda}}{\mathrm{d}\tau^2} + \Gamma^{\lambda}_{00} \left(\frac{\mathrm{d}x^0}{\mathrm{d}t} \right)^2 = 0 \tag{1.4.9}$$

which given a static field and the linearised form of the metric becomes

$$\frac{\mathrm{d}^2 x^\lambda}{\mathrm{d}\tau^2} = \frac{1}{2}\eta^{\lambda\rho}\partial_\rho h_{00}\left(\frac{\mathrm{d}x^0}{\mathrm{d}t}\right)^2. \tag{1.4.10}$$

Of course for $\lambda = 0$, this must become zero as time moves steadily within the Newtonian limit, as $\mathrm{d}\tau \approx \mathrm{d}t$, leaving only the spacial coordinates

$$\frac{\mathrm{d}^2 x^i}{\mathrm{d}t^2} = \frac{1}{2}\eta^{ij}\partial_j h_{00}\left(\frac{\mathrm{d}x^0}{\mathrm{d}t}\right)^2. \tag{1.4.11}$$

If $h_{00} = -2\Phi$, then this equation becomes

$$\frac{\mathrm{d}^2 x^i}{\mathrm{d}t^2} = -\partial_j \Phi. \tag{1.4.12}$$

This giving gravitational acceleration as $\mathbf{g} = -\nabla\Phi$. The Ricci metric in equations 1.4.4 and 1.4.5 reduces by the same assumptions to with the energy-stress tensor $T_{00} = c^2\rho$ to become

$$c^2 R_{00} = 8\pi G\rho = \partial_\lambda \Gamma^\lambda_{00} \tag{1.4.13}$$

and from the same assumptions the Christoffel symbols reduce to

$$\partial_i\partial_i h_{00} = -8\pi G\rho \tag{1.4.14}$$

which as $h_{00} = -2\Phi$ this becomes

$$2\partial_i\partial_i \Phi = 8\pi G\rho \tag{1.4.15}$$

which is of course the Laplacian form of Newtonian gravity in the form of equation 1.2.7.

Much as with NG, methods of determining solutions to the general field equations above depends on the scenario. One of the most famous results from the theory is by Schwarzschild [116], which was achieved by first diagonalising the metric tensor

in spherical coordinates

$$g_{\mu\nu} = 0, \text{ for all } \mu \neq \nu \tag{1.4.16}$$

hence giving a line element

$$\mathrm{d}s^2 = g_{00}\,\mathrm{d}t^2 + g_{11}\,\mathrm{d}r^2 + g_{22}\,\mathrm{d}\theta^2 + g_{33}\,\mathrm{d}\phi^2 \tag{1.4.17}$$

which considering spherical symmetry and time independence leads to the form

$$\mathrm{d}s^2 = A\left(1 + \frac{1}{Br}\right)\mathrm{d}t^2 + \left(1 + \frac{1}{Br}\right)^{-1}\mathrm{d}r^2 + r^2\left(\mathrm{d}\theta^2 + \sin^2\theta\,\mathrm{d}\phi^2\right) \tag{1.4.18}$$

with A and B constants to be determined. These can be determined in the same manner as previously as

$$\begin{aligned} A &= -c^2 \\ B &= -\tfrac{c^2}{2GM} \end{aligned} \tag{1.4.19}$$

giving the Schwarzschild [116] metric in the usual form of

$$\mathrm{d}s^2 = -c^2\left(1 - \frac{2GM}{c^2 r}\right)\mathrm{d}t^2 + \left(1 - \frac{2GM}{c^2 r}\right)^{-1}\mathrm{d}r^2 + r^2\left(\mathrm{d}\theta^2 + \sin^2\theta\,\mathrm{d}\phi^2\right). \tag{1.4.20}$$

This is one of the simplest and most common noted solutions to the Einstein Field equations, and is applicable for time-independent gravitational fields outside any spherical object. This in a sense means that the Schwarzschild metric is applicable to anything from planets to black holes. It is in effect the GR analogy to the spherically symmetric forms of Newtonian gravity, such as equation 1.2.5. It also has a number of interesting properties, including the Schwarzschild radius, given as

$$r_{\mathrm{S}} = \frac{2GM}{c^2} \tag{1.4.21}$$

which in equation 1.4.20 forms a singularity. This of course is not the only valid choice of coordinates, and there exist coordinates under which the event horizon is regular [67]. If a mass M is contained within this radius, it would form what is known as a black hole, that is, light would not be able to escape from within this radius; hence the physical meaning of the singularity. Whilst there exists a singularity at the Schwarzschild radius, there do exist coordinates that are regular across the Schwarzschild radius, and these will be discussed elsewhere in this thesis. These black holes were considered little more than a mathematical curiosity of the equations for decades, with the development of models of stellar collapse they are now considered to be real and important components of cosmology, particularly in regard to galactic dynamics, where most galaxies contain supermassive black holes at their centre, including our own galaxy with Sagittarius A* (SrgA*) [94, 48]. The existence of such is inferred from the behaviour of stars around such dark compact objects at the centre of the galaxy, and their mass may be determined as $M = rV_{\mathrm{circ}}^2/G$ from orbital data and by more sophisticated analyses for non-circular orbits [48].

1.5 Dark Matter

With more robust tools to study gravitational effects, it was natural that an exploration of large scale structures would occur. Whilst GR is in a sense the covariant generalisation of NG, and reduces to it in the non-relativistic limit, it does allow for further dynamics that could be studied, including the previously noted key tests of GR. With this however, issues with GRs interpretation of gravitation would follow with study of large scale effects of gravitation, most notably in rotationally supported galaxies. The theory allows, much as with NG, inferences to be made

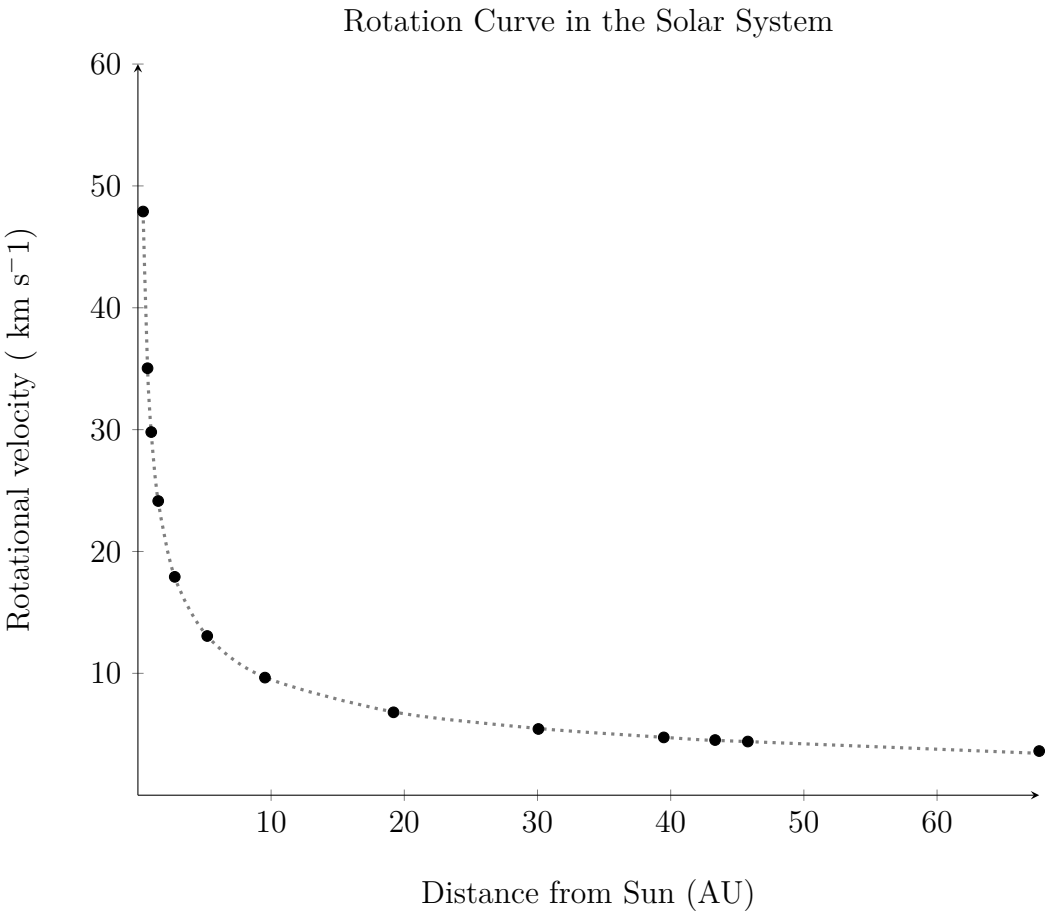

Figure 1.1: Rotation curve in the solar system, with data from [89]. The points represent planets and large gravitationally rounded objects, while the dotted line represents the expected rotation curve from NG alone.

into the amount of enclosed mass at a given distance. It would be here that the so called 'missing mass problem', would first be noted. This effect, and, as it would become known, 'dark matter', was first demonstrated in the dynamics of rotation curves of galaxies. To gain an appreciation of this effect, it is best to first consider the expected curve, starting with the simplified NG case. Consider rotation curves as observed by Kepler, and as they usually appear

$$V_{\text{circ}}^2 = \frac{MG}{r}. \tag{1.5.1}$$

Figure 1.1 shows the rotation curve for the solar system, while figure 1.2 shows a rotation curve of a fairly typical galaxy, this being NGC 3198. Here, whilst the

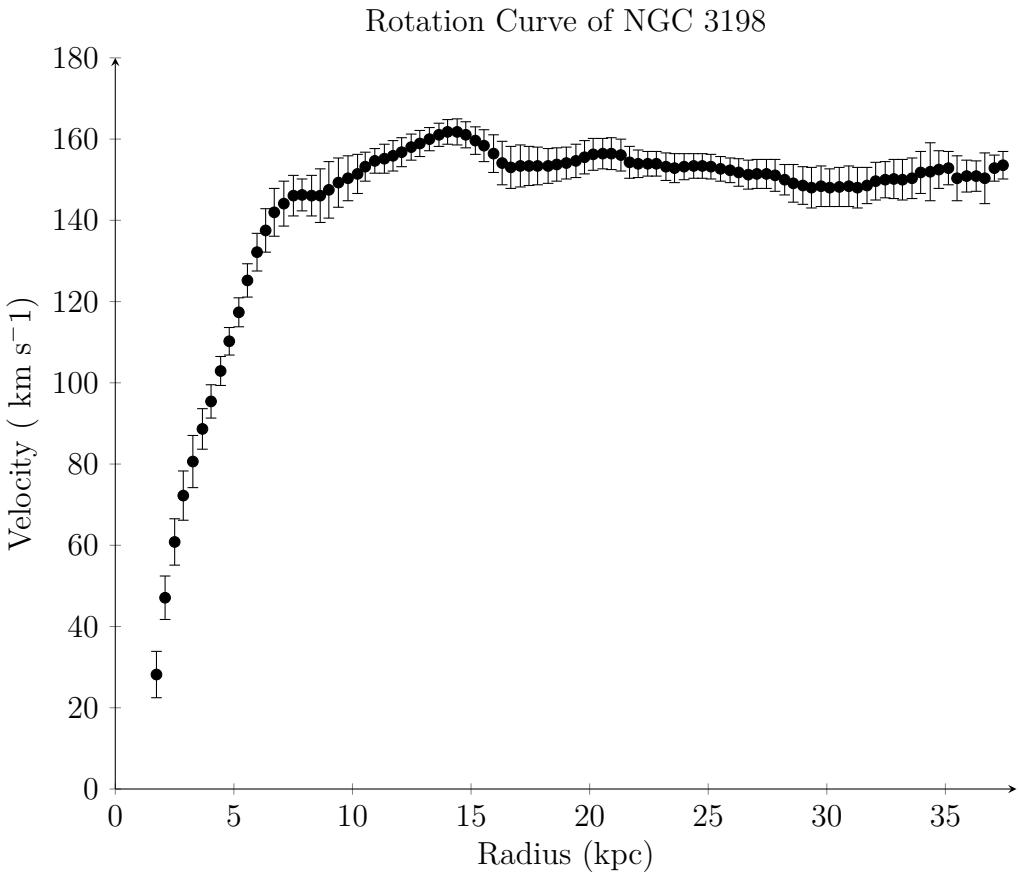

Figure 1.2: Rotation Curve of NGC 3198, data from [38].

total mass of the system is well within the radii this includes, it presents with a near flat rotation curve. Analysed by NG and theories of similar dynamics such as GR alone, this would represent increasing extra mass out to great distance in order to account for this flat region.

This problem is hardly new however. In different forms, the problem with missing mass was reported by Poincaré (1906) [101], Kapteyn (1922) [60], Oort (1932) [93] and Zwicky (1937) [132], though momentum behind the development of it as a serious explanation of observations would not occur until the work of Rubin & Ford Jr [111] in 1970. This was followed up by the influential paper by Rubin, Ford Jr & Thonnard [112] in 1980, which reported from numerous galaxies that the amount of dark matter needed must be in excess of 6 times the visible matter in galaxies. Whilst it is argued that there were movements about dark matter in

the intervening years [12], these observations would be the watershed moment in the development of dark matter theories. Despite nearly four decades having passed, the dark matter remains an unresolved issue within the standard model of cosmology [79], and the search for it remains a key test of the model.

Other theories have been developed to explain these effects in other ways, though these theories have issues of their own. While recent work suggests that dark matter components of rotationally supported galaxies is strongly coupled to the apparent dark matter [80], this not only remains an open question in the field, but one that could still reshape modern understandings of gravitational theory. Of course, concerns with modified gravitational descriptions of dark matter are fraught with concerns of their own, including specific examples such as the bullet cluster, which was claimed to be 'direct empirical proof of the existence of dark matter' [36] at the time of its publication. The gas-rich cluster, resembling a bullet under x-rays, shows disparate mass centres and gas, suggesting that dark matter is moving independently of the mass density. Hence it is regarded as proof of dark matter being a substance rather than an alteration of gravitational laws. Others have challenged this finding however [2, 3], not only suggesting MOND is compatible with the observations, but that in fact the cluster is direct proof of issues with GR due to the collision velocities involved [65], while they are consistent with MOND predictions for the cluster [2, 3]. Equally, the tightness of coupling between baryonic matter and the accelerations seen within rotationally supported galaxies suggests other dynamics at play, and provides a direct challenge to modeling dark matter in galaxies on a case by case basis [80]. Dark matter remains not just an open question within cosmology, but the discovery or non-discovery of direct evidence for it could be considered the key test of gravity within modern cosmology.

1.6 Expansion of the Universe and Dark Energy

Within Einstein's Field Equations a term was included to allow for a static solution to space. This term, the cosmological constant, denoted Λ as it can be seen in equation 1.4.1, acted as a way to fine tune solutions to the expansion of the universe. When Hubble published his results demonstrating the expanding nature of the universe in 1929 [56], this term was quickly discarded. According to Gamow [45], Einstein had remarked that he felt that the cosmological constant was his biggest blunder; without it his Field Equations would have predicted the expansion of the universe prior to its discovery. This in and of itself was no insult against Einstein's work, as a steady state universe was preferred in that era. Gamow for his own part was one of the early adopters of the Big Bang theory as proposed by Lemaître [66]. The name, initially used mockingly, has taken on its own prestige within science and particularly popular science. The very concept of it has captured popular imagination, and has had its own cultural impacts on the modern era.

In order to model the expansion of space, it is assumed that it is homogenous, isotropic and time dependent. Using a scale factor, $R(t)$, in a sense a measure of the size of the universe at one point against any other, it can be written as

$$-c^2\,\mathrm{d}\tau^2 = -c^2\,\mathrm{d}t^2 + R(t)\,\mathrm{d}\boldsymbol{\Sigma}^2 \tag{1.6.1}$$

where $\boldsymbol{\Sigma}$ represents 3-space of some uniform curvature. This is known as the Friedmann–Lemaître–Robertson–Walker metric (FLRW). Depending on the choice of coordinates this may take a number of forms, but solutions with this metric require some assumption about the nature of the energy-stress tensor. For the case of a perfect fluid this can be written as

$$T^{\mu\nu} = \left(\rho + \frac{p}{c^2}\right) U^\mu U^\nu + p g^{\mu\nu} \tag{1.6.2}$$

where ρ is energy density, p is pressure, and U^μ is the velocity vector field of the

fluid. For $U^0 = c$, $U^i = 0$, solutions to the Einstein Field Equation are of the form, with a curvature k

$$\frac{\dot{R} + kc^2}{R^2} = \frac{8\pi G\rho}{3} \tag{1.6.3}$$

$$\frac{\ddot{R}}{R} = -\frac{4\pi G}{3}\left(\rho + \frac{3p}{c^2}\right) + \frac{\Lambda c^2}{3} \tag{1.6.4}$$

these being the Friedmann equations. The Hubble parameter may also be defined as $H \equiv \dot{R}/R$, with H_0 being the current value. From these exists a critical density that determines the behaviour of the expansion of the universe. From the above this exists as

$$\rho_{\mathrm{c}} = \frac{3H^2}{8\pi G} \tag{1.6.5}$$

defining a density parameter $\Omega \equiv \rho/\rho_{\mathrm{c}}$. In the case that there is no cosmological constant, that is $\Lambda = 0$, this would determine where the universe would be

$$\Omega = \begin{cases} < 1, & \text{open} \\ 1 & \text{flat} \\ > 1 & \text{closed} \end{cases} . \tag{1.6.6}$$

This analysis, however, changes with the addition of a cosmological constant. Of course, work by Perlmutter et al. [98] and Riess et al. [106] discovered that in order for the observed redshift data for the expansion of the universe to be consistent with the FLWR metric and Friedmann equations, it would require a considerable cosmological constant. This was termed dark energy, and Perlmutter, Schmitt and Riess would win the 2011 Nobel Prize in Physics for their discovery [99]. This is now a key part of the Λ–Cold Dark Matter model of the universe (ΛCDM). The current best estimates for the key parameters, $\Omega_{\mathrm{m}} = 0.308 \pm 0.012$ and $H_0 = (67.8 \pm 0.9)\,\mathrm{km\,s^{-1}\,Mpc^{-1}}$.

1.7 Strong Unexplained Cosmological Effects

Within cosmology there exist a number of strong relations that behave in much the same way as classical laws of nature. These can be used to determine characteristics and positions of stars, and are generally used to infer other information. Whilst many of these are well known, the behaviours of these relations remain difficult to describe, and at times at odds with current theories of gravity and models of cosmology. It is for this reason that there needs to be some focus upon these, as they may act as a test of sorts, and much as classical laws defined the assumptions that were used to develop the classical theories of gravity, these modern laws may be used in a similar manner.

The relations described herein are by no means an exhaustive list of such, but rather a select few of particular interest to the remainder of this thesis. Those chosen are of particular interest to D3ST as discussed in later chapters. Cases emphasised have been chosen with a focus on where these relations may represent evidence of potential new physics, as opposed to ones where it is more likely to merely be measurement errors or misunderstandings of current phenomena.

1.7.1 Tully-Fisher relation

The Tully-Fisher relation (TFR) is an empirical relationship between the luminosity of a spiral galaxy and its asymptotic rotational velocity [125]. Developed as a method of determining distances to galaxies, the relationship has played a large role in the changing landscape of cosmology in recent decades. Whilst its original statement is in terms of luminosity, a Baryonic Tully-Fisher relation (BTFR) has been developed and is now widely used [77], and has been generalised to gas dominated galaxies [118]. The relation sees a proportionality of $M \propto V_f^4$, where M is the mass of baryons within the system, and V_f is the asymptotic rotational velocity of the system [78]. This calibration for gas dominated galaxies is particularly important

in theories relating baryonic mass to supposed dark matter effects, as it continues the Tully-Fisher relationship in low light galaxies where it broke down in terms of pure luminosity. The tightness of the relationship, as well as the number of orders of magnitude it appears in, means that it has some important properties for study, and can be considered a major test of the dynamics of a gravitational theory [78, 83].

1.7.2 M-σ Relation

There also exists an empirical relation between the mass of a galaxy's central super massive blackhole ($M_\bullet$) and the velocity dispersion of the system (σ) [46], this being applicable both to elliptical galaxies, and the bulges of spiral galaxies [42]. The relation, which can be stated as $M_\bullet \propto \sigma^\beta$, has been found with $\beta = 4.24 \pm 0.41$ for all galaxies and $\beta = 3.96 \pm 0.42$ for elliptical galaxies alone [52]. These more recent values follow on from initial concerns with the differences seen in slopes between different studies, with this being found to be largely down to the methodologies of different groups in estimating the velocity dispersion [123]. The M-σ relationship is noted because of its strong fit to data and limited scatter, which is less than expected from formation processes alone. As such the M–σ may be considered another key test of the dynamics of a gravitational theory.

1.7.3 Bulge-Mass to Black Hole Relation

There is a reported relationship between bulge mass and the mass of the central black hole ($M_\bullet$), this relationship being $M_{\text{bulge}} \propto M_\bullet$ [72, 23]. Whilst this is formulated as a direct proportionality relationship, relationships involving powers that are not exactly 1 are also reported [55, 76], while this relationship has also been explored at low-mass [50]. There have also been reports of this relationship representing roughly $M_\bullet \approx \frac{\alpha}{2} M_{\text{bulge}}$, where α is the fine structure constant [19]. The result considered for the remainder of this thesis is $\log_{10}(M_\bullet/M_\odot) = 8.46 \pm 0.08 + (1.05 \pm 0.11)\log_{10}(M_{\text{bulge}}/M_\odot)$, from [76]. Generally this relation is

considered to be caused by formation processes within galaxies [76], though it has been argued that it could also represent a new type of physics [19, 23, 14, 62].

1.7.4 Baryonic Mass to Rotation Curve Relation

McGaugh, Lelli & Schombert [80] report a strong correlation between radial acceleration traced by rotation curves observed and those predicted by the baryonic mass within galaxies alone. This relationship differs from the BTFR which relates only to the baryonic matter of the galaxy and asymptotic rotational velocity, while this relationship relates the observed radial acceleration to the predicted acceleration within the systems themselves. This relationship is of particular interest as it notes the importance of these relationships within the systems themselves. The study by McGaugh, Lelli & Schombert [80] is of particular interest, however, as it demonstrates this strong coupling between observed and predicted curves, and does so from a sample including 2693 points from 153 rotationally supported galaxies. They note that rotationally supported galaxies were chosen in particular as elliptical and other galaxies have more complicated potentials, though a similar relationship is expected [80]. They report an empirical relationship between $g_{\rm obs}$ to $g_{\rm bar}$ of the form

$$g_{\rm obs} = \frac{g_{\rm bar}}{1 - \mathrm{e}^{-\sqrt{g_{\rm bar}/g_\dagger}}}. \tag{1.7.1}$$

Here $g_{\rm obs}$ is the observed gravitational acceleration, $g_{\rm bar}$ is the gravitational acceleration predicted from the total number of baryons, while $g_\dagger$ a single free fitting parameter with dimensions of acceleration. They report $g_\dagger = 1.20 \pm 0.02\,(\text{random}) \pm 0.24\,(\text{systematic}) \times 10^{-10} \mathrm{m\,s^{-2}}$. On this basis, the authors argue that this could be a potential 'Kepler's Law for rotating galaxies' considering the tightness of fit.

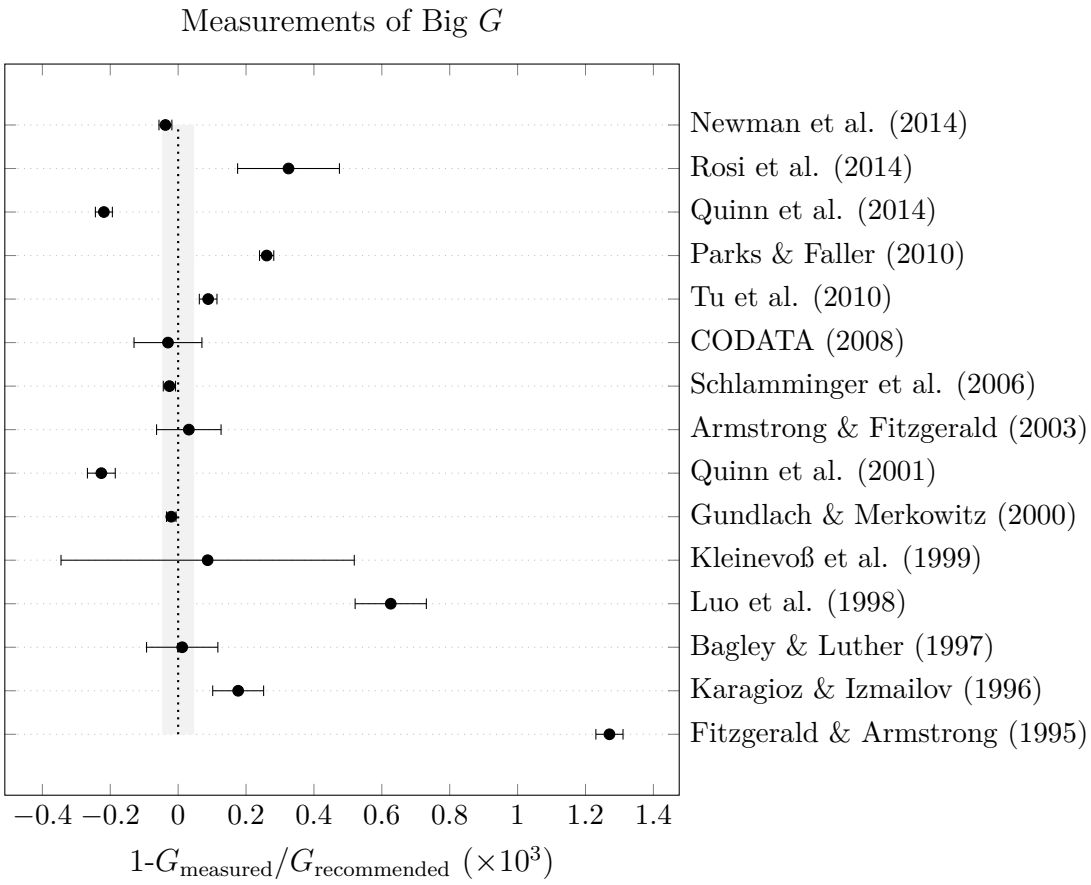

Figure 1.3: A plot of measurements of Big G in terms of fractional difference from the CODATA (2014) recommendation [87], which here is represented by the vertical dotted line with the grey region being the recommended uncertainty.

1.7.5 Measurement of G

While not strictly a cosmological relationship, the measurement of the gravitational constant G has presented issues within gravitational research. Unlike many physical constants, the value of Newton's gravitational constant G remains somewhat alone in that there is still a comparatively large scatter in measured values. Whilst most constants are known to parts per million at worst, values for G still vary in the region of parts per ten thousand [88, 31, 87, 102]. The concerns with the measurement of the gravitational constant G are well established; such concerns have inspired efforts and conferences such as the 2016 one at NIST. The current CODATA recommended value for big G is $(6.67408 \pm 0.00031) \times 10^{-11} \mathrm{m}^3\,\mathrm{kg}^{-1}\,\mathrm{s}^{-2}$ [87]. A plot including some recent values of G with error bars is included as figure

1.3, while the table this was produced from is included as appendix A. As can be seen within the plot, there is a large spread, and this spread of over one part in ten thousand can be clearly seen. There have also been attempts at theoretical values for G [69], though at this point none of these have received widespread attention, nor have these given a sufficient reason for the spread seen in the constant. Equally there have been some less orthodox studies of the gravitational constant in recent years, including suggestions that this may be caused by changes in G over time [1], though their argument that it varies over a period of half a dozen years has been challenged on numerous bases [114]. Overall, the spread in the measurements of the gravitational constant suggests that there may be something else at play here. Whether or not this represents some new physics, or misunderstandings in current measurement protocols, remains to be seen.

1.8 Alternative Theories of Gravity

While GR is the most used and considered standard theory of gravity, there do exist other theories of gravity that attempt to solve some of the problems discussed above. Of particular interest to this thesis are Modified Newtonian Dynamics (MOND) due to similarities arising between its dynamics, and previous work in the topic of this thesis.

1.8.1 Modified Newtonian Dynamics (MOND)

MOND is a theory that attempts to explain the asymptotically flat rotation curves for spiral galaxies by alteration of the gravitational law for small accelerations. The original formulation of the theory was in regard to a modified force law for gravity in the form [10]

$$m\ \mu\left(\frac{g}{a_0}\right) g = \frac{GMm}{r^2} \tag{1.8.1}$$

where m is the mass of the object being accelerated, a_0 is a constant acceleration defining a switching scale for MOND's form of gravity and μ is a function with the property

$$\mu(x) \sim \begin{cases} 1, \ x \gg 1 \\ x, \ x \ll 1 \\ \text{otherwise determined.} \end{cases} . \tag{1.8.2}$$

The acceleration is denoted a_0 and is roughly $\sim 1.5 \times 10^{-10} \mathrm{m\,s^{-2}}$ [83]. There were issues with this form, notably that for Newton's third law to hold, the following would be true

$$\begin{aligned} m\,\mu\left(\frac{g}{a_0}\right) g &= \frac{GMm}{r^2} \\ M\,\mu\left(\frac{g}{a_0}\right) g &= \frac{GMm}{r^2} \end{aligned} \tag{1.8.3}$$

which means that

$$\mu\left(\frac{g}{a_0}\right) = \mu\left(\frac{g}{a_0}\right) \tag{1.8.4}$$

which requires that $\mu(x)$ be a constant, this violating equation 1.8.2. In essence, in the original formulation of the theory as a force law, it violated one of the key laws behind motion. The resolution to this issue a construction of MOND called AQUAL, being name for the term A Quadractic Lagrangian [10, 82, 83]. The AQUAL form of MOND is derived from the Lagrangian [8]

$$\mathcal{L} = -\frac{a_0^2}{8\pi G} F\left(\frac{|\nabla\Phi|^2}{a_0^2}\right) - \rho\Phi \tag{1.8.5}$$

and usually stated in the form

$$\nabla \cdot \left[\mu\left(\frac{|\nabla\Phi|}{a_0}\right)\nabla\Phi\right] = 4\pi G\rho. \tag{1.8.6}$$

The function $F(x)$ is related to the interpolating function as $\mu(x) = \frac{\mathrm{d}F(x^2)}{\mathrm{d}x}$. Using equations (1.8.6) and (1.8.2), gravity outside a spherical system, where $g \equiv |\nabla\Phi| \ll a_0$, is

$$\begin{aligned} \nabla \cdot \left[\frac{|\nabla\Phi|}{a_0}\nabla\Phi\right] &= 4\pi G\rho \\ \frac{g^2}{a_0} &= \frac{GM}{r^2} \\ g &= \frac{\sqrt{GMa_0}}{r}. \end{aligned} \tag{1.8.7}$$

This being the same form as the behaviour initially described in equation 1.8.1. These interpolating functions come in a number of forms, though the most common generally are of the form [131, 47]

$$\mu(x) = \frac{x}{\sqrt{1+x^2}} \tag{1.8.8}$$

or the simple interpolating function

$$\mu(x) = \frac{x}{1+x}. \tag{1.8.9}$$

Application of MOND in the case of $a_0 \gg g$, it produces for spherical orbits

$$V_{\mathrm{circ}}(r) = \sqrt[4]{GMa_0} \tag{1.8.10}$$

that is, a flat rotation curve, as is observed in spiral galaxies. This being MOND's solution for the BTFR [77, 78]. It has been argued that MOND is the best description for these phenomena, and that it is difficult to otherwise understand how there is such a strong correlation between low acceleration environments and dark matter [79].

There also exists a relativistic form of MOND called Tensor-Vector-Scalar gravity (TeVeS) [7, 113, 86, 9], which is derived from the action principle, and allows MOND to account for relativistic phenomena, most notably gravitational lensing.

The theory yields other forms of MOND in the weak field approximation.

1.8.2 Entropic Gravity

Another attempt at describing these effects comes in the form of Entropic Gravity (EG). Through this, the argument is essentially that we can model the universe and objects within it as information [126]; this not too dissimilar to the starting point for Process Physics. The theory follows a postulate that

$$\Delta S = 2\pi k_B \frac{mc}{\hbar}\Delta x \tag{1.8.11}$$

argued as [126]

$$\Delta S = 2\pi k_B \quad \text{when} \quad \Delta x = \frac{\hbar}{mc} \ . \tag{1.8.12}$$

From this it follows that

$$k_B T = \frac{1}{2\pi}\frac{\hbar a}{c}. \tag{1.8.13}$$

Within this theory, Newton's law of universal gravitation is returned by first considering a number of bits N that it takes to describe an object, enclosed within a surface A, with the number of bits given as [126]

$$N = \frac{Ac^3}{G\hbar}. \tag{1.8.14}$$

Here, area and a set of constants were introduced and it was assumed that number of bits was proportional to area [126]. Following the standard equipartition rule

$$E = \frac{1}{2}Nk_B T, \tag{1.8.15}$$

assuming that the energy enclosed by the surface follows the standard

$$E = Mc^2, \tag{1.8.16}$$

and that

$$A = 4\pi r^2 \tag{1.8.17}$$

this becomes

$$F = \frac{GMm}{r^2} \tag{1.8.18}$$

which is the standard form of Newton's universal law of gravitation as in equation 1.2.2. Whilst Verlinde does note that this comes about by design of the equations [126], it is argued that this does form a new argument for the origin of gravity. That is, gravitation can be described as an entropic force. These arguments are also generalised for the Poisson equation, and Einstein equations for gravity, though the arguments follow similar lines [126].

Verlinde [127] has also formulated arguments for an explanation for dark matter within galaxies as an entropic phenomena related to the amount of entropy removed from a region by the addition of matter. In effect, the theory relates added mass to the expansion of the universe, and derives a 'dark matter' like effect from it. Notably, it is argued that the acceleration scale of MOND, a_0 may in fact be determined theoretically, in this case as for an Anti-de Sitter space with a finite horizon, that the surface acceleration κ can be modeled as [127]

$$\kappa = cH_0 = \frac{c^2}{L} = a_{\mathrm{EG}}. \tag{1.8.19}$$

Here L is a Hubble scale and this a_{EG} (written as a_0 in Verlinde's paper) being the same acceleration as identified within MOND. This however is only similar to the one used, and is related by $a_0 = a_{\mathrm{EG}}/6$. This would give $a_0 \approx 1.2 \times 10^{-10}$ m s^{-2},

this comparable to the value generally seen in MOND [83].

There exist criticisms of EG both on a theoretical basis and a observational basis. Visser [128] argues that Verlinde's formulation of the theory causes problems with how the entropic forces need to be set up. Pardo [96] argues that EG fails to predict the maximum velocity in rotation curves for small gas dominated galaxies. How this relates to the relationship as described by McGaugh, Lelli & Schombert [80] is unclear. Despite such concerns, the theory appears to work fairly well in an area where there is still no clear solution to problems.

Concluding Remarks

The development of gravitational theories has lead to a strong understanding of gravity within our own neighbourhood. Kepler's laws having been explained by Newton were a turning point in the understanding of modern physics, and offered a link between the motions of bodies from the scale of dust to astronomical bodies. Unlike under the work of Aristotle, it was no longer a case of different types of motion for different types of objects. With this however, whilst we have now explained our own solar system to great detail, at large scales our theories of gravity now require a new Vulcan. Not just one either, but two, normally named dark matter and dark energy, without which our understanding of the universe falls flat. Whilst there exist other theories that attempt to explain these phenomena, such as MOND and EG, there still remains no full explanation for the dynamics of the universe at a large scale.

This chapter has outlined the development of modern gravitational theories from their classical origins, and noted some areas of interest to the rest of this thesis. Of particular interest include elements of GR, MOND, and large scale astronomical relations.

Chapter 2

An Introduction to Dynamical 3-Space Theory

With the current developments in other theories of gravitation in mind, consideration of the basis for this research within its field, as well as where it has come from, is appropriate. This chapter seeks to outline the basis for, and direction in, research into D3ST with reference to its Process Physics origins, and in doing so justify and highlight the direction of the rest of the thesis. In particular, this chapter outlines key results in the theory to this point, and will be used as a basis for discussion within chapters 3 and 4. In addition to this, while drawing on the knowledge of past papers within this field, work by Rothall [108] has been noted to improve previous definitions within the theory.

2.1 Process Physics

Process Physics is a theory that seeks to model reality from a viewpoint that does not contain *a priori* elements [15]. Inspired by work on self-referential syntactical information systems, as described by Gödel and Chaitin [35], the theory attempts to model space and quantum realities as emergent entities, rather than syntactical ones. It does so in a way that models time as a non-geometric process [15]. Cahill

[22] argues that whilst geometric modeling of time has useful mathematical elements, such representations of time offer little resemblance to its reality. Of notable concern is that time itself can be seen to have three separate phases which are difficult to capture geometrically, that is

1. The Past: events that have happened and have clearly defined results.
2. The Present: a boundary separating the past and the future, and interacting directly with reality.
3. The Future: undecided and unknowable.

Whilst it is undeniable that there are uses of geometric modeling of time within physics, and in understanding classical laws of physics, care should be taken not to confuse this with the ontology of time as has arguably happened with other theories [22]. Within SR and GR, the concept of a spacetime, in a way wedded together inseparably, is argued to be confusing useful modeling tools with an understanding of reality itself. Whilst there is undeniably value in such modeling, particularly in terms of the results of such theories, this theory is argued on the basis of process time.

The philosophical side of the theory focuses on concerns with the limitations of many physical theories, and the over-reliance on metarules and metaphysical assumptions to overcome these limitations. In particular, the theory is concerned with understanding how quantum processes come about, and considering elements such as the Born measurement metarule to model the non-process structures in a way congruent with syntactical theories.

To this end the theory models reality as a stochastic neural network, and time as a self-ordering process, rather than a geometric one [15]; in effect, the system is bootstrapped by some start-up process and modeling and description can be performed herein. Here the self-ordering and stochastic processes in a sense compete as the system iterates. Containing no *a priori* concept of geometry, fields or physical

laws, these elements emerge from these processes, rather than being a designed part of the system. Whilst the initial aims of the theory were to attempt to understand the emergent properties of reality and explore how this can be done without these prior assumptions, what it instead found was new and interesting properties that could be tested against observational and experimental phenomena. In a sense, what was found was that these systems formed a quantum foam-like structure that behaved roughly as a 3-space, with topological defects acting as sinks. This, along with other behaviours of the defects, sees its behaviour identified with that of matter; this argued to be a possible unification of space and matter [15], as well as an explanation of quantum, inertial and gravitational behaviour.

To this end, Process Physics appeared to give rise to behaviours such as inertia, gravity, 3-space and such without the need for prior assumptions. It has also been suggested that under these models, the universe would form as an S^3 space [24], that is the 3-dimensional surface of a 4-dimensional sphere. This, for a sufficiently sized universe, would appear flat locally, though there should exist some real curvature of space should this be verifiable. In any case, at this time a method of transitioning this modeling to that of a more traditional syntactical theory has yet to be found. To this end, D3ST was developed to fill this void, and to be a theory of gravity derived from principles of this theory.

2.2 3-Space Velocity

While Process Physics at this time has not been completely unified with D3ST, it does serve as the motivation for it, as well as the processes seen within it. Whilst NG treats gravity as a force field and GR treats it as warping of a 4D sheet like spacetime, within D3ST gravity is modeled by changes in a velocity field denoted $\boldsymbol{v}$. This velocity field is suggested to be one of a background quantum foam which acts as a dynamical 3-space. From considering behaviours of this from Process Physics,

this theory attempts to describe these processes embedded in a 3-space. This 3-space itself is used merely as an embedding space for the velocity field, and is not believed to have ontological significance within the theory [22, 24, 29]. In this sense the idea of gravitation being equivalent to accelerations takes on a clear and well defined meaning, as within this theory it is defined as the changes in the velocity field. This can be defined by taking the change of the velocity field over a step in time, and hence gravitational acceleration may be defined by

$$\begin{aligned} \boldsymbol{a}\left(\boldsymbol{r},t\right) &= \frac{\mathrm{d}\boldsymbol{v}}{\mathrm{d}t} \\ &= \lim_{\Delta t\to 0}\frac{\boldsymbol{v}\left(\boldsymbol{r}+\boldsymbol{v}\left(\boldsymbol{r},t\right)\Delta t, t+\Delta t\right)-\boldsymbol{v}\left(\boldsymbol{r},t\right)}{\Delta t} \\ &= \frac{\partial \boldsymbol{v}}{\partial t}+\left(\boldsymbol{v}\cdot\nabla\right)\boldsymbol{v}. \end{aligned} \tag{2.2.1}$$

This here is also known as the material derivative. The above form would suggest that this acceleration $\boldsymbol{a}$ should be identified with gravitational acceleration $\boldsymbol{g}$. The definitions here can be considered to be a statement of the equivalence principle in a sense, here gravitation is not only identified as being indistinguishable from an acceleration, but in a sense is a true acceleration within the field. From this, the above can be identified with Gauss' form of gravitation (equation 1.2.6), this would suggest a form for a 3-space equation of

$$\nabla\cdot\left(\frac{\partial \boldsymbol{v}}{\partial t}+\left(\boldsymbol{v}\cdot\nabla\right)\boldsymbol{v}\right)=-4\pi G\rho \tag{2.2.2}$$

or equivalently as

$$\nabla\cdot\frac{\mathrm{D}\boldsymbol{v}}{\mathrm{D}t}=-4\pi G\rho. \tag{2.2.3}$$

Whilst the first is the standard form of the equation seen in the theory, for this thesis the second will be preferred for brevity as $\frac{\mathrm{D}\boldsymbol{v}}{\mathrm{D}t}\equiv\frac{\partial \boldsymbol{v}}{\partial t}+\left(\boldsymbol{v}\cdot\nabla\right)\boldsymbol{v}$, this being the definition of the material derivative. These forms of the equation represent a simple form of the dynamical 3-space equation, but one that behaves identically to NG. To

that end, consider solutions to the above for a mass M at distance r in the form

$$\boldsymbol{v}\left(r\right) = -\hat{\boldsymbol{r}}\sqrt{\frac{2GM}{r}} \tag{2.2.4}$$

which yields a gravitational acceleration of

$$\boldsymbol{g}\left(r\right) = -\hat{\boldsymbol{r}}\frac{GM}{r^2} \tag{2.2.5}$$

this being the same behaviour as with NG. Equally, this velocity field can as such be seen as being equivalent to escape velocity for a single source, or total escape velocity for a collection of sources. This here gives some physical meaning to the velocity field beyond it acting as a generator for gravitational acceleration.

Equally, for the case of zero vorticity and time-independence, it is possible to associate $v^2 \equiv \boldsymbol{v} \cdot \boldsymbol{v}$ with gravitational potential as

$$v^2 = -2\Phi \tag{2.2.6}$$

which of course in equation 2.2.3 produces the Poisson form of gravitation

$$\nabla^2\Phi = -4\pi G\rho. \tag{2.2.7}$$

Which again shows the equivalence between 3-space gravitational theory and other gravitational theories in this form. Alternatively, for zero vorticity, this would become, keeping velocity notation

$$\nabla \cdot \left(\frac{\partial \boldsymbol{v}}{\partial t} + \nabla\left(\frac{v^2}{2}\right)\right) = -4\pi G\rho \tag{2.2.8}$$

or for the gravitational acceleration

$$\boldsymbol{g}\left(\boldsymbol{r}, t\right) = \frac{\partial \boldsymbol{v}}{\partial t} + \nabla\left(\frac{v^2}{2}\right) \tag{2.2.9}$$

which is useful in some circumstances.

In a sense, under this formulation, 3-space is simply a velocity field formulation of NG. Whilst there may exist a temptation to associate this theory with luminiferous aether theories, it is actually very different in both its construction and consequences. Aether theories required the medium's existence to explain how light propagated, while this theory is instead interested in the geometry that the universe is embedded in. It is not a substance within the geometry of the universe that is flowing, but rather a change in the geometry itself. It is actually closer to the construction of GR than aether theories, the difference is the focus. As will be discussed in chapter 4, the theory may actually be constructed in a near identical way to GR, and maintain the same behaviours. There is nothing particularly mysterious about this construction of a gravitation, and it in terms of gravitational phenomena at the very least, behaves in an identical fashion in the Newtonian and relativistic limits at the very least. It is at this point that the new dynamics of the theory need to be considered however.

2.3 Dynamics of the 3-Space

The version of the dynamical 3-space equation as can be seen as 2.2.3 may be generalised by considering other possible terms. In order to expand possible dynamics considered by this theory, other terms that may fit within the equation of gravity were considered, such that they could be compared to observations. Considering minimal terms of dimension t^{-2} which are invariant under translation and rotation, these added to equation 2.2.3 produces

$$\nabla \cdot \frac{\mathrm{D}\boldsymbol{v}}{\mathrm{D}t} + \alpha_1 \left(\mathrm{tr}D\right)^2 + \alpha_2 \mathrm{tr}\left(D^2\right) = -4\pi G\rho \tag{2.3.1}$$

where here

$$D_{ij} = \frac{1}{2}\left(\frac{\partial v_i}{\partial x_j} + \frac{\partial v_j}{\partial x_i}\right). \tag{2.3.2}$$

In order for these terms to produce no unusual behaviour outside of spherically symmetric objects, this requires that $\alpha_2 = -\alpha_1$, that is, the two extra terms are required to be equal and opposite. For this reason α_1 may be replaced with simply α. This is how the theory was originally set up, and older work saw the dynamical 3-space equation published as [22, 29]

$$\nabla \cdot \frac{\mathrm{D}\boldsymbol{v}}{\mathrm{D}t} + \frac{\alpha}{8}\left((\mathrm{tr}D)^2 - \mathrm{tr}\left(D^2\right)\right) = -4\pi G\rho \tag{2.3.3}$$

however a reanalysis by Rothall [108] found issues with the original analysis of some observations, and instead proposed the form

$$\nabla \cdot \frac{\mathrm{D}\boldsymbol{v}}{\mathrm{D}t} + \frac{\pi^2\alpha}{8}\left((\mathrm{tr}D)^2 - \mathrm{tr}\left(D^2\right)\right) = -4\pi G\rho. \tag{2.3.4}$$

This form will be used for the remainder of this thesis. The value of α has been found independently using bore hole data to be $\alpha \approx 1/137$ [18, 108]. This has been observed to be similar to the fine structure constant $\alpha = 1/137.036$ within error, and it has been suggested that this may be the constant observed [18]. It is also convenient to rewrite this in the form $\alpha' \equiv \frac{\pi^2\alpha}{2}$ due to the frequent instances of $\frac{\pi^2\alpha}{2}$ seen within the theory, giving the form

$$\nabla \cdot \frac{\mathrm{D}\boldsymbol{v}}{\mathrm{D}t} + \frac{\alpha'}{4}\left((\mathrm{tr}D)^2 - \mathrm{tr}\left(D^2\right)\right) = -4\pi G\rho. \tag{2.3.5}$$

Of course, the above can also be solved for outside a spherical mass M at distance r as before, firstly for the velocity field

$$\boldsymbol{v}\left(r\right) = -\hat{\boldsymbol{r}}\sqrt{\frac{2GM\left(1+\alpha'\right)}{r}} \tag{2.3.6}$$

and secondly the gravitational acceleration

$$\boldsymbol{g}(r) = -\hat{\boldsymbol{r}}\frac{GM(1+\alpha')}{r^2}. \tag{2.3.7}$$

The above could also be represented by defining these changes as $M_{\mathrm{DM}} = \alpha' M$ such that

$$\boldsymbol{g}(r) = -\hat{\boldsymbol{r}}\frac{G(M + M_{\mathrm{DM}})}{r^2}. \tag{2.3.8}$$

This 'dark matter' term here represents extra effective matter caused by the α term in equation 2.3.5. That is, the extra apparent mass that would appear should this be analysed with a purely Newtonian theory of gravitation. Of course, this would present in effect a small offset to the data, and could represent part of the issue in measurements of the gravitational constant as discussed in section A.

Further expansion of the dynamics of this theory were done including a further term, this being the topic of my previous research. It was argued to require the following that [31, 14, 62]

1. It must maintain the case of NG outside spherically symmetric matter systems.

2. Dark matter effects seen where $\alpha \neq 0$.

The form that was tested included a new term of the form

$$\delta^2\nabla^2\left((\mathrm{tr}D)^2 - \mathrm{tr}\left(D^2\right)\right) \tag{2.3.9}$$

and may be incorporated into the dynamical 3-space equation as

$$\nabla\cdot\frac{\mathrm{D}\boldsymbol{v}}{\mathrm{D}t} + \left(\frac{\alpha'}{4} + \delta^2\nabla^2\right)\left((\mathrm{tr}D)^2 - \mathrm{tr}\left(D^2\right)\right) = -4\pi G\rho \tag{2.3.10}$$

where here δ is some small, Plank-like length. This form prevents inflow velocity for systems going to infinite at the origin in spherical and cylindrical coordinates. Whilst this was not a major concern as the theory had to this point been interested

in effects far away from the origin, this still posed theoretical issues in some isolated cases, such as cosmic filaments [31]. The solutions to this version of the 3-space equation has well-behaved solutions even at small scales.

Equation 2.3.10 may also be represented as

$$\nabla \cdot \frac{\mathrm{D}\boldsymbol{v}}{\mathrm{D}t} = -4\pi G \left(\rho + \rho_{\mathrm{DM}}\right) \tag{2.3.11}$$

where

$$\rho_{\mathrm{DM}} = \frac{1}{32\pi G}\left(\frac{\alpha'}{4} + \delta^2\nabla^2\right)\left(\left(\mathrm{tr}D\right)^2 - \mathrm{tr}\left(D^2\right)\right). \tag{2.3.12}$$

This form has been chosen for brevity as well as allowing the equation to remain consistent regardless of choice of α and δ value, as will be discussed further in this chapter. It also allows any further terms to be included simply without any changes to the rest of the equation, nor standard formulae used within the theory. This choice of writing the equation also highlights a key component of the equation, that all effects that differ from NG represent some new form of physics and under Newtonian theories will appear to behave as some form of apparent mass.

At this time, exact solutions to this form of the equation for outside a spherical mass are unknown [31, 108], by analogy to previous solutions however it is expected that they will come in a similar manner, with the original Newtonian Inverse Square Law, followed by additional terms which can be packaged in a similar manner. That is, in the same manner as equation 2.3.8, solutions to equation 2.3.11 may be written as

$$\boldsymbol{g}\left(r\right) = -\hat{\boldsymbol{r}}\frac{G\left(M + M_{\mathrm{DM}}\right)}{r^2} \tag{2.3.13}$$

which, whilst not a full solution, with some understanding of the behaviour of M_{DM}, does suggest its behaviour. For a full discussion of the known behaviour of M_{DM}, see section **2.11**. Of course, the other way of defining this would be

$G_{\text{obs}} \equiv G\left(1+\frac{M_{\text{DM}}}{M}\right)$ giving the form

$$\boldsymbol{g}(r) = -\hat{\boldsymbol{r}}\frac{G_{\text{Obs}}M}{r^2}. \tag{2.3.14}$$

That is, we could represent these changes as being a perturbation to the gravitational constant. This however assumes that M_{DM}/M is a constant value for $\delta \neq 0$, which is not a given, unlike in the $\alpha \neq 0$ case for spherically symmetric systems. In any case, even an approximate form of this relation could be a cause for the difficulty in measuring G as discussed in section 1.7.5.

2.4 Characteristics of the 3-Space

The dynamics of the theory are highly non-local and instantaneous [29]. To see this action at a distance, the integro-differential form of equation 2.3.12 can be written as

$$\frac{\partial \boldsymbol{v}}{\partial t} = -\frac{\mathrm{D}\boldsymbol{v}}{\mathrm{D}t} - 4\pi G\int \mathrm{d}^3 s\ \left(\rho(\boldsymbol{s},t) + \rho_{\text{DM}}(\boldsymbol{s},t)\right)\ \frac{\boldsymbol{r}-\boldsymbol{s}}{|\boldsymbol{r}-\boldsymbol{s}|^3} \tag{2.4.1}$$

which, beyond being non-local, is also non-linear in changes in ρ and ρ_{DM} [29]. It is worth noting that this apparent dark matter density behaves exactly as baryonic matter within this formulation. This may also be generalised considering the effective velocity to an object moving against the 3-space, this being

$$\boldsymbol{v}_{\text{R}}(\boldsymbol{r}_{\text{O}}(t),t) = \boldsymbol{v}_{\text{O}}(t) - \boldsymbol{v}(\boldsymbol{r}_{\text{O}}(t),t) \tag{2.4.2}$$

where $\mathbf{v}_0$ is defined as the velocity of the object, which in the case of $v_{\text{R}} \ll c$ can be used to determine the vorticity vector field $\boldsymbol{\omega}(\mathbf{r},t) = \nabla \times \mathbf{v}$ as [29]

$$\boldsymbol{\omega}(\boldsymbol{r},t) = \frac{2G}{c^2}\int \mathrm{d}^3 s\ \frac{\rho_{\text{DM}}(\boldsymbol{s},t)+\rho(\boldsymbol{s},t)}{|\boldsymbol{r}-\boldsymbol{s}|^3}\boldsymbol{v}_{\text{R}}(\boldsymbol{s},t)\times(\boldsymbol{r}-\boldsymbol{s}) \tag{2.4.3}$$

which has been used to analyse experiments such as the procession of gyroscopes

in gravity probe B experiment [21, 29].

Equally, approximate velocity superposition effects have previously been studied within the theory, and it has been demonstrated that both the velocity field and gravitational acceleration are invariant with change of observers [16].

2.5 Direct Observations

It has been reported that direct observations of this 3-Space have been made, with the most famous experiment claimed to show such an effect being the Michelson-Morley experiment of 1887 which was concluded to be null [81, 28]. The theory is argued to have Lorentzian relativistic effects relative only to the background 3-space [29]. A reanalysis of the Michelson-Morley experiment by [20] reported a velocity of in excess of 300 km s^{-1}, arguing that the original analysis did not take into account dynamical effects. This is a stark contrast to the originally reported 8 km s^{-1} as reported by Michelson & Morley [81], and far in excess of the 30 km s^{-1} that they had originally expected. Further experiments by Miller (1925/26) [84], Torr and Kolen (1981) [122], De Witte (1991) [26], Cahill (2006) [25] and Rothall & Cahill (2014) [109] using various methods have shown the same result [29] under Cahill's theory. Another characterisation of the 3-space velocity was found using spacecraft Earth Flyby Doppler shift data to be $486 \text{km} \cdot \text{s}^{-1}$ in the direction Right Ascension (RA)= 4.3hrs, Declination (Dec)= $-75°$ [28], confirming that this velocity could be determined from multiple different types of sources.

The inflow velocity has been confirmed to be in a different direction to the Cosmic Microwave Background frame, as is expected [16]. This is because, for the inflow interpretation to be self-consistent, it requires that inflow in our local region be dominated by gravitational effects in our local region. These are, namely, the inflow towards the centre of the galaxy, and the inflow towards the Sun and Earth proper. This is also on top of motion of the solar system, galaxy and such against

the background frame.

The most recent method of detecting these changes in $\mathbf{v}$ has also been reported using RF coaxial cables and zener diodes [32], with this reported to be potentially related to the Schnoll effect [17]. It is believed that the zener diode based detectors work due to a hypothesised change in the tunneling current caused by the velocity of the 3-space [33]. These experiments have confirmed independently a velocity in the direction RA$\sim$ 5hrs, Dec $\sim -80^\circ$ with a speed of $\sim 500\text{km} \cdot \text{s}^{-1}$[109].

Despite this reported success other groups checking the results have had less success. There have been two recent tests using Cahill's Zener Diode experiments. Whilst Seaver [117] reported an effect, they reported that it was a response to local electromagnetic disturbances. Equally, they noted that it appeared that it was the similar natures of the diodes that lead to the apparent correlations. Equally a recent test by Baer, Reiter & Jabs [5] reported a null result from similar tests. The authors noted that they felt that this was not an overall null result for the effect, but rather that they simply were not able to see the same effect as reported by Cahill.

Overall it appears that whilst there are reports of direct detection of 3-space velocities, there do remain concerns about both the methodology and previous findings. Whilst the results in and of themselves are interesting, without results being confirmed independently, and correlated by multiple teams, the claimed effect by Cahill and colleagues at this time should be taken as a potentially interesting effect, but one that is in no way proven. Whether or not 3-space may be directly detected is however not of key importance to the rest of this thesis, which is primarily focused on gravitational phenomena. Whilst there is a relationship between the reported effect and these gravitational phenomena, particularly in how D3ST is constructed, whether or not direct detection is possible does not impact later sections.

2.6 Emergent Quantum Gravity

This theory also allows for a quantum explanation of gravity. A unique generalisation of the Schrödinger equation allows a wave function associated with a mass m to respond to the velocity field $\mathbf{v}$ with respect to the 3-Space [24]. That is, the theory provides a candidate for a quantum explanation of gravity, and motion relative to the 3-space, or more directly, quantum foam. The generalised Schrödinger equation with a velocity field $\mathbf{v}$ is

$$i\hbar\left(\frac{\partial}{\partial t}+\boldsymbol{v}\cdot\nabla+\frac{1}{2}\nabla\cdot\boldsymbol{v}\right)\psi\left(\boldsymbol{r},t\right)=-\frac{\hbar^{2}}{2m}\nabla^{2}\psi\left(\boldsymbol{r},t\right). \tag{2.6.1}$$

Here $\boldsymbol{v}$ is the 3-Space velocity field, while $\psi\left(t\right)$ is the wave function. This may also be represented as the Hamiltonian

$$\hat{H}\left(t\right)=-\frac{\hbar^{2}}{2m}\nabla^{2}\psi\left(\boldsymbol{r},t\right)-i\hbar\left(\boldsymbol{v}\cdot\nabla+\frac{1}{2}\nabla\cdot\boldsymbol{v}\right). \tag{2.6.2}$$

This form includes the dynamics of the 3-space in the same manner as previously, except with an extra term of $\frac{1}{2}\nabla\cdot\boldsymbol{v}$ to maintain the Hermitian and symmetric properties of the operator, as well as its invariance.

From the above, the quantum wave packet propagates as

$$\boldsymbol{g}\equiv\frac{\mathrm{d}^{2}}{\mathrm{d}t^{2}}\left(\psi\left(t\right),\boldsymbol{r}\psi\left(t\right)\right)=\frac{\mathrm{D}\boldsymbol{v}}{\mathrm{D}t}+\left(\nabla\times\boldsymbol{v}\right)\times\boldsymbol{v}_{\mathrm{R}}+\ldots \tag{2.6.3}$$

where $\boldsymbol{v}_{\mathrm{R}}\equiv\boldsymbol{v}_{\mathrm{O}}-\boldsymbol{v}$, that is the velocity $\boldsymbol{v}_{\mathrm{R}}$ is the velocity of the object relative to the local 3-space. The last term in (2.6.3) accounts for the Lense-Thirring effect within the theory [24]. This explanation of gravity is not only a quantum account of gravity, but it is also an explanation of the equivalence principle from quantum systems.

A similar analysis can be performed with the Dirac equation as well. In this case the suggested form becomes

$$i\hbar\left(\frac{\partial}{\partial t}+\boldsymbol{v}\cdot\nabla+\frac{1}{2}\nabla\cdot\boldsymbol{v}\right)\psi=-i\hbar c\boldsymbol{\alpha}\cdot\nabla\psi+\boldsymbol{\beta}mc^2\psi. \tag{2.6.4}$$

Here $\boldsymbol{\alpha}$ and $\boldsymbol{\beta}$ are the Dirac matrices. This here allows the generalisation of the previous effect for relativistic phenomena. This can be solved in the same manner as before to find the propagation of the quantum wave packet as

$$\boldsymbol{g}\equiv\frac{\mathrm{D}\boldsymbol{v}}{\mathrm{D}t}+(\nabla\times\boldsymbol{v})\times\boldsymbol{v}_{\mathrm{R}}-\frac{1}{2}\frac{\boldsymbol{v}_{\mathrm{R}}}{1-(v_{\mathrm{R}}^2/c^2)}\frac{\mathrm{d}}{\mathrm{d}t}\left(\frac{v_{\mathrm{R}}^2}{c^2}\right)+\ldots \tag{2.6.5}$$

which generalises 2.6.3 and introduces a limit to the speed a wavepacket may travel relative to the 3-space to $|\boldsymbol{v}_R|<c$, and causes elliptical orbits to precess [29]. In effect, this defines the gravitational acceleration due to the 3-space within the theory, and has been derived from a quantum base. Of course, these two additional effects tend to zero in the case of zero vorticity and $|\boldsymbol{v}_{\mathrm{R}}|\ll c$ this tends towards the standard formulation.

In effect, this formulation represents a quantum gravitational theory, and one congruent with both Process Physics and D3ST at large. As well as being an interesting result within the theory, it is also used in justification for a number of key results. This includes results such as the equivalence of GPS systems within the theory [16], and predictions for Gravity Probe B [21]. In essence, the quantum formulation of gravity is an important part of the construction of D3ST [24, 29], and an important part of the formulation of this theory.

2.7 Maxwell-Hertz Equations

D3ST also includes alterations to the Maxwell equations to include reference to the 3-space velocity [27], given in the form

$$\left(\frac{\partial}{\partial t}+\boldsymbol{v}\cdot\nabla\right)\boldsymbol{H}=-\nabla\times\boldsymbol{E} \tag{2.7.1}$$

$$\frac{1}{c^2}\left(\frac{\partial}{\partial t}+\boldsymbol{v}\cdot\nabla\right)\boldsymbol{E}=\nabla\times\boldsymbol{H} \tag{2.7.2}$$

$$\nabla\cdot\boldsymbol{H}=0 \tag{2.7.3}$$

$$\nabla\cdot\boldsymbol{E}=0 \tag{2.7.4}$$

this being the source-free Maxwell equations as in equations 1.3.1–1.3.4 with the replacement $\frac{\partial}{\partial t}\rightarrow\frac{\partial}{\partial t}+\boldsymbol{v}\cdot\nabla$. This alteration of the equations is required for many of the elements of the theory to be self-consistent, notably including the speed of light. Their inclusion here is self-justified, and, far from being new physics, were actually proposed by Hertz [27]; they are merely the result of including such a velocity field to describe the behaviour of the geometry, and this impact will become more evident when discussing other phenomena. Of course, as would be expected, this will lead to alterations in the group velocity for light, with new plane wave solutions of

$$\begin{aligned}\boldsymbol{E}\left(\boldsymbol{r},t\right)&=\boldsymbol{E}_0\mathrm{e}^{\mathrm{i}(\boldsymbol{k}\cdot\boldsymbol{r}-\omega t)}\\ \boldsymbol{H}\left(\boldsymbol{r},t\right)&=\boldsymbol{H}_0\mathrm{e}^{\mathrm{i}(\boldsymbol{k}\cdot\boldsymbol{r}-\omega t)}\\ \omega\left(\boldsymbol{k},\boldsymbol{v}\right)&=\frac{|\boldsymbol{k}|}{\sqrt{\mu_0\epsilon_0}}+\boldsymbol{v}\cdot\boldsymbol{k}\end{aligned} \tag{2.7.5}$$

where $c^{-1}=\sqrt{\mu_0\epsilon_0}$. This means that the group velocity is

$$\boldsymbol{v}_{\text{group}}=\nabla_{\boldsymbol{k}}\omega\left(\boldsymbol{k},\boldsymbol{v}\right)=c\hat{\boldsymbol{k}}+\boldsymbol{v}. \tag{2.7.6}$$

This means that within D3ST that c is only the speed of light at rest to the 3-space, and is otherwise affected by the 3-space velocity $\mathbf{v}$. The previously discussed direct observations of the 3-space velocity may be justified by such self-consistent mechanics. In order for many gravitational phenomena to manifest within the theory, these changes are required. Much as with the quantum effects previously discussed,

these alterations are a key part of how this theory is structured.

2.8 Lensing

Lensing within D3ST is a result of the above alterations to Maxwell's equations, with the velocity of space only being c in respect to the 3-space reference frame. The time-dependent and homogeneous elements of the above as such lead to bending of light, and explain such phenomena within this theory. This behaviour is of course the same as seen within GR up to ρ_{DM} effects. Consider the minimisation of travel time problem with an object traveling at $\mathbf{v}_{\mathrm{R}}$, using equations 2.4.2 and 2.7.6, travel time may be minimised as [29]

$$\tau = \int_{s_1}^{s_2} \frac{\mathrm{d}s}{\left| c\hat{\boldsymbol{k}}\left(s\right) + \boldsymbol{v}\left(\boldsymbol{r}\left(s\right), t\left(s\right)\right)\right|} \left|\frac{\mathrm{d}\boldsymbol{r}}{\mathrm{d}s}\right| \tag{2.8.1}$$

from which the angle of reflection may be calculated as

$$\hat{\theta} = 2\frac{v^2}{c^2} = \frac{4GM_{\mathrm{Obs}}}{c^2 r} \tag{2.8.2}$$

where r is distance from the object, and $\hat{\beta}$ is the angle of deflection. In essence, this is the same as GR up to the same correction term included above, which as previously discussed would merely represent a change in the expected mass, or a change to the gravitational constant. This means that gravitational lensing could be seen as not only a key behaviour within this theory, but as a direct measure of the 3-space inflow velocity in the form

$$v = \sqrt{\frac{\hat{\theta}c^2}{2}} \tag{2.8.3}$$

and has been suggested to have uses in determining inflow velocities [29]. This has important implications for how D3ST may be generalised to include further dynamics, as will be discussed in chapter 3.

2.9 The Spherically Symmetric Case

One of the simplest solutions to the D3ST equation (equation 2.3.11) is the spherically symmetric case. More specifically, one may take the case for irrotational and time independent flows as to simplify the equations. Taking the case of spherically symmetric flows where one sets $\mathbf{v}(\mathbf{r},t) = v(r)\,\hat{r}$, $\nabla \times \mathbf{v} = 0$, the equation becomes, including the expanded 'dark matter' term [62]

$$\begin{aligned}(v')^2 + \frac{2vv'}{r} + vv'' + \alpha'\left(\frac{2v^2+4rvv'}{r^2}\right) + \\ \frac{\delta^2}{r^4}\left(v^2 + r^2v'\left(v'+3rv''\right) + rv\left(-2v' + r\left(v''+rv'''\right)\right)\right) = -4\pi G\rho.\end{aligned} \tag{2.9.1}$$

Using $\Phi = -\frac{v^2}{2}$, the above becomes

$$\left(\frac{\alpha'}{r^2}+\frac{\delta^2}{r^4}\right)\Phi + \left(\frac{2}{r}+\frac{\alpha'}{r}-\frac{\delta^2}{r^3}\right)\Phi' + \left(1+\frac{\delta^2}{2r^2}\right)\Phi'' + \frac{\delta^2}{2r}\Phi''' = -4\pi G\rho. \tag{2.9.2}$$

It is worth noting that in this theory, it is roughly linear in terms of v^2 or Φ for spacial components, and linear in v for time dependent components. This means that in solving problems outside spherical mass systems, use of Φ may be a useful and compact notation, despite it still being used to model the 3-space velocity. In order to investigate effects of the equation in this instance, the first method is to solve the equation for the case of $\alpha' = 0$, $\delta = 0$, giving

$$\frac{2}{r}\Phi' + \Phi'' = -4\pi G\rho \tag{2.9.3}$$

which is a standard form of the Laplacian form of NG. The above has solutions

$$\Phi(r) = \frac{-A}{r} + \frac{-G}{r}\int_0^r 4\pi s^2\rho(s)\,\mathrm{d}s - G\int_r^\infty 4\pi s\rho(s)\,\mathrm{d}s. \tag{2.9.4}$$

Here $A = 0$ by comparison with the solution in vector form, as $\nabla^2 \left(\frac{A}{r}\right) \neq 0$, and would create imaginary mass, hence not be a solution to the original form of the 3-space equation.

2.9.1 α-effects

The inclusion of α–effects from here can be achieved in a similar manner. Consider equation 2.9.1 with $\alpha' \neq 0$ and $\delta = 0$, giving

$$\frac{\alpha'}{r^2}\Phi + \left(\frac{2}{r} + \frac{\alpha'}{r}\right)\Phi' + \Phi'' = 4\pi G\rho \tag{2.9.5}$$

which may be written in a Poisson like form [75]

$$\frac{1}{r^2}\frac{\mathrm{d}}{\mathrm{d}r}\left(r^{2-\alpha'}\frac{\mathrm{d}}{\mathrm{d}r}\left(r^{\alpha'}\Phi\right)\right) = 4\pi G\rho. \tag{2.9.6}$$

This form demonstrates the altered Poisson form of the dynamics produced. This can be solved in the form

$$\begin{aligned}\Phi(r) = \frac{-A}{r} + \frac{-B}{r^{\alpha'}} + \frac{-G}{(1-\alpha')\,r}\int_0^r 4\pi s^2\rho(s)\,\mathrm{d}s + \\ \frac{-G}{(1-\alpha')\,r^{\alpha'}}\int_r^\infty 4\pi s^{1+\alpha'}\rho(s)\,\mathrm{d}s.\end{aligned} \tag{2.9.7}$$

As before $A = 0$ due to it not being a solution to the full 3-Space equation under the same parameters, while B acts as a 'dark matter' source of sorts [29]. This is generally referred to as a primordial black hole within D3ST. The total extra 'dark matter' beyond the B term may be written in the form [75]

$$\rho_{DM} = \frac{\alpha'}{4\pi G r^2}\frac{\mathrm{d}}{\mathrm{d}r}(r\Phi). \tag{2.9.8}$$

Which are all equivalent to Newtonian Gravity in the case where $\alpha' = 0$ [75]. The potential in (2.9.7) also creates a singularity at the center with gravitational

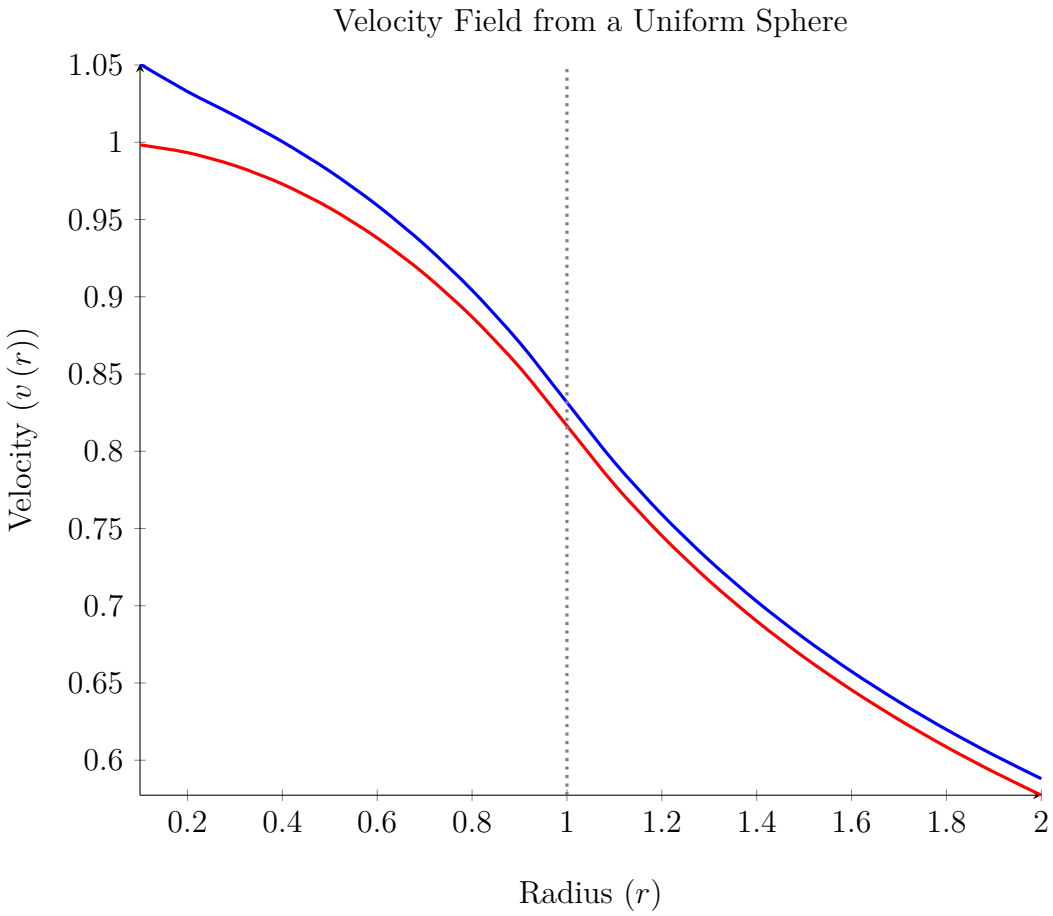

Figure 2.1: Graph of the 3-space velocity for NG (red, $\alpha = 0$) and D3ST (blue) for a uniform sphere. The dotted gray line represents the radius of the matter density. This has been done with from equations 2.9.11 and 2.9.12.

potential even in the case $\gamma = 0$ as

$$\Phi(r) = \frac{G}{(1-\alpha')\, r^{\alpha'}} \int_0^\infty 4\pi s^{1+\alpha'} \rho(s)\, \mathrm{d}s. \tag{2.9.9}$$

A simple case is the solution for a uniformly dense sphere with $\rho(r) = \rho_0$ for $0 \leq r < R$, where ρ_0 is a constant. Using the above form for $\Phi(r)$

$$\Phi(r) = \frac{-B}{r^{\alpha'}} + \frac{-G}{(1-\alpha')\, r} \int_0^r 4\pi s^2 \rho_0 \,\mathrm{d}s + \frac{-G}{(1-\alpha')\, r^{\alpha'}} \int_r^\infty 4\pi s^{1+\alpha'} \rho_0 \,\mathrm{d}s \tag{2.9.10}$$

which for a sphere with finite radius R this becomes a gravitational potential of

the form

$$\Phi(r) = \frac{-B}{r^{\alpha'}} + \frac{-4\pi G\rho_0 r^2}{3(1-\alpha')} + \frac{-4\pi G\rho_0\left(R^{2+\alpha'} - r^{2+\alpha'}\right)}{(2+\alpha')(1-\alpha')r^{\alpha'}} \tag{2.9.11}$$

which outside the sphere becomes

$$\Phi(r) = \frac{-B}{r^{\alpha'}} + \frac{-GM}{(1-\alpha')r}. \tag{2.9.12}$$

For $B = 0$ and outside the mass M, this is essentially the same form as Newtonian Gravity with a small extra mass as previously. This system has been used to produce figure 2.1, which graphs the above's inflow velocity $v(r)$ to demonstrate its effects in the case $\alpha \neq 0$ and $\delta = 0$. Note how the 3-space velocity increases as r approaches zero in the $\alpha \neq 0$ case. This is the manifestation of the dark matter effect, and for the above form at exactly $r = 0$, the 3-space velocity will go to infinite. Here it is also worth noting that the change in mass caused by α in the previous equation is

$$\frac{M}{(1-\alpha')} - M \approx \alpha' M. \tag{2.9.13}$$

This here is considered the total dark matter from α effects alone. Where using $\alpha \approx 1/137 = 7.30 \times 10^{-3}$ gives this to be a 3.60% change in mass for the exact equation and 3.74% for the approximate one. This mass difference would be built into measurements using other theories and offers no change to the observable result. The main difference in the gravitational potential that occurs in this spherical case is to do with the interior of a system.

2.9.2 δ-effects

In the case of $\alpha' \neq 0$ and $\delta \neq 0$, the equation again becomes

$$\left(\frac{\alpha'}{r^2}+\frac{\delta^2}{r^4}\right)\Phi+\left(\frac{2}{r}+\frac{\alpha'}{r}-\frac{\delta^2}{r^3}\right)\Phi'+\left(1+\frac{\delta^2}{2r^2}\right)\Phi''+\frac{\delta^2}{2r}\Phi'''=-4\pi G\rho. \quad (2.9.14)$$

At this time there are no known solutions to the equation in the case of $\rho \neq 0$ [62, 108], there are however solutions for where $\rho = 0$, here given as

$$\begin{aligned}
\Phi_1 &= \frac{1}{r} \\
\Phi_2 &= \frac{\delta^2\left({}_1F_1\left(\frac{-1}{2}+\frac{\alpha'}{2};\frac{-1}{2};\frac{-r^2}{\delta^2}\right)-1\right)}{r\left(2\alpha'-2\right)} \\
\Phi_3 &= \frac{2^{\alpha'}\sqrt{\pi}}{3r}\left(\frac{3\delta^2\left(\left({}_1F_1\left(\frac{-1}{2}+\frac{\alpha'}{2};\frac{-1}{2};\frac{-r^2}{\delta^2}\right)-1\right)\right)}{r\left(2\alpha'-2\right)\Gamma\left(1/2-\frac{\alpha'}{2}\right)}-\right. \\
&\quad \left.\frac{r^3\,{}_1F_1\left(1+\frac{\alpha'}{2};\frac{5}{2};\frac{-r^2}{\delta^2}\right)}{\delta\Gamma\left(-\alpha'/2\right)}\right).
\end{aligned} \quad (2.9.15)$$

Here ${}_1F_1\left(a;b;z\right)$ represents the confluent hypergeometric functions, which are defined as

$$M\left(a,b,z\right)\equiv {}_1F_1\left(a;b;z\right)=\sum_{n=0}^{\infty}\frac{\left(a_i\right)_n}{\left(b_i\right)_n}\frac{z^n}{n!} \quad (2.9.16)$$

with $\left(x\right)_n$ being the Pochhamme symbol defined as

$$\left(x\right)_n\equiv\begin{cases}1, & n=0\\ x\left(x+1\right)\ldots\left(x+n-1\right), & n>0\end{cases}. \quad (2.9.17)$$

The full solutions of this form of the dynamical 3-space equation can be written as a linear sum of the three answers with constants, i.e.

$$\Phi\left(r\right)=A\Phi_1+B\Phi_2+C\Phi_3 \quad (2.9.18)$$

yet here, once again $A = 0$ for the same reasons as previously. This means that this can be represented in the more compact form

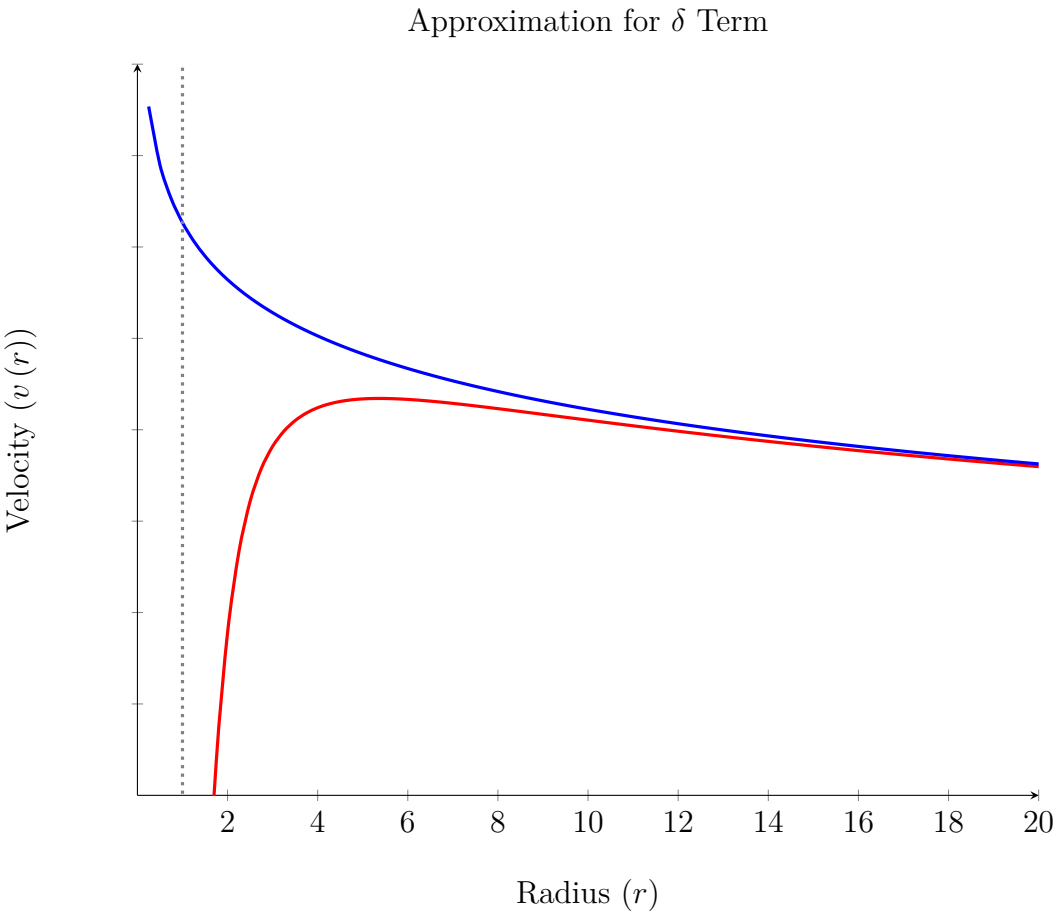

Figure 2.2: A plot of the approximation for $\delta \neq 0$ case (blue) with the actual solution (red), demonstrating how it behaves as $r \gg \delta$. Here the value of δ has been set to 1 and is represented by a vertical gray dotted line. Note that $v(r)$ for the exact case goes to zero at the origin.

$$\begin{aligned}\Phi(r) = &-\frac{B(1-C)}{r}\left(M\left(\frac{-1}{2}+\frac{\alpha'}{2},\frac{-1}{2},\frac{-r^2}{\delta^2}\right)-1\right)\\ &-BC\frac{2r^2(2\alpha'-2)\,\Gamma\left(1/2-\frac{\alpha'}{2}\right)M\left(1+\frac{\alpha'}{2},\frac{5}{2},\frac{-r^2}{\delta^2}\right)}{3\delta^3\Gamma\left(-\frac{\alpha'}{2}\right)}.\end{aligned} \tag{2.9.19}$$

The above can be approximated for large arguments of r in the form [62]

$$\Phi(r) \approx -\frac{2\sqrt{\pi}B}{\Gamma\left(-\frac{\alpha'}{2}\right)\delta^{1-\alpha'}r^{\alpha'}} - \frac{B(C-1)}{r} \tag{2.9.20}$$

or relabeling the constants

$$\Phi(r) \approx -\frac{B}{r^{\alpha'}} - \frac{C\delta^{1-\alpha'}}{r}. \tag{2.9.21}$$

A comparison between these forms and the form in equations 2.9.19 and 2.9.20 can be seen in figure 2.2. Here B has the same form as in the case for $\alpha \neq 0$, and we have a new free parameter term with C and the length scale δ. One issue that had existed previously within the theory was the case of cosmic filaments 2.10, where they did not have well defined inflows. One of the effects of the δ term, arguably its most important effect, is that it creates well defined inflows at the origin of spherical potentials, with all inflows tending to zero. This can be seen particularly well in figure 2.2 which shows the approximate solution going to infinite at the origin, and the exact solution going to 0. This is particularly important for the case of cosmic filaments as in the following section, as unlike spherical inflows, considerable issues are introduced without $\delta \neq 0$ for cylindrical inflows.

2.10 Cosmic Filaments

The Dynamical 3-Space equation may also be solved in the case of spherical symmetry and time independence, which has its own set of spacial inflow solutions. Consider the equation in terms of spherical coordinates [31, 14]

$$\frac{1}{r}\frac{\partial v}{\partial t} + \frac{\partial v'}{\partial t} + \frac{vv'}{r} + v'^2 + vv'' + \frac{\alpha'}{2}\frac{vv'}{r} = 0 \tag{2.10.1}$$

where here r is perpendicular to the z axis. This has static solutions with a free parameter μ of the form

$$v(r) = -\frac{\mu}{r^{\alpha'/4}} \tag{2.10.2}$$

and hence gravitational acceleration of

$$g(r) = -\frac{\alpha'\mu^2}{4r^{1+\alpha'/2}}. \tag{2.10.3}$$

This form here causes some issues however. Considering the divergence form of the above

$$\int \nabla \cdot \boldsymbol{g}\, \mathrm{d}V = \int \boldsymbol{g} \cdot \mathrm{d}\boldsymbol{A} = \frac{\alpha'\mu^2\theta d}{4}\left(\frac{1}{R_1^{\alpha'/2}} - \frac{1}{R_2^{\alpha'/2}}\right) \tag{2.10.4}$$

which requires and suggests that there must exist some $R_1 > 0$ outside the filament axis itself. This problem was used as a partial justification for the introduction of the δ term which allows such solutions to be well behaved towards the origin. In this instance, the $\delta \neq 0$ form of this equation is [62]

$$v(r)^2 = v_0^2 \left(\frac{r}{\delta}\right)^2 \; M\left[1 + \frac{\alpha'}{4}, 2, -\frac{1}{2}\left(\frac{r}{\delta}\right)^2\right] \tag{2.10.5}$$

which is well behaved towards the origin, unlike the $\delta \neq 0$ form. This also includes a gravitational acceleration of

$$g(r) \sim \frac{1}{r^{1+\alpha'/2}} \tag{2.10.6}$$

for $r \gg \delta$ and otherwise behaves the same as the previous solution. In effect, the only difference is the behaviour on scales of r near δ. The presence of the δ term again regulates solutions as $r \to 0$ such that $v(r) \to 0$. That is, the δ–dynamics of the theory regulate the behaviour of inflows near their origin, which has important implications for these particular dynamics. At this time however, no solutions exist to be able to determine the scale of δ itself. Beyond being on a small enough scale to not impact gravitational effects currently observed, the length is otherwise left undetermined.

2.11 Dark Matter-Like Effects

As previously noted this theory contains a number of non-Newtonian results, which here are broadly termed 'dark matter' effects. This is not meant to represent actual dark matter, that is, non-baryonic matter. Rather, these terms are meant to represent gravitational effects that are predicted within the theory that would otherwise be misattributed to such non-baryonic matter. Consider Gauss' form of gravity

$$\nabla \cdot \boldsymbol{g} = -4\pi G\rho. \tag{2.11.1}$$

Any additional effects that are not predicted by NG would be placed in the ρ term when analysing gravitational fields, and as such we can consider the form previously given as

$$\nabla \cdot \boldsymbol{g} = -4\pi G\left(\rho + \rho_{\mathrm{DM}}\right). \tag{2.11.2}$$

It is for this reason that within this theory terms such as ρ_{DM} is used. For the most part however, there are effects within the theory that add small amounts of well defined extra mass, and this could either be considered as a change of the total mass, or as an alteration to the gravitational constant. Beyond these however there are some more significant contributions that are beyond these other effects, the two most important are termed as primordial black holes, and matter-like black holes; these coming from α and δ effects within the 3-space equation.

In cases where dark matter densities may not be found in other ways, they may be numerically calculated using iterative methods [75] by using the baryonic matter density ρ, and putting it through the non-Newtonian part of the matter density ρ_{DM} in the form of equation 2.3.12.

2.11.1 Primordial Black Holes

Consider the solutions to the spherical 3-space equation in section 2.9.1, which include a free parameter B. It has been suggested that these black holes may be the cause of the flat rotation curves of spiral galaxies [29, 30] due to the properties of gravitational accelerations caused by them. Consider equation 2.9.7 in the case of $A = 0$ and $M(r) = 0$, which gives

$$\Phi(r) = \frac{-B}{r^{\alpha'}} \tag{2.11.3}$$

which produces gravitational acceleration of

$$g(r) = -\frac{-B\alpha'}{r^{1+\alpha'}} \tag{2.11.4}$$

which are asymptotically flat up to a factor of α'. Defining apparent enclosed mass for analysis by a Newtonian theory as

$$M(r) = \frac{r^2 g}{G} \tag{2.11.5}$$

the above becomes, with a relabeled constant

$$M(r) = M_0 \left(\frac{r}{r_s}\right)^{1-\alpha'} \tag{2.11.6}$$

where r_s is defined by $M(r_s) = M_0$, which in turns returns a gravitational acceleration of

$$g(r) = \frac{GM_0}{r_s^{1-\alpha'} r^{1+\alpha'}}. \tag{2.11.7}$$

This form has a few key behaviours, notably the plot rotation curves that are observed and argued as the basis for dark matter as discussed in section 1.5. Equally, consider circular orbits which have the relation

$$\frac{V_{\text{circ}}^2}{r} = a \tag{2.11.8}$$

which from the above produces the form

$$V_{\text{circ}}(r) = \sqrt{\frac{GM_0}{r_{\text{s}}^{1-\alpha'} r^{\alpha'}}} \tag{2.11.9}$$

which is in effect flat due to the small magnitude of α', this being D3ST's original resolution to the Tully-Fisher relations [62]. Further work on this topic demonstrated that should there exist an acceleration where the Newtonian and non-Newtonian components of acceleration were of equal magnitude for all systems, and this was a constant for all systems, that the above would reduce to exactly the Tully-Fisher relation [62]. This was termed the g_0–hypothesis, and will be expanded in more details as the introduction to chapter 3, which focuses on refining the understanding of the above effect and improving it.

2.11.2 Matter-like Black Holes

By analogy with the above, consider the case with the approximation for $\delta \neq 0$ as in equation 2.9.21, which may be redefined as

$$M(r) = M_0 \left(1 + \left(\frac{r}{r_{\text{s}}}\right)^{1-\alpha'}\right) \tag{2.11.10}$$

where $M(r_s) = 2M_0$. Figure 2.3 shows a log-log plot of the apparent enclosed mass as found from 2.3 with $M_0 = 1$, graphing in r/r_s, demonstrating the change seen. Figure 2.3 shows how this in effect would look for a galactic system. At the switching distance r_{s} it changes from the flat regime to the linearly increasing one. This becomes more apparent at higher length scales, particularly after the switching distance r_s. Here it is important to note that this apparent increase in mass effect is caused entirely by the primordial black hole within this example, and not a baryonic matter density.

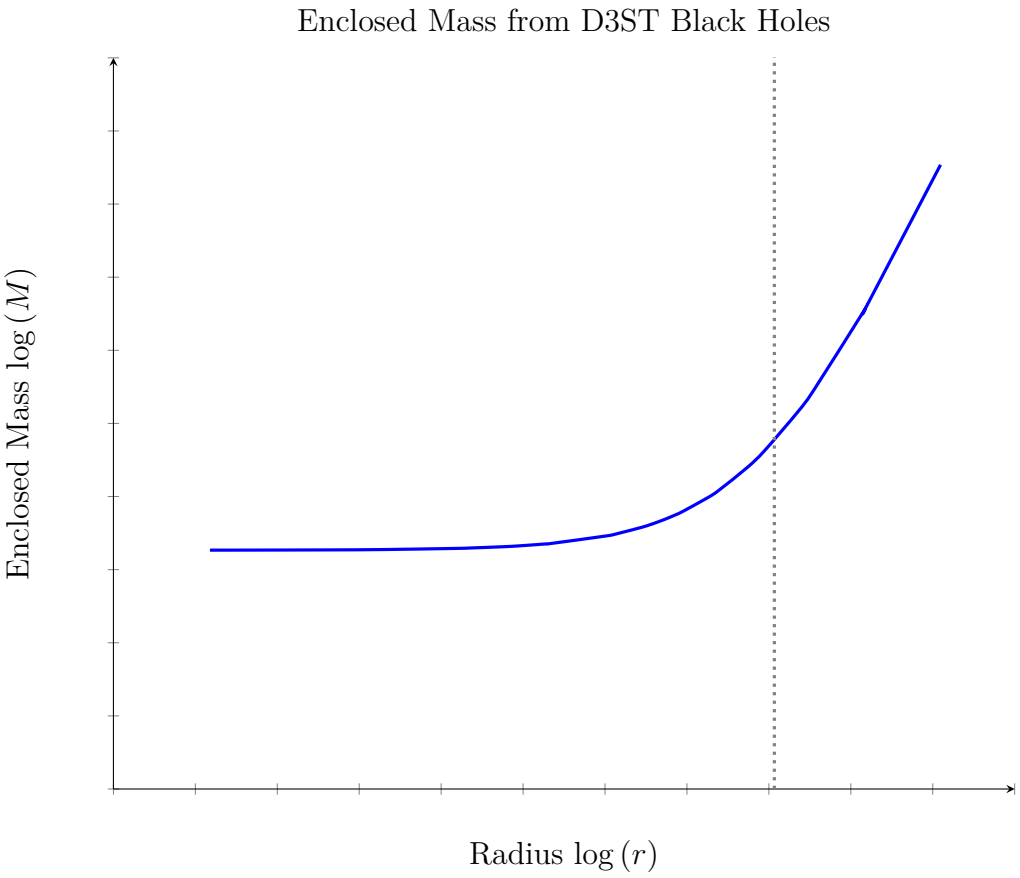

Figure 2.3: This plot has been produced from equation 2.11.10. Here showing the switching behaviour caused by the length scale r_s, which is represented by a vertical dotted line.

2.11.3 Enclosed Matter Parametrisation and Srg. A*

This particular form has also been compared to the motions of stars in the galactic core [14, 62]. The two parameters in (2.11.10) can also be used to predict the asymptotic velocity in spiral galaxy rotation curves by using equation (2.11.8)

$$V_{\text{circ}}^2(r) = GM_0 \left(\frac{r_s}{r}\right)^{\alpha'} \frac{1}{r_s} \approx \frac{GM_0}{r_s}. \tag{2.11.11}$$

Which is again, the form predicted by the BTFR, as previously noted. For later comparison with chapter 3, a previous analysis of this system using data from the star orbits about Srg A* has been used to determine an apparent enclosed mass toward the center of the galaxy [94, 14, 62]. Figure 2.4 shows this data and using

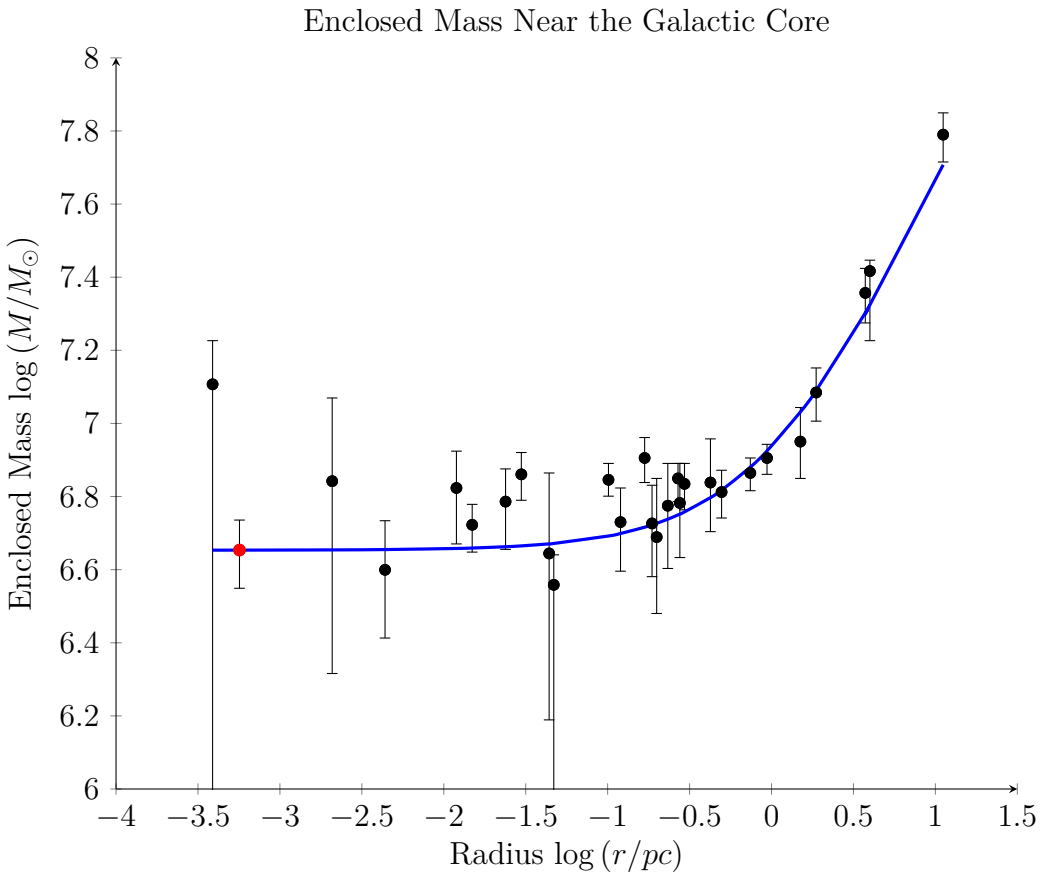

Figure 2.4: The enclosed mass parameterisation around SrgA* and nearby stars. Here using $r_s = 1.08$ pc and $M_0 = 4.5 \times 10^6 M_\odot$ and data from [48].

the parametrisation as in equation 2.11.10 a best fit can be made, here shown in blue. Here the red point represents an added point showing the data point found from S2 from [48] which has $M_0 = (4.5 \pm 0.4) \times 10^6 M_\odot$ and this is assumed to be the value of the mass M_0 under this analysis. The other data has been scaled by 2 as compared to the original data in [94], which had already been scaled to fit better with their model. Originally, the best fit here was $r_s = 1.33$ pc [14, 62], while a newer analysis by Rothall [108] using the replacement $\alpha \to \pi^2\alpha$ reanalysis found $r_s = 1.08$ pc. Using 2.11.11, the asymptotic circular velocity is $V_{\text{circ}} = 120$ km s^{-1} by the old analysis, and $V_{\text{circ}} = 135$ km s^{-1} by the new one. These differ to the values given in [62] and [108] due keeping the values of α and δ constant in the calculation. Both of these are considerably less than the $V_{\text{circ}} = 254 \pm 16\text{km} \cdot \text{s}^{-1}$ observed [105]; the observed value of r_s would be 0.300 pc. This could have a number of causes,

and has been identified as a problem previously [62, 108].

Using the form of 2.11.10 and 2.11.10 can also be used to give the gravitational potential of the system in terms of these parameters

$$\Phi(r) = -\frac{2M_0 r_{\mathrm{s}}^{\alpha'-1}}{\alpha r^{\alpha'}} - \frac{GM_0}{r}. \tag{2.11.12}$$

Whilst the dark matter density may be calculated with the δ term, for all functional systems the impact of this term is negligible, and as such it is generally better to take approximations in the case of $\delta \approx 0$. Whilst the δ term is required for matter-like black holes to exist within the theory, the inclusion of such in the final results merely complicates the expressions, and unlike $\alpha \neq 0$ effects, it does not change the predictions of the theory. In any case, taking this approximation produces the following form

$$\rho_{\mathrm{DM}}(r) \approx \frac{M_0(1-\alpha')}{4G\pi r_{\mathrm{s}}^{1-\alpha'} r^{2+\alpha'}} \tag{2.11.13}$$

Which falls off in the same manner as observed dark matter density does of the form $g^{-1} \sim r^{2+\alpha'}$ as has been observed [13].

2.12 Expanding Solutions

There exists a solution to the 3-space equation in the absence of matter density with a Hubble-solution [29]. This can be found using the spherically symmetric case with $\delta = 0$ using 2.9.5 with the centreless flow $v(r) = H(t)\, r$ giving the form

$$\dot{H} + \left(1 + \frac{\alpha'}{4}\right) H^2 = 0. \tag{2.12.1}$$

Here note that as the equation is linear in terms of v in this instance, v was preferred to Φ. Here $\dot{H}$ is the time derivative of H. In the usual manner the scale factor $R(t)$ may be introduced as $H(t) = \dot{R}(t)/R(t)$. In terms of scale factor, this equation is [108]

$$4R\ddot{R} + 2\alpha'\dot{R}^2 = \frac{-16}{3}\pi G R^2 \rho. \tag{2.12.2}$$

This being a kind of Friedmann equation for D3ST. These equations have solutions for $H(t)$ of

$$H(t) = \frac{1}{(1+\alpha'/2)\,t} = H_0 \frac{t_0}{t} \tag{2.12.3}$$

with $R(t)$ being found to be

$$R(t) = R_0 \left(\frac{t}{t_0}\right)^{1/(1+\alpha'/2)} \tag{2.12.4}$$

with definitions $H_0 \equiv H(t_0)$ and $R_0 \equiv R(t_0)$. This demonstrates that within D3ST the universe expands with a centreless flow at a near linear rate without the need for introducing dark matter or dark energy. This has been shown to be in agreement with observations [30]. This may also be expressed as

$$t(a) = t_0 \left(\frac{a}{a_0}\right)^{\alpha'/2}. \tag{2.12.5}$$

Rothall [108] demonstrated that the above equations contain a very rapid inflation epoch, with a singularity at $t = 0$. This presents a possible emergent solution to the Horizon Problem, as this inflation is inherent to the structure and form of the equations. That is, D3ST offers an inflation solution to the Horizon Problem, something that was expected from the understanding of the problem [54].

As demonstrated by Cahill [29], it is possible to find a solution for the case of non-zero energy density. This can be done by introducing energy density in the form

$$\rho(\boldsymbol{r}, t) = \frac{\rho_{\mathrm{m}}}{a(t)^3} + \frac{\rho_{\mathrm{r}}}{a(t)^4} + \Lambda. \tag{2.12.6}$$

Where here ρ_{m} is the matter density, ρ_{r} is radiation and Λ is a cosmological constant. It is argued that this Λ is unnecessary. Using this (Spherical 3DST) becomes [29]

$$\frac{\ddot{R}}{R}+\frac{\alpha'}{2}\frac{\dot{R}^2}{R^2}=-\frac{4\pi G}{3}\left(\frac{\rho_{\mathrm{m}}}{a^3}+\frac{\rho_{\mathrm{r}}}{a^4}+\Lambda\right) \tag{2.12.7}$$

giving

$$\dot{R}^2=\frac{8\pi G}{3}\left(\frac{\rho_{\mathrm{m}}}{R}+\frac{\rho_{\mathrm{r}}}{R^2}+\Lambda R^2\right)-\alpha'\int\frac{\dot{R}^2}{R}\,\mathrm{d}R. \tag{2.12.8}$$

This has the solution

$$\dot{R}^2=\frac{8\pi G}{3}\left(\frac{\rho_{\mathrm{m}}}{(1-\alpha')\,a}+\frac{\rho_{\mathrm{r}}}{(1-\alpha'/2)\,R^2}+\frac{\Lambda R^2}{(1+\alpha'/2)}+bR^{-\alpha'}\right) \tag{2.12.9}$$

where b is a constant of integration. This can be expressed as

$$\begin{aligned}t\,(R)=&\sqrt{\frac{3}{8\pi G}}\int_{R_0}^{R}\mathrm{d}R\left(\frac{\rho_{\mathrm{m}}}{(1-\alpha')\,R}+\frac{\rho_{\mathrm{r}}}{(1-\alpha'/2)\,R^2}+\right.\\&\left.\frac{\Lambda a^2}{(1+\alpha'/2)}+bR^{-\alpha'}\right)^{-1/2}.\end{aligned} \tag{2.12.10}$$

Which in the case of $\rho_{\mathrm{m}}=\rho_{\mathrm{r}}=0$ and $\Lambda=0$ becomes equation (2.12.5) as expected. In a universe of minimal energy density, being around 1 proton for every 4 cubic metres [11], it is expected that this final term b would dominate the expansion with the other terms being only minor, with there being no need for Λ to be non-zero. As shown by Cahill [29], forcing $b=0$ and curve fitting with only ρ_{m}, ρ_{r} and Λ leads to the standard model's interpretation of the expansion of the universe. This has been confirmed by Rothall [108]. The combination of the two Friedmann equations in effect under the standard model requires that $b=0$, hence ΛCDM cosmology's requirement of $\Lambda\neq 0$.

2.13 Curved Spacetime Formalism

Within the theory a spacetime metric can be induced in the same manner as GR, and the metric below is in fact the Painlevé–Gullstrand class of metrics (PG), of the form [95, 51, 67, 29]

$$c^2 \, \mathrm{d}\tau^2 = g_{\mu\nu} \, \mathrm{d}x^\mu \, \mathrm{d}x^\nu = c^2 \, \mathrm{d}t^2 - \left(\mathrm{d}\boldsymbol{r} - \boldsymbol{v}\left(\boldsymbol{r}, t\right) \, \mathrm{d}t\right)^2 . \tag{2.13.1}$$

This class of metrics is notable in that it allows the coordinates to be regular across the event horizon, unlike the case with Schwarzschild coordinates [73]. In fact, there is a natural sense in this metric, and one that will be unpacked later in this thesis 4, with the behaviour here and relation to the theory as a whole investigated.

We may also consider the behaviour in minimum time intervals

$$\tau = \int \mathrm{d}t \sqrt{g_{\mu\nu} \frac{\mathrm{d}x^\mu}{\mathrm{d}t} \frac{\mathrm{d}x^\nu}{\mathrm{d}t}} \tag{2.13.2}$$

this recovering the standard geodesic behaviour in the form

$$\tau\left[\mathbf{r}_0\right] = \int \mathrm{d}t \sqrt{1 - \frac{\boldsymbol{v}_{\mathrm{R}}^2}{c^2}}. \tag{2.13.3}$$

This formulation is potentially interesting due to how time is modeled within it, and for this reason it was chosen as an idea to be explored as part of this thesis.

Concluding Remarks

This chapter has outlined the currently investigated elements of D3ST with references to its Process Physics origins. D3ST is still a developing theory, and yet it has so far seen some success in dealing with the nature of the expansion of the universe, as well as success in dealing with dark matter on a universal scale. On a galactic scale, while the theory has scope for dealing with rotation curves of galaxies, this is an area that is as yet incomplete. Other dark matter effects, and smaller

scale sections of the theory have also been developed, but are largely outside the scope of this project. Part of D3ST of particular interest to the remainder to this thesis includes the nature of the equation's behaviour in the spherical case for modeling simple galactic scale dynamics, the expanding solutions of the equation, and the incomplete discussions of how covariant formalisms may be included within the theory.

Outline of the Thesis

The remainder of this thesis covers new research into D3ST, and the behaviour of a number of large scale relations. Chapter 3 begins by discussing some previous work on how dark matter distributions may be modeled and predicted within D3ST, first discussing and dissecting previous efforts within the theory in sections 3.1 and 3.1.1. This is done by first identifying the nature of the relationship between D3ST and MOND, and then identifying issues in the original formulation. From here, a more robust version of this previous work is discussed, and determined through comparison with another theory, MOND. From this, previous analyses performed are repeated with an emphasis on the predictive capabilities. Despite improvements upon previous work, and extending the theory's capabilities with a number of observed galactic scale relations, this chapter has failed to identify a potential source of the phenomena as such, and this is still considered a key area for future work. For this reason this effect has been broadly dubbed the g_0–conjecture within this theory.

Beyond this, chapter 4 then considers the relationship between D3ST and the GR. This is done with a particular focus on the PG class of metrics, and the similarities between the flow-like characteristics seen and the behaviour of D3ST. This both generalises previous work within the theory, and in turn allows a number of key results from the theory to be rederived from this basis. From here the nature of the expanding universe within the theory is reconsidered and discussed, in particular, the reasons for D3ST allowing for a uniformly expanding universe are discussed

and reconsidered through this lens. This thesis concludes with a short summary of the work as presented, as well as a discussion of potential future work proposed following.

Chapter 3

g_0–Conjecture

The g_0–conjecture was originally formulated as the g_0–hypothesis, which presented the idea of there existing a point at which the Newtonian and non-Newtonian components of gravitational acceleration within D3ST would be equal. This was initially done as a manner of setting the strength of free parameter black holes within D3ST. In effect, there appeared to exist some critical radius r_0 at which the Newtonian and non-Newtonian components seen within the theory may be equal for the case of a primordial black hole. This radius for each system would be set by a universal constant acceleration, denoted g_0. This form was used to set the strength of these primordial black holes, and the idea was tested, and used to make a no-free-parameters prediction for the M–σ relation with a simple model. Hence, this worked as a test of a simplified case, setting the asymptotically flat rotation curves with a parameter, though offering no reasoning as to why this would occur. Whilst it was consistent with observations in the cases considered, this was of course by design as D3ST naturally predicts asymptotically flat rotation curves from free parameters; this merely setting the value of those free parameters. This chapter begins with a description, then reanalysis of the results of the previous g_0–hypothesis work, notably discussing issues with the original formulation, as well as limitations of the results. Within this, the similar characteristics between this formulation and MOND were

identified, and the theory has been compared with MOND on this basis. From here, this comparison with MOND, along with other observations is used to generalise the dynamics of D3ST, and new analyses of the previous work is performed, finding that whilst the previous work was limited, it can be considered a limiting case of the more general formulation.

3.1 Background

In its original form, referred to as the g_0–hypothesis, the conjecture was framed as being related to using the free parameters within the $\delta \neq 0$ form of the theory in order to produce a self-consistent description of how the BTFR may occur [62]. The gravitational acceleration for a system with a significant free parameter B as in equation 2.11.3 has an acceleration of the form

$$g\left(r\right) = \frac{GM\left(r\right)}{r^2} + \frac{\alpha' B}{r^{1+\alpha'}}. \tag{3.1.1}$$

Here the first term is the standard Newtonian acceleration, while the second term is a free parameter black hole as discussed in 2.11.1. From the form it is clear that for small r the Newtonian term will dominate, but as $r \to \infty$ the non-Newtonian term will dominate. There exists some point r_0 at which these two terms will become equal, that is

$$g\left(r_0\right) = \frac{GM\left(r_0\right)}{r_0^2} = \frac{\alpha' B}{r_0^{1+\alpha'}}. \tag{3.1.2}$$

such that defining $2g_0 \equiv g\left(r_0\right)$ and $M_0 \equiv M\left(r_0\right)$ this can be written

$$2g_0 = \frac{GM_0}{r_0^2} + \frac{\alpha' B}{r_0^{1+\alpha'}} \tag{3.1.3}$$

which with the two terms equal means that

$$\frac{GM_0}{r_0^2} = g_0 \tag{3.1.4}$$

hence this can also be used to calculate the distance r_0 as

$$r_0 = \sqrt{\frac{GM}{g_0}}. \tag{3.1.5}$$

This in turn means we can calculate the parameter B in this instance as here this essentially represents the acceleration at which the two terms become equal. From this, the behaviour of this primordial black hole can be considered. B can be found as

$$\begin{aligned} B &= \frac{1}{\alpha'}\sqrt{(GM_0)^{1+\alpha'}\, g_0^{1-\alpha'}} \\ &\approx \frac{1}{\alpha'}\sqrt{GM_0 g_0}. \end{aligned} \tag{3.1.6}$$

Here, the above could be redefined such that $G^{1+\alpha'} \to G$, $g_0^{1-\alpha'} \to g_0$, etc., however for the sake of this analysis the approximation $1 \pm \alpha' \approx 0$ has been preferred for simplicity. It is worth noting that in order to include these effects overall, it has to be done from this step to avoid other issues occurring. This gives a form for gravitational acceleration to be

$$g\left(r\right) \approx \frac{GM}{r^2} + \frac{\sqrt{GMg_0}}{r}. \tag{3.1.7}$$

$$\frac{GM}{r^2} = \frac{\sqrt{GMg_0}}{r} \tag{3.1.8}$$

This result being exact in the limit $\alpha \to 0$. This can be used to find the circular velocity at large distance considering that $g = V_{\text{circ}}^2/r$ as

$$V_{\text{circ}}\left(r\right) = \sqrt{\frac{GM}{r} + \sqrt{GMg_0}}. \tag{3.1.9}$$

For large r the above becomes

$$V_{\text{circ}}(r) = \sqrt[4]{GMg_0} \tag{3.1.10}$$

which is the form of the BTFR [78]. The above form however only produces the BTFR in the case that g_0 is a constant, hence suggesting that g_0 is a universal constant. It is worth noting that the above formulation would identify, up to correction terms for α and δ effects, the constant g_0 as being the constant a_0 as reported within MOND [83, 78]. As these additional effects exist within D3ST however, g_0 is left as being considered a different constant for the sake later comparison. This in a sense is the concept behind the g_0–hypothesis as it was, that there exists an acceleration at which the Newtonian and non-Newtonian elements of the gravitational acceleration are of equal value, this being $2g_0$.

Of interest to later sections, the above formulation has the interesting effect of being set by mass enclosed within some critical radius r_0, yet this effect would exist within that radius. Equally, as this analysis has only been performed on static systems, how this may or may not respond to changes to the matter density, or mass contained within the critical radius are unknown. These remained as key issues to be considered from the original work.

It is also worth noting that with the α dynamics that there still remains a $g^{-1/2} \propto r^{\alpha'}$ component in the circular velocity when not approximating, yet for large r it is clear that the non-Newtonian term dominates. Consider some $r = 10^9 r_0$, for which $r^{\alpha'} = 2.11 r_0^{\alpha'}$. In effect, whilst this can have an impact, it is not large enough to justify for comparisons of asymptotic velocities on a galactic scale, but may be useful for comparisons on a much larger scales. What is interesting in this regard is that in effect these α dynamics have their key effects on very small and very large scales, but otherwise in the theory to this point act as little more than a bootstrapping for these primordial black holes. For this reason α dynamics will be largely neglected for this section with them approximated to $\alpha' \approx 0$, though they can be included in a fairly rudimentary manner.

3.1.1 Previous Results

The g_0–hypothesis in the above case was applied to data from the BTFR (section 1.7.1) and bulge-mass to black hole (section 1.7.3) relation, and from there used to create a simple prediction for the M–σ relation (section 1.7.2) with no free parameters. The data from [77, 62] was used to calculate $g_0 = (1.46 \pm 0.490) \times 10^{-10}$ m s^{-2}. Considering a second conjecture, that the bulge mass of a galaxy is related to the mass of its central black hole by the relation

$$M_\bullet = \eta M_{\text{bulge}} \tag{3.1.11}$$

and this being found from data to be $\log \eta = -2.77 \pm 0.280$ from [55, 62]. Using this pair of values a prediction of the M-σ relation could be produced. This was done in [62] by considering the Jeans equation [57] for a spherically symmetric system in the form

$$\langle V_r \rangle \frac{\partial \langle V_r \rangle}{\mathrm{d}r} = -\frac{\partial \Phi}{\partial r} - \frac{1}{\nu} \frac{\mathrm{d}\left(\nu \sigma^2\right)}{\mathrm{d}r} \tag{3.1.12}$$

where $\langle V_r \rangle$ is the expected velocity in r of particles and ν is the number density. As this is modeling a galaxy, it is reasonable to assume that there is no average velocity away or towards the origin and hence $\langle V_r \rangle = 0$, from which this can be solved, which associating ν with ρ becomes

$$\sigma^2 = \frac{1}{\rho} \int \rho g \, \mathrm{d}r. \tag{3.1.13}$$

From this, the values for g_0, η and a simple isothermal sphere model for matter density in the form

$$\rho\left(r\right) = \frac{\rho_0 R_0^2}{r^2} \tag{3.1.14}$$

which was used to find that

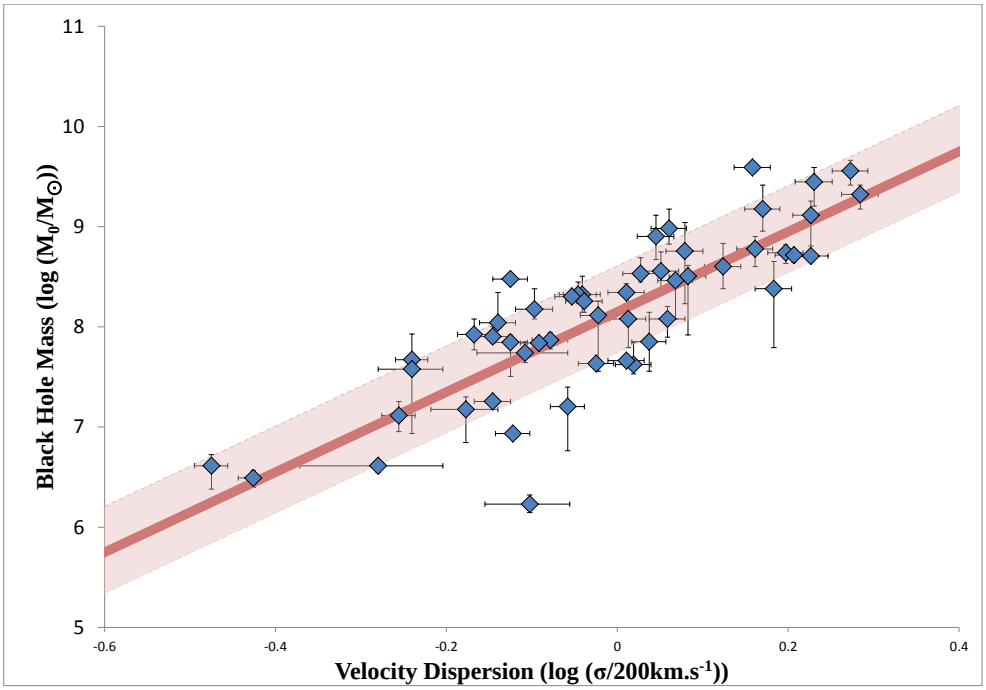

Figure 3.1: Predicted M–σ relation using the g_0–hypothesis, here the data points are observed systems, the red line is the prediction and the shaded area covers the error in the prediction, graph and result from [62].

$$\sigma\left(r\right) \approx \sqrt[4]{G\eta^{-1}M_{\text{bulge}}g_0}. \tag{3.1.15}$$

Using this, a predicted M-σ relationship was found as $\log\left(M_\bullet/M_\odot\right) = 8.12 \pm 0.433 + 4\log\left(\sigma/200\text{ km s}^{-1}\right)$ as compared to the observed relation of $\log\left(M_\bullet/M_\odot\right) = 8.12 \pm 0.08 + \left(4.24 \pm 0.41\right)\log\left(\sigma/200\text{ km s}^{-1}\right)$ [52, 62]. A plot of the result of this against observations can be seen as figure 3.1. This was of course a very simple model, and did not take into account more complicated dynamics of even roughly spherical galaxies. It did however demonstrate how the M–σ relationship could be modeled using the results of the g_0-hypothesis with the free parameters set by other observational data.

3.2 Similarities with MOND

To begin the reanalysis of the previous work, it seemed appropriate to compare this construction to MOND, due to the similar nature of the results at great distance. Particularly given the similar motivations of MOND, comparing these two theories more directly may be considered a useful method of generalising the g_0–hypothesis. Of course, it is worth noting the difference in many aspects of these theories however, including notably how gravity comes about within D3ST. In any case, consider again the interpolating functions used within MOND as in section 1.8.1, and notably the behaviour that

$$\mu\left(\frac{|\nabla\Phi|}{a_0}\right) \sim \begin{cases} 1, \ |\nabla\Phi| \gg a_0 \\ |\nabla\Phi|/a_0, \ |\nabla\Phi| \ll a_0 \\ \text{otherwise determined.} \end{cases} . \tag{3.2.1}$$

This is the same behaviour as seen in from the g_0–hypothesis. This suggests rewriting equation 3.1.7 in the form

$$\mu\left(\frac{g}{a_0}\right) g = \frac{GM}{r^2}. \tag{3.2.2}$$

That is, attempting to define the result in terms of a MOND-like interpolating function in the spherically symmetric case. Here the right hand side is a Newtonian inverse square law, while the left hand side is MOND's force law. The substitution $u = \frac{GM}{r^2}$, and $x = \frac{g}{a_0}$ allows the above to be defined as

$$\mu(x)\, x = u \tag{3.2.3}$$

from which we can write the same to equation 3.1.7 in the form

$$x = u + \sqrt{u} \tag{3.2.4}$$

and hence can be solved from the substitution

$$x = \mu(x)\, x + \sqrt{\mu(x)\, x}. \tag{3.2.5}$$

This has the solution for $\mu(x)$ of

$$\mu(x) = \frac{\sqrt{1+4x} - 1}{\sqrt{1+4x} + 1} \tag{3.2.6}$$

which has appropriate behaviour for an interpolating function. This interpolating function has been used and derived within the TeVeS form of MOND [7, 131]. This in effect is the result of having as a requirement that the Newtonian and non-Newtonian elements add linearly. This particular interpolating function however has been criticised when compared to the more standard interpolating functions as it switches slower; this property will be discussed more in section 3.4.1, which discusses interpolating functions and the choice of which in more depth.

It is at this point that the differences between the theories become apparent however. The first and most obvious here being that whilst within MOND, the non-Newtonian gravitational acceleration only applies to matter enclosed, the form presented as the g_0–hypothesis depends on mass at some radius r_0, and hence the acceleration from the primordial black hole does not depend on the structure of the matter density in the same manner. That is, the strength of the primordial black hole remains constant at all length scales up to α–effects as described in the previous section. This means that whilst MOND and the g_0–hypothesis for the D3ST would agree outside of matter systems in the deep MOND regime, the two theories will disagree within matter systems, it will cause issues for rotation curves for galaxies as a whole. This in particular is problematic as MOND in general provides a good description of rotation curves of galaxies [83, 79, 80], and having behaviour that is comparable only outside the systems themselves should be seen as somewhat of an issue. Equally, previous work discussing the nature of the centre of the galaxy

within D3ST had indeed confirmed that the strength of the black hole at the galactic centre was too large to confidently determine the strength of this primordial black hole directly [62]; this will be discussed in more detail in the next section.

3.3 Concerns with Original Formulation

As noted, D3ST with the g_0–hypothesis is capable of explaining asymptotically flat rotation curves, but at this time has no explanation for the behaviour of rotation curves within the matter system itself, particularly towards the centre of systems. For this reason it is worth reconsidering how D3ST in general deals with these phenomena.

Firstly consider the rotation curves of galaxies, which under NG, D3ST and MOND with the simple fitting function in equation 1.8.9, which have gravitational accelerations of

$$g = \frac{GM\left(r\right)}{r^2} \qquad \text{NG} \qquad (3.3.1)$$

$$g = \frac{GM\left(r\right)}{r^2} + \frac{\sqrt{GM_0 g_0}}{r} \qquad \text{D3ST} \qquad (3.3.2)$$

$$g = \frac{GM\left(r\right) + \sqrt{G^2 M\left(r\right)^2 + 4GM\left(r\right) a_0 r^2}}{2r^2} \qquad \text{MOND} \qquad (3.3.3)$$

which as $V_{\text{circ}} = \sqrt{rg}$ we get

$$V_{\text{circ}} = \sqrt{\frac{GM\left(r\right)}{r}} \qquad \text{NG} \qquad (3.3.4)$$

$$V_{\text{circ}} = \sqrt{\frac{GM\left(r\right)}{r} + \sqrt{GM_0 g_0}} \qquad \text{D3ST} \qquad (3.3.5)$$

$$V_{\text{circ}} = \sqrt{\frac{GM\left(r\right) + \sqrt{G^2 M\left(r\right)^2 + 4GM\left(r\right) a_0 r^2}}{2r}} \qquad \text{MOND} \qquad (3.3.6)$$

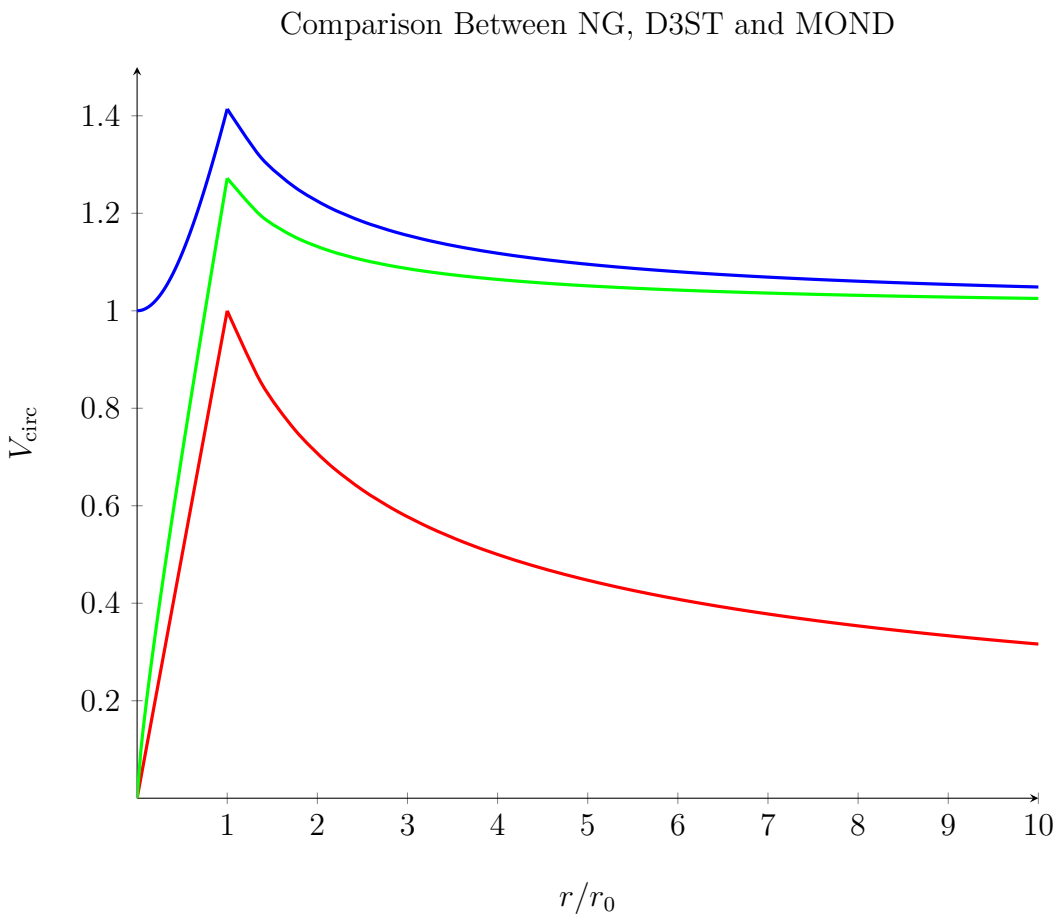

Figure 3.2: Comparison of Rotational Velocities between NG (red), D3ST (blue) and MOND (green). Here units have been chosen such that at $r/r_c = 1$ that $GM_0 = 1$ and $a_0 = g_0 = 1$. Of particular interest here is the behaviour of D3ST inside the sphere, and at great distance from the sphere. Keep in mind that this is for the interpolating function $\mu(x) = x/(1+x)$.

which from the forms alone have vastly different predictions, particularly near the origin as can be seen in figure 3.2. This shows a case of a uniformly dense sphere, but on a scale where g_0 is significant. Note that here $g_0 = a_0 = 1$ for the sake of comparison, with $GM(r_0) = 1$. Of particular note here is the behaviour of D3ST within the matter system and towards the origin. Here, unlike MOND or NG, the circular velocity does not go to zero, and instead tends to a value set entirely by the primordial black hole term. This behaviour occurs in both the g_0 and non-g_0 case, as the g_0–conjecture is merely setting the value for this term. This in effect is one of the larger issues with the g_0–hypothesis, the flat rotation curves at great

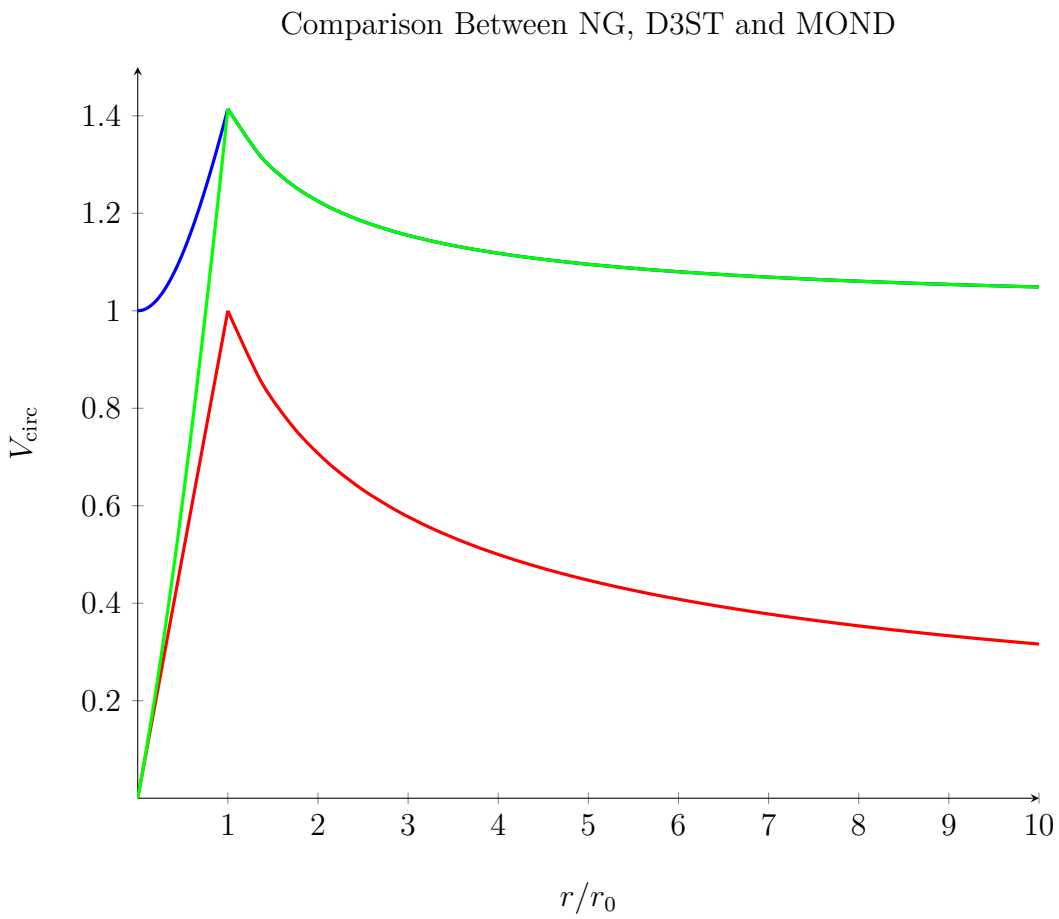

Figure 3.3: Comparison of Rotational Velocities between NG (red), D3ST (blue) and MOND (green). Here units have been chosen such that at $r/r_c = 1$ that $GM_0 = 1$ and $a_0 = g_0 = 1$. Of particular interest here is the behaviour of D3ST inside the sphere, and at great distance from the sphere. In this instance the MOND interpolating function is from equation 3.2.6.

distances remains as a linear addition to the Newtonian curve, yet this is not what is observed inside galaxies [100, 77, 38].

The above can also be repeated in the case of the MOND interpolating function from equation 3.2.6, which gives new MOND versions from the above of

$$g = \frac{GM(r)}{r^2} + \frac{\sqrt{GM(r)\,a_0}}{r} \tag{3.3.7}$$

$$V_{\text{circ}} = \sqrt{\frac{GM(r)}{r} + \sqrt{GM(r)\,g_0}} \tag{3.3.8}$$

which will match the behaviour of D3ST exactly outside of matter systems. As can be seen in figure 3.3, this other form sees D3ST and MOND match exactly outside matter systems. The difference here is in terms of the rate that this switch occurs. The interpolating function that can be derived from D3ST has been criticised for not matching data strongly due to the rate at which it switches from the NG to deep MOND regime [131].

The other related issue is related to a previous analysis presented in [14, 62] in relation to the galactic core, and the object SrgA*. Previous analyses of this object with this theory have centred around enclosed mass parameterisations as in 2.11.10, relating it to the free parameters for matter-like and primordial black holes. This parameterisation was elegant, but the results found left something to be desired. As noted in section 2.11.3, the fit value for the switching distance r_s was found to be 1.08 pc [108], which leads to an asymptotic circular velocity of $V_{\text{circ}} = 106$ km s^{-1}, which is less than half the $v_c = 254 \pm 16\text{km} \cdot \text{s}^{-1}$ observed [105]. This is a fairly significant result, in that it suggests that there are considerable issues here with the analysis. In fact, from figure 3.4, it is clear that what is seen could be produced from already known matter profiles near the centre of the galaxy, and a compact mass $M_0 = (4.5 \pm 0.4) \times 10^6 M_{\odot}$ [48] . This problem was identified originally [62], and it was suggested that the concern was that it would be difficult to remove actual matter density from the observed density data; this however brings into question whether this situation can actually be considered evidence of a primordial black hole effect at all. If it is impossible to separate the effect of matter densities and this effect, then the analysis itself tells us nothing useful, hence the considerably different result. Particularly considering, as noted, that the effect from primordial blackhole is otherwise not seen close to the centre in galactic rotation curves.

Alternatively, considering the mass functions as discussed in [58], density functions appear as

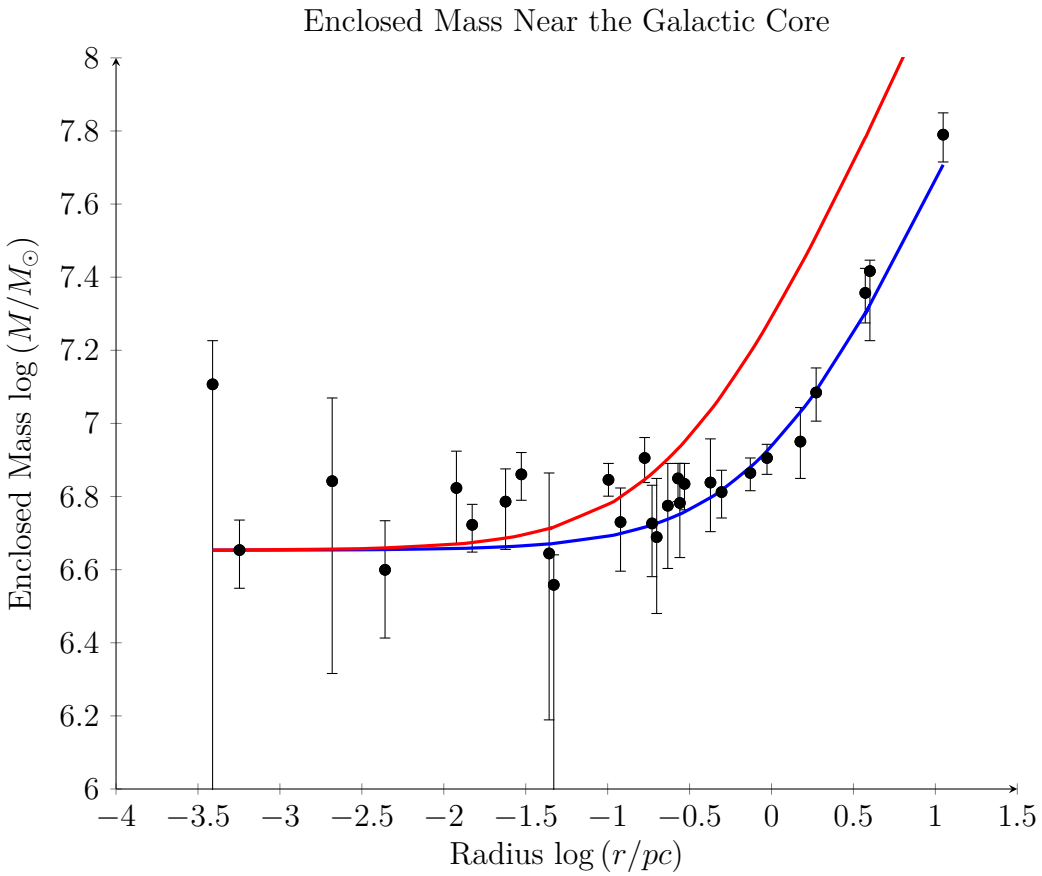

Figure 3.4: Apparent enclosed mass plot from the same data as figure 2.4, the fitted value for r_s of 1.08 pc in blue, with the value of r_s observed from the asymtotic velocity of the galaxy of 0.30 pc included in red.

$$\rho(r) \propto \left(\frac{r_b}{r}\right)^{2.4} \tag{3.3.9}$$

which including the mass of SrgA* itself would give a mass function of the form

$$M(r) = M_0 + Ar^{0.6} \tag{3.3.10}$$

which can of course be written in the exact same manner as equation 2.11.10

[Figure has been removed due to copyright restrictions; original can be found as figure 7 in [41].]

Figure 3.5: Orbit stars around the galactic core, including projected orbits demonstrating their elliptical nature, graphic from [41].

$$M(r) = M_0 \left(1 + \left(\frac{r}{r_s}\right)^{0.6}\right) \qquad \text{Baryonic Matter} \qquad (3.3.11)$$

$$M(r) = M_0 \left(1 + \left(\frac{r}{r_s}\right)^{1-\alpha'}\right). \qquad \text{Free Parameters} \qquad (3.3.12)$$

Equation 2.11.10 has been reproduced here to demonstrate the similar forms. Plotted on a log-log plot, the only differences here will be the slope, and as can be seen in figure 3.4, this data alone is not only not enough to differentiate, but it is fully expected that there will be baryonic matter within this region which cannot be easily removed from this analysis. Consider figure 3.4, where the red line is the observed value of r_s of 0.30. Here it is clear that the parameterisation used above produces a form that is not in agreement with the observations, which again, as with the full rotation curve, suggests that a constant value for this free parameter does not match observations. As such it appears that having a constant strength primordial black hole is not consistent with the observations, and hence some other effect may be occurring here.

Even with all this in mind however, SrgA* remains a candidate for a matter-like black hole under D3ST. Indeed, figure 3.5 shows the orbits of stars around the SrgA*, showing the elliptical nature of the orbits. Even if a constant primordial black hole potential were valid from other data, this alone would mean that SrgA* remains a candidate for a matter-like or matter black hole, with nothing presented here capable of differentiating between those two possibilities. That is, there is an object that appears as a dense mass here, the question in terms of D3ST is only if it is a matter or matter-like black hole. Furthermore, the only concern here is that

primordial black holes appear to not behave in a way consistent with observations, and hence a new model needs to be developed to explain observations within the theory. That is, the concern is with the constant nature of the primordial black hole within the theory, and whether or not there is another way of modeling this, as the inclusion of them as they are currently considered within D3ST is not consistent with the range of observations we currently have.

3.4 Reconstruction of the Conjecture

With these issues in mind, it is clear that modeling spiral galaxies by use of a primordial black hole as previously discussed has been unsuccessful to an extent, only being able to describe behaviour of velocity curves further out. For D3ST to be able to correctly model such systems, it requires that

- Non-Newtonian r^{-1} accelerations respond to enclosed matter density, rather than matter contained at some radius.
- The transition from Newtonian to non-Newtonian must be slower.

This in effect means that solutions with a clear linear addition of Newtonian and non-Newtonian components are not valid when compared to the observations. A possible method of dealing with these issues would be to consider what other effects that flowing space may have on an object. Consider a rudimentary unit analysis for the system of variables; $\left|\frac{\mathrm{D}\boldsymbol{v}}{\mathrm{D}t}\right|$, the change in the velocity field; $\boldsymbol{g}_{\mathrm{obs}}$ the gravitational acceleration observed; g_0, a constant of units acceleration. By collecting these in terms of unitless sets this gives; $(1/g_0)\,\frac{\mathrm{D}\boldsymbol{v}}{\mathrm{D}t}$ and $\boldsymbol{g}_{\mathrm{obs}}/g_0$. This means that such can be expressed as

$$\frac{\boldsymbol{g}_{\mathrm{obs}}}{g_0} = f\left(\frac{1}{g_0}\frac{\mathrm{D}\boldsymbol{v}}{\mathrm{D}t}\right) \tag{3.4.1}$$

where $f(x)$ is some function relating the two. Of course, the trivial solution

from this is

$$\frac{\boldsymbol{g}_{\rm obs}}{g_0} = \frac{1}{g_0}\frac{\mathrm{D}\boldsymbol{v}}{\mathrm{D}t} \tag{3.4.2}$$

which simply gives $\boldsymbol{g}_{\rm obs} = \frac{\mathrm{D}\boldsymbol{v}}{\mathrm{D}t}$, which is the standard form of acceleration from the 3-space velocity neglecting higher order effects. The other simple version that could be used is analogous to the original g_0–conjecture, this being

$$\frac{\boldsymbol{g}_{\rm obs}}{g_0} = \frac{1}{g_0}\frac{\mathrm{D}\boldsymbol{v}}{\mathrm{D}t} + \sqrt{\frac{g_0}{\left|\frac{\mathrm{D}\mathbf{v}}{\mathrm{D}t}\right|}}\frac{1}{g_0}\frac{\mathrm{D}\boldsymbol{v}}{\mathrm{D}t} \tag{3.4.3}$$

which in terms of $\boldsymbol{g}_{\rm obs}$ becomes

$$\boldsymbol{g}_{\rm obs} = \frac{\mathrm{D}\boldsymbol{v}}{\mathrm{D}t} + \sqrt{\frac{g_0}{\left|\frac{\mathrm{D}\boldsymbol{v}}{\mathrm{D}t}\right|}}\frac{\mathrm{D}\boldsymbol{v}}{\mathrm{D}t}. \tag{3.4.4}$$

This in effect relates the observed gravitational acceleration to the calculated velocity field from solely baryonic matter. As expected, by construction this will have the same behaviour as equation 3.1.7, except here this is written in vector form. Taking the example of a standard solution for a spherical mass $M(r)$, with $\alpha = 0$ and $\delta = 0$, this becomes

$$\boldsymbol{g}_{\rm obs} = -\hat{\boldsymbol{r}}\frac{GM(r)}{r^2} - \hat{\boldsymbol{r}}\frac{\sqrt{GM(r)\,g_0}}{r}. \tag{3.4.5}$$

This form solves one but not both of the issues noted at the start of this section; this acceleration responds only to matter enclosed, but it fails to have a slower switching phase. This form will of course produce the BTFR exactly as the previous formulation, though that is entirely by design. This is of course only one possible choice of the function $f(x)$, and one merely to compare to the previous formulation. The choice of $f(x)$ here however should be to better suit the observations, and hence agree with the second of the two points as well. This in effect, creating the D3ST form of MOND, and this function $f(x)$ is not only analogous to MOND, but can be directly compared, in the $\alpha = 0$ and $\delta = 0$ form of D3ST. Following a similar

procedure to section 3.2, considering that

$$\mu(x)\, x = u \tag{3.4.6}$$

and that $f(x)$ is defined in the form

$$x = f(u) \tag{3.4.7}$$

which hence becomes

$$\mu(x) = \frac{f^{-1}(x)}{x}. \tag{3.4.8}$$

This generating the more general result for comparison in the spherically symmetric case. The reverse of this is non-trivial however, and should be solved on a case by case basis. Here exists however a manner of comparing the velocity based D3ST and the action based AQUAL form of MOND, and one that may be useful for the remainder of this chapter.

3.4.1 The Function $f(x)$

As described above, whilst the forms previously discussed show the expected behaviours within the highly Newtonian and highly non-Newtonian domains, observational data shows some differences to this formulation. That is, the choice of the function of how this transition from the Newtonian to non-Newtonian regimes is not as trivial as a linear sum of the Newtonian and non-Newtonian contributions in the deep regimes of both. In order to find the most appropriate fitting function however the behaviour seen in the observations is required. Newer findings have found a correlation between observed acceleration and acceleration predicted solely by baryonic mass; this correlation being observed in cases where 'dark matter' dominates, as well as cases where baryonic matter dominates [80]. The relationship found in [80] is

Table 3.1: Fitting functions for $\mu(x)$

Function	$\mu(x)$	Colour on Figure 3.6
D3ST Original	$\frac{\sqrt{1+4x}-1}{\sqrt{1+4x}+1}$	Green
MOND Common	$\frac{x}{\sqrt{1+x^2}}$	Blue
MOND Simple	$\frac{x}{1+x}$	Red
Empirical Law [80]	No Analytical Function	Black

$$g_{\text{obs}} = \frac{g_{\text{bar}}}{1 - \mathrm{e}^{-\sqrt{g_{\text{bar}}/g_\dagger}}} \tag{3.4.9}$$

where g_{obs} is the observed acceleration, g_{bar} is the expected acceleration from baryonic mass and $\mathrm{g}_\dagger$ is a fitting parameter with units acceleration, this value being found to be $g_\dagger = 1.20 \times 10^{-10}\mathrm{m}\cdot\mathrm{s}^{-2}$. Here $\mathrm{g}_\dagger$ may be identified with g_0 and a_0, that is, an acceleration scale for the theory in question. Comparisons of the above with the MOND interpolating function $\mu(x)$ are not originally clear, as the above is non-trivial to solve for the MOND interpolating function. Other methods for performing such a comparison as such need to be used this thing case. First writing the above in terms of a dimensionless function, as with the other fitting functions

$$f(x) = \frac{x}{1 - \mathrm{e}^{-\sqrt{x}}} \tag{3.4.10}$$

the power expansion of this around $x = 0$ becomes for the first 5 terms becomes

$$f(x) = \sqrt{x} + \frac{x}{2} + \frac{x^{3/2}}{12} - \frac{x^{5/2}}{720} + \frac{x^{7/2}}{30240} + \mathcal{O}\left(x^{9/2}\right). \tag{3.4.11}$$

Whilst $\mu(x)$ may not be derived simply from the original function, this can

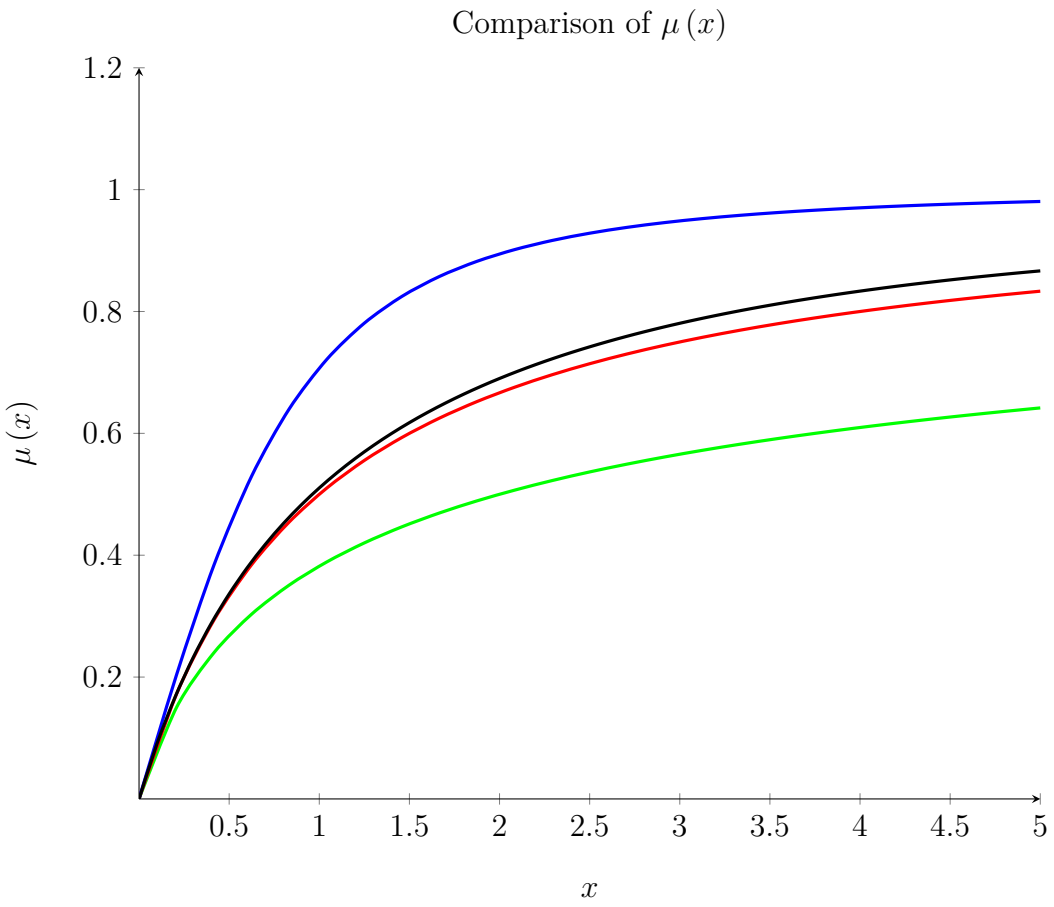

Figure 3.6: Comparison of $\mu(x)$ over the range $x \in [0, 5]$. The green function is the original form from D3ST, while the blue and red functions are the common and simple $\mu(x)$ respectively. Black is the numerically calculated version of the empirical law found by [80].

be used to graph an approximate version of it for comparison. In this instance a numerical version of $\mu(x)$ for empirical law was made from the first three terms of 3.4.11.

Figure 3.6 shows this comparison of some selected interpolating functions. The functions used for the comparison can be seen in table 3.1. The MOND interpolating function $\mu(x)$ was used for this comparison as the behaviour of $\mu(x)$ is clearer to illustrate by graphing. Whilst $f(x)$ displays switching properties, this switching is from $f(x) \sim x$ to $f(x) \sim \sqrt{x}$, the MOND interpolating function goes from $\mu(x) \sim 1$ to $f(x) \sim x$ for small x, hence a clearer visible change and better for demonstration purposes. Of course, the change in slope in a log-log plot from 1 to 1/2 would also

provide another method of making the change clearer, but still not as clear as in terms of $\mu(x)$.

From figure 3.6 the value of the simple MOND interpolating function can be seen. Whilst the one originally seen in the comparison with D3ST appears far below the other functions, and the common MOND interpolating function switches far quicker, the simple MOND interpolating function remains quite close to the value of the empirically found value, suggesting that it is not only a simple interpolating function for use, but that it may well be the best simple estimate of its behaviour. This may serve as a reason for this simpler fitting function performing better for some galaxies, notably the Milky Way as noted in [131].

On this basis, the following function is likely the best to be used for the time being

$$\mu(x) = \frac{x}{1+x} \tag{3.4.12}$$

in cases where $\mu(x)$ is required, while the function

$$f(x) = \frac{x}{1-\mathrm{e}^{-\sqrt{x}}} \tag{3.4.13}$$

in cases where the function $f(x)$ may be used. Of course, the nature of this functions means that even in cases where $f(x)$ is applicable, it may not be the ideal form to use. This will allow the interpolation to behave in the manner as observed, and hence should give a better fit for observations in cases where the observed function is not appropriate. Comparing the opposite form of the simple MOND interpolating in the form

$$f(x) = \frac{x+\sqrt{x^2+4x}}{2}. \tag{3.4.14}$$

the error caused by using this has a maxima at 4.68%, although this occurs around $x \approx 7$. Of course, for these fitting functions the issue with errors is when

they exist in this very range, as this is the switching range for MOND, but the overall error is quite minor compared to other interpolating functions. A family of functions could be constructed in the sense of

$$\mu(x) = \frac{x}{(1+x^n)^{1/n}} \tag{3.4.15}$$

as has been suggested by some authors [131], where here n controls the rate of switching seen in the theory. From this, a best fit with the empirical law can be found for n, although due to the different shapes of the functions this depends heavily upon the point at which they are compared, hence the 'best' fit can only truly be decided on a case by case basis. In any case though, values of n from 1.04–1.11 are good fits for $\mu(x) \in [1, 7]$. This however removes the single most valuable aspect of the $n = 1$ case, this being the simplicity in constructing analytical solutions. Hence the simple function will be the one used for the remainder of this chapter where this property is useful, while the empirically found function will be used where analytical solutions are less important.

3.4.2 Critical Radius

It is worth noting that in the limiting case for most matter systems, for example spherically symmetric systems as discussed in section 2.9. For a given matter distribution $M(r)$ outside which $M(r) = M$ for r greater than some critical radius, the above formulation reduces to that discussed in section 3.1 up to choice of $f(x)$. Equally, where $g(r) \ll g_0$ the results in this regime become identical. This being the reason that the original formulation worked in the sense that it did, at great distance outside a matter distribution, the results converge; that is, the comparison was largely being made in the highly non-Newtonian regime.

Also of interest is the point that the Newtonian and non-Newtonian components of the theory become identical. Assuming the case outside of a spherically symmetric

matter distribution, and using the simple MOND equivalent of $f(x)$, we have that

$$\frac{GM}{r_0^2} = \frac{-GM + \sqrt{G^2M^2 + 4GMg_0r_0^2}}{2r_0^2} \tag{3.4.16}$$

which solving for r_0 gives

$$r_0 = \sqrt{\frac{2GM}{g_0}}. \tag{3.4.17}$$

This being the replacement for the original form seen in equation 3.1.5. This can be done more generally in the form

$$g_{\mathrm{N}}(r_0) = g_{\mathrm{obs}}(r_0) - g_{\mathrm{bar}}(r_0) \tag{3.4.18}$$

which can also be stated in differential terms in $\boldsymbol{v}$ as

$$2\left|\frac{\mathrm{D}\boldsymbol{v}}{\mathrm{D}t}\right| = g_0 f\left(\frac{1}{g_0}\left|\frac{\mathrm{D}\boldsymbol{v}}{\mathrm{D}t}\right|\right). \tag{3.4.19}$$

The above version can be used more generally when considering a switching distance between matter systems themselves, and is not simply limited to just the behaviour of $f(x)$. This in turn allows the above to be useful in calculating this in a range of other circumstances. Whilst not overly useful in most circumstances, this above can give a good idea of the rate at which the switching occurs. That is, the above is useful in terms of demonstrating this switching effect, but outside of a discussion of the switching point itself, serves little function.

This can also be used to consider the acceleration at which they are equal. Of interest with the above result however is that the simple MOND interpolating function, as well as the one discussed by McGaugh, Lelli & Schombert [80], tend toward the acceleration that the two terms are equal as being g_0 rather than $2g_0$ as seen in the original formulation in section 3.1. This in turn might be suggesting something about the dynamics themselves may have led to this effect, though at

this time the impact itself is unknown. This does however suggest that the family of solutions to equation which result in $r_0 = \sqrt{2GM/g_0}$ may be important, noting that for spherically symmetric systems that

$$g_{\mathrm{N}}(r_0) = \frac{GM}{r_0^2} = \frac{g_0}{2} \tag{3.4.20}$$

for all such cases, and hence where the two contributions are equal this will remain the case. Indeed, the solution to the function discussion in McGaugh, Lelli & Schombert [80] in this instance is

$$r_0 = \frac{1}{\log 2}\sqrt{\frac{GM}{g_0}} \tag{3.4.21}$$

here noting that $\log 2 \approx 2^{-1/2}$, while we also know that the described relationship is empirical in nature. This in effect suggests that not only is the simple interpolating function a good fit for the remainder of this chapter, but that it may be a close approximation to the actual relationship. This in turn may be useful in determining the nature of why this occurs, regardless of theory used for initial analysis, and may offer some sense of future direction is how to examine how this effect may arise from the theory itself.

3.4.3 Apparent Enclosed Mass

Another important property of these switching functions, and new form of the conjecture in general is the apparent enclosed mass. The existence of dark matter is inferred from its effects on the universe around it, notably due to the effects it has on galactic dynamics as discussed in section 1.5. With this in mind, it is worth considering how the above changes predictions about apparent enclosed mass within D3ST. As an example, the rotation curve of the galaxy NGC3198 will be used. This particular galaxy has been chosen due to its previous use as an example for work in D3ST Rothall [108], as well as for its fairly typical rotation curve. The data

Table 3.2: The three different models, and enclosed mass.

Model	Enclosed Mass from $V(r)$ ($M(r)$)
Newtonian	$\frac{rV_{\text{circ}}^2(r)}{G}$
D3ST Before	$\frac{r}{G}\left(V_{\text{circ}}^2 - \sqrt{GM_0g_0}\right)$
D3ST After	$\frac{V(r)^4}{G\left(g_0 + V(r)^2/r\right)}$

used here however is of greater resolution than previously used within work on the theory, this new data coming from the THINGS survey [38]. From the rotation curve of NGC3198, apparent enclosed mass may be calculated using the various models discussed above. Consider three different models of gravitation from a galaxy as in table 3.2

Of course, the drastically lower amount of enclosed mass than expected from the original model towards the centre of a galaxy renders the 'D3ST before' model effectively useless here, and it will return extremely large negative values for enclosed mass. This can be demonstrated by comparing the expected curve of a galaxy to the fitted one, as in figure 3.7. The curve in the figure was produced using the original form of the g_0–hypothesis as discussed in section 3.1, using the $\alpha \neq 0$ formulation. Note that this fitting issue is not unique to the g_0–hypothesis work, and existed in all fitting of spiral galaxies with this free parameter within previous D3ST work. For this reason only the Newtonian and new D3ST models are included in figure 3.8.

Figure 3.8 demonstrates the drastic difference in total enclosed mass between the Newtonian and non-Newtonian models here, as would be expected. In this figure the red line represents the Newtonian enclosed mass, while the blue line represents the non-Newtonian enclosed mass with the new model used within D3ST. As can

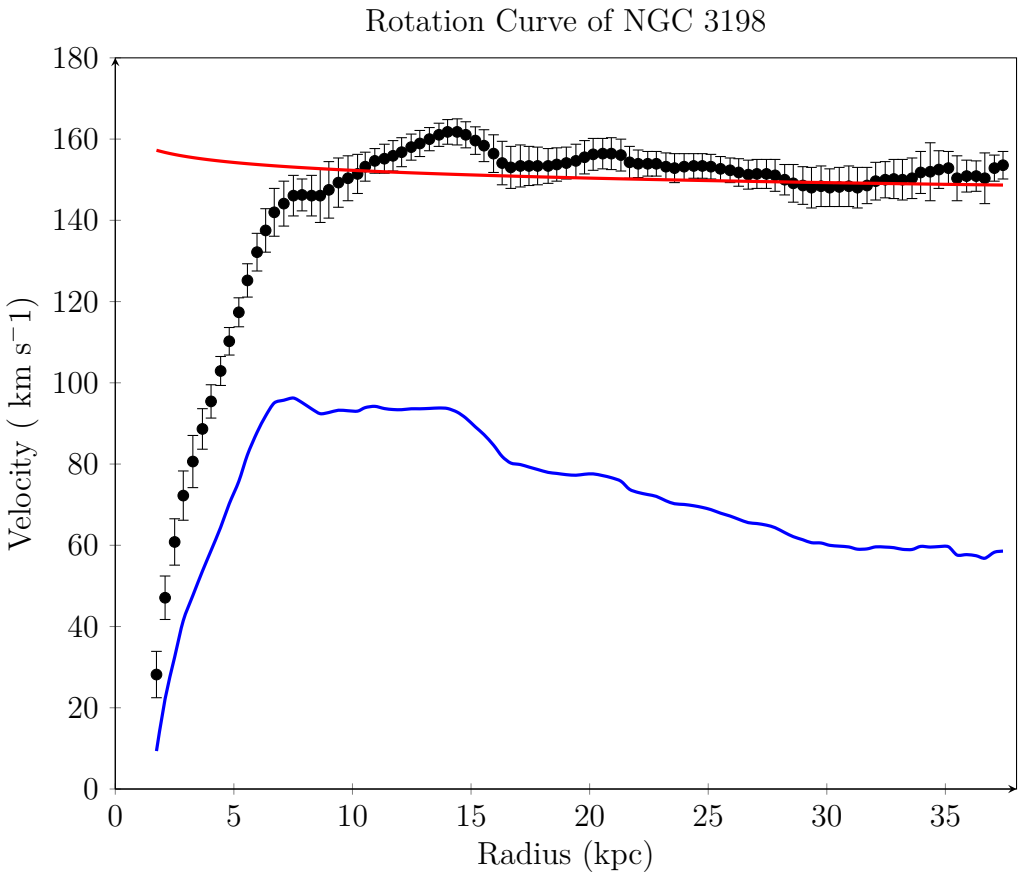

Figure 3.7: Example rotation curve fit with old modelling in D3ST to the galaxy NGC3198 with data from [38]. The red line is the fit from the original formulation of D3ST with $\alpha \neq 0$, while the blue line is the acceleration from solely baryonic matter with the new model.

be seen, the amount of mass required to generate the observed rotation curve is an order of magnitude less using the new form of the g_0–conjecture, this being the same effect as in MOND.

Within this representation, however, this is merely reproducing the effects seen within MOND within D3ST, and for this reason repeating large scale comparisons of rotations curves would serve limited purpose when specific analyses of these rotation curves with a similar theory already exist, and indeed the effectiveness of MOND fitting for such galaxies has been demonstrated at the large scale [80]. Indeed, through this comparison there exists limited need to investigate whether this form of D3ST can reproduce these results, as this has already been done up to the difference seen with α and δ effects, neither of which are of significant contribution here. Rather

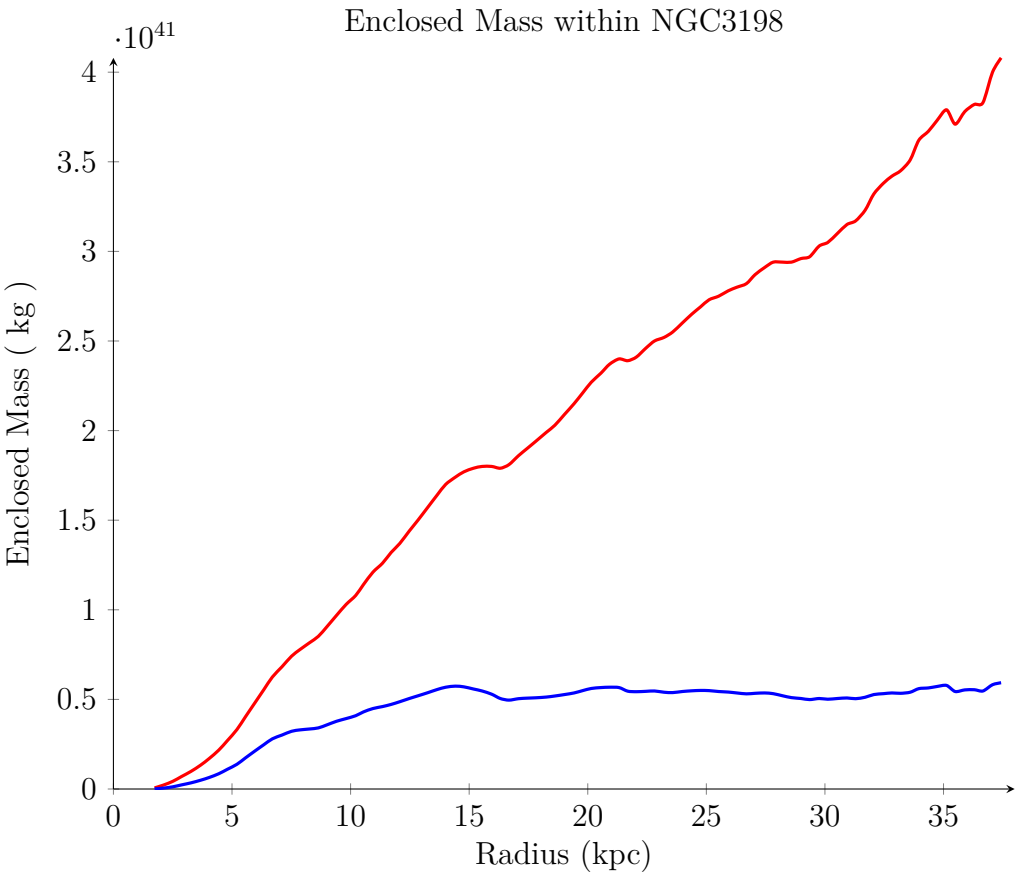

Figure 3.8: Enclosed mass as analysed with a Newtonian model (red) and the new model within D3ST (blue).

now attention turns to exactly how this works within wider D3ST.

3.4.4 Effective Dark Matter Density

The above of course leads to a question about how this will change the effective dark matter densities as discussed in section 2.11. In order to determine the effective dark matter distributions arising from the above, how dark matter is surveyed again needs to be considered. In effect, effective dark matter is matter beyond the observable matter when considering gravitational effects in terms of the gravitational acceleration. This means that taking equation 3.4.1 for the gravitational acceleration, the additional acceleration from non-baryonic sources may be defined as

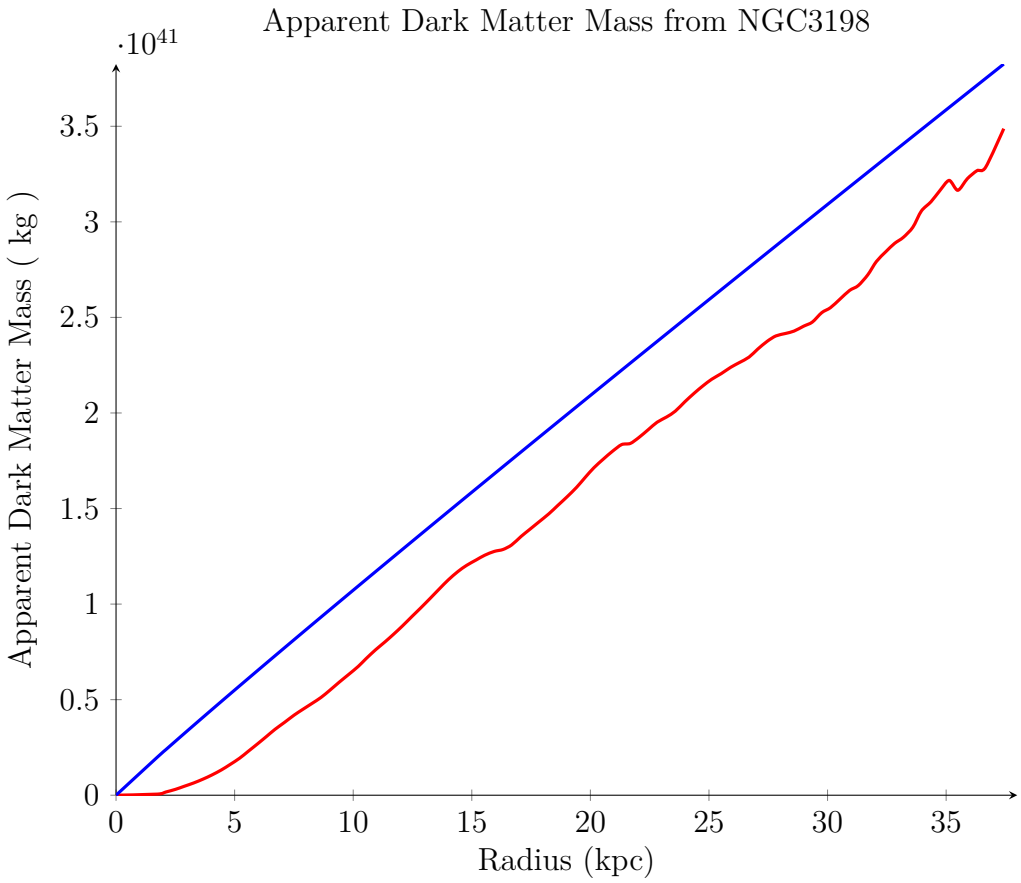

Figure 3.9: Comparison of effective 'dark matter' predictions between original g_0–hypothesis (blue), and MOND simple (red) for NGC3198 in terms of radius r in kpc, data for the rotation curve from [38].

$$g_{\text{obs}} - g_{\text{bar}} = g_0 f\left(\frac{1}{g_0}\left|\frac{\mathrm{D}\boldsymbol{v}}{\mathrm{D}t}\right|\right) - \left|\frac{\mathrm{D}\boldsymbol{v}}{\mathrm{D}t}\right| \tag{3.4.22}$$

up to vorticity and relativistic effects. This allowing the determination of expected dark matter distributions as analysed by different theories. The behaviour of the above depends heavily on the choice of $f(x)$ used. For example, for the function originally suggested in equation 3.4.3 this would become

$$g_{\text{obs}} - g_{\text{bar}} = \sqrt{\frac{g_0}{\left|\frac{\mathrm{D}\boldsymbol{v}}{\mathrm{D}t}\right|}}\frac{\mathrm{D}\boldsymbol{v}}{\mathrm{D}t} \tag{3.4.23}$$

that is, the non-Newtonian component in the acceleration alone. Of course, the switching behaviour seen in this as noted previously is different to what is observed.

The function discussed in McGaugh, Lelli & Schombert [80] becomes

$$g_{\text{obs}} - g_{\text{bar}} = \frac{1}{\mathrm{e}^{\sqrt{\left|\frac{\mathrm{D}\boldsymbol{v}}{\mathrm{D}t}\right|/g_0}} - 1} \frac{\mathrm{D}\boldsymbol{v}}{\mathrm{D}t}. \tag{3.4.24}$$

The simple MOND interpolating function here becomes

$$g_{\text{obs}} - g_{\text{bar}} = \frac{-1 + \sqrt{1 + 4g_0/\left|\frac{\mathrm{D}\boldsymbol{v}}{\mathrm{D}t}\right|}}{2} \frac{\mathrm{D}\boldsymbol{v}}{\mathrm{D}t}. \tag{3.4.25}$$

From this, the effective matter density can be found as done in section 2.11. Here, the key comparison is between the new function used within D3ST and what was previously used. Figure 3.9 shows this comparison. Of course, the old form used within D3ST was not responsive to enclosed mass, and hence appears near linear here, save for a slight curve due to the $r^{-\alpha'}$ factor. It also starts and remains at a higher mass, this caused by the difference near the centre of the galaxy, where the observed rotation curves show a near solid body rotation profile, as opposed to the flat curve originally expected within D3ST.

3.5 g_0–Conjecture and D3ST

With all this in mind, the question now is how this all fits into the rest of the theory. The first and most pressing concern is the nature of the behaviour already discussed. Whilst this is modeled up to here as relating observational gravity to predicted gravity, the actual meaning of this has not been explored. One possibility would be altering the gravitational acceleration from a velocity flow in the form, that is, changing equation 2.6.3 to become

$$\frac{\boldsymbol{g}}{g_0} = f\left(\frac{1}{g_0}\frac{\mathrm{D}\boldsymbol{v}}{\mathrm{D}t}\right) + \frac{1}{g_0}\left(\nabla \times \boldsymbol{v}\right) \times \boldsymbol{v}_R - \frac{1}{2g_0}\frac{\boldsymbol{v}_R}{1 - (\boldsymbol{v}_R^2/c^2)}\frac{\mathrm{d}}{\mathrm{d}t}\left(\frac{\boldsymbol{v}_R^2}{c^2}\right). \tag{3.5.1}$$

From here then the g_0–hypothesis can be restated in a new form as the g_0–conjecture. Here this can be stated as

> The gravitational acceleration caused by changes in the 3-space is some function in the material derivative of the 3-space, divided by a universal acceleration constant g_0.

with the previous equation being a possible statement of this. It is also worth noting that the requirement that the Newtonian and non-Newtonian components of the acceleration being equal at exactly g_0 could be an important constraint on this.

In any case, this formulation would however have large implication for lensing within the theory. Lensing is a result of refraction through changing velocity (as discussed in section 2.8), so a further acceleration from the same velocity field would not result in further lensing by current construction, and hence observations of dark matter from gravitational lensing [59, 130, 36] would not be explained by this effect. An alternative change would be to alter the 3-space equation to accommodate these effects in the same sense as MOND

$$\nabla \cdot \left(\mu \left(\frac{1}{g_0} \left| \frac{\mathrm{D}\boldsymbol{v}}{\mathrm{D}t} \right| \right) \frac{\mathrm{D}\boldsymbol{v}}{\mathrm{D}t} \right) = -4\pi G \left(\rho_{\mathrm{DM}} + \rho \right) \tag{3.5.2}$$

where here ρ_{DM} contains the α and δ terms as before. This in a sense would represent a D3ST version of MOND, but including other dynamics. Of course, when analysing observations in the standard manner, the difference of α' falls within standard modeling parameters, and hence may be neglected in most cases, unless specifically testing for α' dynamics.

This in a sense would be an interesting prospect to test, but still lacks a dynamical explanation for the effects. For the time being however this will be the form preferred. The other advantage of this form, at least for the time being, is that up to α and δ effects, the above theory is comparable with the AQUAL form of MOND, yet has lensing dynamics and relativistic effects. In essence, the above

would represent a MOND-like version of D3ST, with the additional effects such as lensing that are included from other parts of the theory. That is, it is in effect a flow-dynamic form of MOND, and not requiring other elements from theories such as TeVeS.

With this all considered however it is important to note that this does not represent a complete explanation of the phenomena being discussed, but rather a method of modeling it within D3ST. At this time there still does not exist a reason for how this comes about as part of the theory itself, although potential solutions for where this may come from have been presented in work of other theories, such as EG (see section 1.8.2), which presents a manner by which these acceleration scale effects may be caused by the entropy of the system. Whilst D3ST and EG represent significantly different theories, such potential explanations could be further expanded with further consideration of how Process Physics transitions into D3ST. Equally, the empirically observed relation that the Newtonian and non-Newtonian components are of equal strength at g_0 may also be part of a future explanation.

Concluding Remarks

This chapter has expanded previous work in the theory on the behaviour of free parameters, replacing it instead with a MOND-like modification of the 3-space equation. This in turn has solved a number of key issues previously arising out of both the free parameter description of spiral galaxies used within D3ST, as well as the set parameters as in the g_0–hypothesis. The utility of this within D3ST has been demonstrated through an exploration of various new effects that may be tested, as well as checking that select previous results remain as they had before. Within this however, the theory has taken on a number of MOND-like characteristics, up to α and δ effects, and for this reason under these methods the theory faces the same successes and issues as seen in the AQUAL form of MOND, although D3ST deals

with relativistic phenomena differently, notably including lensing. This distinction is important to remember, as D3ST is based on the concept of a velocity flow model for gravity, as opposed to how MOND models gravity. Equally, it has raised the interesting point of Newtonian and non-Newtonian components of gravity being equal at the overall gravitational acceleration being g_0 as opposed to $2g_0$ as with the original formulation, although the significance of this has not been fully investigated. Overall, the reconstruction of the g_0–hypothesis into the more usable g_0–conjecture offers an interesting new direction for describing these dynamics within D3ST, and allows for better comparison with results seen in other theories such as MOND.

Chapter 4

Covariant 3-Space Theory

D3ST is the result of generalising the dynamics of a fluid flow form of NG in order to understand other effects that may be emergent out of Process Physics. The focus on the quantum foam nature of space and geometry underpins this research. To this end however, covariant formulations of the theory have to this point been limited to ad-hoc discussions of how the various results from other theories may be compared, as opposed to a full examination of how a covariant form of the flow metric may behave. As noted in section 2.13, there exists a class of metrics which show similar behaviour to D3ST, these being the PG class of metrics. Aside from being regular across the event horizon, these metrics can be written in a way to effectively relate a velocity field $\boldsymbol{v}$ to the curvature of space time, and in doing so, relate D3ST-like language to covariant theories. The PG class of metrics are usually used as a form of coordinates for the Schwarzschild metric, and hence consideration of their behaviour beyond this is not usually performed, where the primary concern is to the behaviour across the event horizon of a black hole. Here however the concern is to the behaviour of the velocity field itself, and how this relates to a number of key results within D3ST.

This chapter begins with an analysis of the impacts of the PG class of metrics as a 3-space velocity metric, with regard to key results within D3ST, notably including

rederiving elements of the 3-space equation in the $\alpha = 0$, $\delta = 0$ case, before showing that the familiar results, including within electro-magnetism, are a natural result of using this metric. This will then be used to create a simple model of the expansion of the universe, and demonstrate the utility of such coordinates as a generalisation of D3ST in the $\alpha = 0$, $\delta = 0$ case. From here this is then used as a method of arguing the case for modifications to the Einstein field equations for the case of D3ST, and from this, exploring the behaviour of this new form with regard to a key result in this theory, the expansion of the universe.

4.1 Construction of the Metric

Consider a 3-space four-vector constructed as $V^0 = c$, in which the spacial components are simply the three values of the standard 3-space velocity field. Let 3-space and time be representable by some smooth pseudo-Riemann manifold (M, g), where g is the metric tensor on this manifold. Constructing from this a representation of this metric tensor, with a flat 3-space represented by $\eta^{\mu\nu}$ with $\eta^{00} = \eta^{i0} = \eta^{0i} = 0$ and the tensor product of the velocity field with itself, divided by the speed of light squared defining the time-like components. That is, constructing the metric in the form

$$g^{\mu\nu} = \eta^{\mu\nu} - \frac{1}{c^2} V^\mu V^\nu \tag{4.1.1}$$

$$g^{\mu\nu} = \begin{pmatrix} -1 & -\beta^1 & -\beta^2 & -\beta^3 \\ -\beta^1 & \eta^{11} - (\beta^1)^2 & \eta^{12} - \beta^2\beta^1 & \eta^{13} - \beta^3\beta^1 \\ -\beta^2 & \eta^{21} - \beta^1\beta^2 & \eta^{22} - (\beta^2)^2 & \eta^{23} - \beta^3\beta^2 \\ -\beta^3 & \eta^{31} - \beta^1\beta^3 & \eta^{32} - \beta^2\beta^3 & \eta^{33} - (\beta^3)^2 \end{pmatrix}. \tag{4.1.2}$$

which for a flat 3-space in Cartesian coordinates, has the inverse of

$$g_{\mu\nu} = \begin{pmatrix} \beta^2 - 1 & -\beta_1 & -\beta_2 & -\beta_3 \\ -\beta_1 & 1 & 0 & 0 \\ -\beta_2 & 0 & 1 & 0 \\ -\beta_3 & 0 & 0 & 1 \end{pmatrix} \tag{4.1.3}$$

where here $\beta_i \equiv \eta_{ij}\beta^j$. Of course discussing the metric in terms of a particular set of coordinates is rather inefficient, but here is used for illustration of the key point. That is, how the metric itself is represented in the above. In any case, more generally the above leads to line element

$$\mathrm{d}s^2 = -c^2\,\mathrm{d}t^2 + \left(\mathrm{d}\boldsymbol{r} - \boldsymbol{v}\left(\boldsymbol{r}, t\right)\,\mathrm{d}t\right)^2. \tag{4.1.4}$$

This is the metric as discussed in section 2.13. Noting here despite how the time and spacial components are separated, there is the interaction in the right hand term. This has the alternative form

$$\mathrm{d}s^2 = -\left(1 - \beta\left(\boldsymbol{r}, t\right)^2\right) c^2\,\mathrm{d}t^2 + \mathrm{d}\boldsymbol{r}^2 - 2\mathrm{d}\boldsymbol{r}\cdot\boldsymbol{v}\left(\boldsymbol{r}, t\right)\,\mathrm{d}t. \tag{4.1.5}$$

Here the cross term behaviour of the PG class of metrics is more apparent. This of course is the same version of the PG metric as discussed in 2.13, yet here it is created entirely from the 3-space velocity. The metric has the property $g_{\mu\nu}g^{\nu\lambda} = \delta^{\lambda}_{\mu}$, of course, while $\eta_{\mu\nu}\eta^{\nu\lambda} = \delta^{l}_{m}$ where $\mu,\ \nu,\ \lambda \in [0, 3]$ and the associated $m,\ n,\ l \in [1, 3]$ by convention. This property occurs as $\eta^{00} = 0$ in this construction.

The properties of the metric tensor for this manifold also tend towards a standard flat spacetime in the condition that $v \to 0$, and this induces from the properties of the 3-space velocity alone, this producing the standard Minkowski Metric, as opposed to the one used here. This property is a consequence of defining a time component of velocity to be related to the speed of light, the same standard construction as within SR and GR four-vectors. One interesting property of the above metric however is

that even at small scales, there exists this velocity $\boldsymbol{v}(\boldsymbol{r}, t)$, which even if constant is still apparent in the metric, this relating back to the original formulation of D3ST. That is, even if the velocity field $\boldsymbol{v}(\boldsymbol{r}, t)$ is not producing curvature effects, it still exists within this construction. This is of course expected within D3ST, particularly if direct detection of the 3-space velocity can be verified further as discussed in section 2.5. This was of course an effect also discussed with the original formulation of PG coordinates [95, 51].

Of course, this formulation depends strongly on the behaviour of the velocity field itself. For this reason, whilst this form is a useful representation of D3ST in a covariant form, using the above metric is in a sense non-trivial. This brings up the second main point with this above formulation however, with this class of metrics there are a number of well known properties. Most notably that they are related to more standard coordinate systems by a transformation involving time in the form

$$t' = t - f(\boldsymbol{r}, t) \tag{4.1.6}$$

which for $\mathrm{d}t$ becomes

$$c\,\mathrm{d}t = c\,\mathrm{d}t' + c\,\mathrm{d}f(\boldsymbol{r}, t) \tag{4.1.7}$$

this here depends heavily on the formulation of the velocity field, and hence to understand the connection between these coordinates and other sets, it requires a number of assumptions and knowledge of the behaviour of the velocity field $\boldsymbol{v}(\boldsymbol{r}, t)$ where this relation may be used. Here, some behaviour of this function can be considered more generally. In this instance, the form in equation 4.1.5 suggests that the transformation

$$c\,\mathrm{d}t = c\,\mathrm{d}t' + \frac{\beta}{1-\beta^2}\,\mathrm{d}r \tag{4.1.8}$$

is appropriate given that it reduces equations 4.1.4 and 4.1.5 to

$$\mathrm{d}s^2 = -\left(1-\beta^2\right)c^2\,\mathrm{d}t'^2 + \frac{\mathrm{d}r^2}{1-\beta^2} + \mathrm{d}\boldsymbol{\Omega}^2 \tag{4.1.9}$$

this being the standard form used in Schwarzschild coordinates. A simple example of this would be to consider a 3-space inflow as usually predicted within the theory in the form of equation 2.2.4. Inputting this gives the following form for the metric in equation 4.1.5

$$\mathrm{d}s^2 = -c^2\left(1-\frac{2GM}{c^2r}\right)\mathrm{d}t^2 + \left(\mathrm{d}r + 2\sqrt{\frac{2GM}{r}}\,\mathrm{d}t\right)\mathrm{d}r + \mathrm{d}\boldsymbol{\Omega}^2. \tag{4.1.10}$$

which given the previous transformation becomes

$$\mathrm{d}s^2 = -c^2\left(1-\frac{2GM}{c^2r}\right)\mathrm{d}t'^2 + \left(1-\frac{2GM}{c^2r}\right)^{-1}\mathrm{d}r^2 + \mathrm{d}\boldsymbol{\Omega}^2. \tag{4.1.11}$$

which is the standard form of the Schwarzschild metric. This hence defines the behaviour of this particular metric, and its relationship to more standard GR. The form presented in the coordinate transformation in equation 4.1.8 in the case that $\beta \to 0$ reduces to a perfectly flat metric, with both sets of coordinates agreeing. From here however, the concern moves from the relationship between this theory and GR, to whether or not the PG class of metrics is capable of describing the various elements of D3ST, notably including various standard forms of the theory, as well as required elements such as the Maxwell-Hertz equations, which are how lensing and other such effects are described within the theory.

4.2 Requirements of a 3-Space Metric

Considering this class of metrics in the form presented, this can be used to determine a number of different results previously used as part of D3ST. Here, rather than simply using them as a self-consistent set of rules, this section seeks to demonstrate

that they are in fact a natural consequence of this particular formulation. Whilst at this point α and δ effects are not built into this formulation, by demonstrating that GR in an inflow formalism is congruent with previous results, it presents a manner by which D3ST can be built into a proper covariant framework. As such, this section will explore a number of key elements within this, and confirm that they reduce to the usual expected results within D3ST. In essence, for this metric to be able to model D3ST in a standard sense, it is a requirement that in the non-relativistic case that it reduces to the standard equations within D3ST.

This section of course is attempting to recover a number of results within D3ST, and do so in a manner consistent with those seen in chapter 2. As such, relativistic effects are neglected in a number of cases, but do present areas where D3ST can be generalised to include such effects from this construction. This means that the main concern here is the case that $v \ll c$, and hence the parameter $\beta \to 0$, and terms which will not include coefficients of c will tend to be negligible in many instances. This is particularly important when dealing with covariant derivatives as will be discussed later, as whilst this is crucial in relativistic cases, and hence has future value, the case where $v \ll c$ is where almost all previous study of D3ST has been focused and hence this represents the best options for a proper comparison. That is, as long as results are consistent in this regime, this may be considered an effective representation of the theory.

4.3 Length contractions

Length contractions are discussed heavily in much of the work referred to in section 2.5, and present a key part in the question of whether or not the velocity field $\boldsymbol{v}$ is actually observable. Here it is worth noting that the important component for length contractions is the velocity with respect to the 3-space, that is, the velocity $\boldsymbol{v}_{\mathrm{R}} \equiv \boldsymbol{v} - \boldsymbol{v}_{\mathrm{O}}$ as previously discussed. For objects at rest in a particular reference

frame, $\boldsymbol{v}_{\mathrm{R}} = \boldsymbol{v}$, yet this distinction itself is important to remember. In considering this point of course, time dilatation and length contractions come out of this formulation naturally. Here, as usually defined, proper time is related to length step as $c^2\mathrm{d}\tau^2 = -\mathrm{d}s^2$. Consider the form of the PG metric in equation 4.1.5, which can be manipulated by replacing the differentials with differentials in time as

$$-\left(\frac{\mathrm{d}\tau}{\mathrm{d}t}\right)^2 = -1 + \frac{1}{c^2}\left(\frac{\mathrm{d}\boldsymbol{r}}{\mathrm{d}t} - \boldsymbol{v}\left(\boldsymbol{r}, t\right)\right)^2. \tag{4.3.1}$$

which gives using the previous definition $\boldsymbol{v}_{\mathrm{R}}$ and as $\boldsymbol{v}_{\mathrm{O}} \equiv \frac{\mathrm{d}\boldsymbol{r}}{\mathrm{d}t}$

$$-\left(\frac{\mathrm{d}\tau}{\mathrm{d}t}\right)^2 = -1 + \frac{v_{\mathrm{R}}^2}{c^2} \tag{4.3.2}$$

which hence defines

$$\frac{\mathrm{d}t}{\mathrm{d}\tau} = \gamma\left(\boldsymbol{v}_{\mathrm{R}}\right). \tag{4.3.3}$$

This is of course the Lorentz factor for the velocity of an object relative to the 3-space $\boldsymbol{v}_{\mathrm{R}}$ as previously discussed, and discussed in chapter 2. This in turn defines all time contractions within the theory as defined against movement relative to the 3-space, exactly as expected. This can be demonstrated in the form

$$\frac{\mathrm{d}x^i}{\mathrm{d}\tau} = \frac{\mathrm{d}x^i}{\mathrm{d}t}\frac{\mathrm{d}t}{\mathrm{d}\tau} = \gamma\left(\boldsymbol{v}_{\mathrm{R}}\right)\boldsymbol{v}_{\mathrm{R}}. \tag{4.3.4}$$

This form of course defines contractions as length to go along contractions in time by this Lorentz factor in terms of velocity relative to the defined velocity field. This indeed is the same type of relativistic behaviour described within this theory previously as discussed in section 2.6. This here being a key result within the theory, and describing the kind of relativistic behaviour required. Hence, for the standard relativistic effects assumed within D3ST, this construction does indeed produce the expected result.

In considering proper time, we can find the comparison between proper time intervals and time intervals in the standard sense. Consider a proper time interval of the form

$$c\Delta\tau = \int_{\Delta\tau} \sqrt{c^2\,\mathrm{d}t^2 - \left(\mathrm{d}\boldsymbol{r} - \boldsymbol{v}\left(\boldsymbol{r},t\right)\,\mathrm{d}t\right)^2} \tag{4.3.5}$$

which can hence be rewritten in the form

$$c\Delta\tau = \int_{\Delta\tau} \sqrt{c^2 - \boldsymbol{v}_{\mathrm{R}}^2}\,\mathrm{d}t \tag{4.3.6}$$

which is

$$\Delta\tau = \int_{\Delta\tau} \frac{\mathrm{d}t}{\gamma\left(\boldsymbol{v}_{\mathrm{R}}\right)}. \tag{4.3.7}$$

This comes out the same as the above discussion about length contractions, and, as would be expected, is again in terms of velocity relative to the 3-space. That is, all dilation and contractions are relative only to the 3-space.

In any case, these results are consistent with D3ST up to this point, and these are consistent with key results to do with the nature and behaviour of length and time contractions within the theory. These occur only relative to the 3-space itself, and do so in the manner expected. This in effect covers the previously studied relativistic behaviour within the theory.

4.4 Speed of Light

The speed of light itself is an important point within the theory, given that detection of anisotropy in the speed of light has been claimed to be one of the methods of detection of the 3-space velocity as discussed in section 2.5. The same process as above can be applied to light rays to find the speed of light. Consider as before equation 4.3.1, except here $\mathrm{d}\tau = 0$ for a ray of light. Hence we can find that

$$c = |\boldsymbol{v}_{\mathrm{O}} - \boldsymbol{v}(\boldsymbol{r}, t)| . \tag{4.4.1}$$

which is $\boldsymbol{v}_{\mathrm{R}}$ as previously defined, and hence a light ray moves at exactly the speed of light relative to the 3-space, as expected. This behaviour is of course exactly the same as discussed in section 4.3, but determining it more directly remains important. This in turn defines why these behaviours are apparent within the theory, as its relative movement against the 3-space, at which the speed of light is exactly c. This has interesting properties, but in effect here $\boldsymbol{v}_{\mathrm{O}}$, that is, the velocity of the light ray, and the velocity of the three space, must together have the length of the speed of light. Due to the previous relation, we can use

$$\boldsymbol{c} = \boldsymbol{v}_{\mathrm{O}} - \boldsymbol{v}(\boldsymbol{r}, t) \tag{4.4.2}$$

that is, $\boldsymbol{c} \equiv c\hat{\boldsymbol{v}_{\mathrm{R}}}$, such that

$$\boldsymbol{v}_{\mathrm{O}} = \boldsymbol{c} + \boldsymbol{v}(\boldsymbol{r}, t) . \tag{4.4.3}$$

The speed of light in these coordinates is the speed of light in the direction of $\boldsymbol{v}_{\mathrm{R}}$ plus the speed from the velocity field, as expected in wider D3ST. This is particularly important for the results of section 2.5. This effect is a natural result of the coordinates of the PG class of metrics, and this formulation remains self consistent with a covariant construction. Indeed, the real question is whether or not a 3-space velocity is detectable, and hence demonstrable, rather than if it is self-consistent within a modern formulation of gravitation.

These definitions are of course congruent with those defined in section 2.7, while further in this chapter, section 4.8 will present another definition as a consequence of the Maxwell equations in this construction for the sake of comparison.

4.5 Velocity Field 4-Gradient

Another key result discussed throughout the theory is the replacement of a partial derivative in time $\frac{\partial}{\partial t}$ with the material derivative. This has been noted in section 2.7 in particular, but is an important point within the theory. Considering equation 1.3.16 for ∂_μ the above metric may also be used to find the material derivative form discussed within the theory. Consider the form of the operator as created from the definition of $g^{\mu\nu}$. From this ∂^μ can be found as

$$\partial^0 = -\frac{1}{c}\partial_t - \beta^i\partial_i \tag{4.5.1}$$

$$\partial^i = \frac{-\beta^i}{c}\partial_t - \beta^i\beta^j\partial_j + \partial_i \tag{4.5.2}$$

which suggests from the form of the metric in equation 4.1.4 alone that the replacement seen in 3-space theory of the form [27, 29] where appropriate

$$\frac{\partial}{\partial t} \to \frac{\partial}{\partial t} + \boldsymbol{v}\cdot\nabla \tag{4.5.3}$$

is direct result of that initial form. Indeed, equation 4.5.1 is this replacement exactly, while the spacial components include only small relativistic corrections, which tends to zero in the case that $\beta \to 0$. Whilst this on its own suggests that the formulations for the Maxwell-Hertz equations discussed in 2.7, further consideration of this will be made later in the chapter with specific reference to their construction.

Due to the behaviour of form of the PG metric used, this also defines the wave operator in the form

$$\partial^\mu\partial_\mu = -\frac{1}{c^2}\left(\partial_t\partial_t + 2v^i\partial_i\partial_t + v^iv^j\partial_i\partial_j\right) + \partial_i\partial_i \tag{4.5.4}$$

which can be written in vector form as

$$\partial^\mu \partial_\mu \equiv \Box = -\frac{1}{c^2}\left(\frac{\partial^2}{\partial t^2} + 2\left(\boldsymbol{v}\cdot\nabla\right)\frac{\partial}{\partial t} + v^2\nabla^2\right) + \nabla^2. \tag{4.5.5}$$

this here being the wave operator within this formulation. Of particular interest here is that this can also be written in the form

$$\Box = -\frac{1}{c^2}\left(\frac{\partial^2}{\partial t^2} + 2\left(\boldsymbol{v}\cdot\nabla\right)\frac{\partial}{\partial t}\right) + \gamma^{-2}\nabla^2 \tag{4.5.6}$$

where $\gamma^{-2} = 1 - \beta^2$ as it is usually formulated. This showing the relativistic behaviour of the operator with respect to the 3-space. Of course, all of these behaviours go to the standard forms of the above in the case of $\boldsymbol{v} = 0$, as should be expected.

4.6 Christoffel Symbols

Of course, the metric tensor defines the Christoffel symbols for the manifold, and these will be important for results from here. Using the metric in equation 4.1.4, these may be defined in the form

$$\Gamma^\alpha_{\beta\gamma} = \frac{1}{2}g^{\alpha\epsilon}\left(g_{\beta\epsilon,\gamma} + g_{\gamma\epsilon,\beta} - g_{\beta\gamma,\epsilon}\right) \tag{4.6.1}$$

where here we know that

$$g^{\mu\nu} = \eta^{\mu\nu} - \frac{1}{c^2}V^\mu V^\nu \tag{4.6.2}$$

and $g_{\mu\nu}$ is defined as

$$\begin{aligned} g_{00} &= \beta^2 - 1 \\ g_{i0} = g_{0i} &= -\beta_i \\ g_{ij} &= \eta_{ij}. \end{aligned} \tag{4.6.3}$$

Here as noted previously $\eta_{\mu\nu}\eta^{\nu\epsilon} = \delta^{e}_{m}$, while $\beta_i\beta^i \equiv \beta^2$ where here Greek symbols α, β, γ and ϵ include the time coordinate, and associated Roman symbols a, b, c and e are only in spacial dimensions. This allows the above to remain invariant under coordinate transformations and rotation. The Christoffel symbols $\Gamma^{\alpha}_{\beta\gamma}$ may be calculated from the above as

$$\begin{aligned}
\Gamma^{0}_{00} &= \beta^{\epsilon}\left(\beta_{\epsilon,0} + \frac{1}{2}\beta^{2}_{,\epsilon}\right) \\
\Gamma^{a}_{00} &= \left(\beta^{a}\beta^{\epsilon} - \eta^{a\epsilon}\right)\left(\beta_{\epsilon,0} + \frac{1}{2}\beta^{2}_{,\epsilon}\right) \\
\Gamma^{0}_{b0} &= \beta^{\epsilon}\beta_{[\epsilon,b]} \\
\Gamma^{a}_{b0} &= \left(\beta^{a}\beta^{\epsilon} - \eta^{a\epsilon}\right)\beta_{[\epsilon,b]} \\
\Gamma^{0}_{bc} &= \beta^{\epsilon}\left(\eta_{b[c,\epsilon]} - \frac{1}{2}\eta_{c\epsilon,b}\right) \\
\Gamma^{a}_{bc} &= \left(\beta^{a}\beta^{\epsilon} - \eta^{a\epsilon}\right)\left(\eta_{b[c,\epsilon]} - \frac{1}{2}\eta_{c\epsilon,b}\right)
\end{aligned} \tag{4.6.4}$$

with the immediate consequence that most of these terms will go to zero for the case that $\beta \to 0$ within the geodesic equation. Whilst some time components, notably Γ^{0}_{00} and Γ^{a}_{00} will have some significant component in some cases, others will quickly vanish under this requirement, as will be discussed below. It is also important to remember the importance of using the defined $\eta^{\mu\nu}$ here to allow this to behave as designed, as these allow the transformations required with the Christoffel symbols. This can be used to calculate the Riemann and Ricci tensors, although expressing the full tensors would be inefficient in this regard. The above is only produced to demonstrate how results are being produced in the following sections.

4.7 Geodesics

It is also worth considering the behaviour of geodesics in the non-relativistic limit, and hence compare the motions of test particles with D3ST. It should be expected that from the geodesic equation that the acceleration induced by the 3-space be

recovered, up to the assumptions made. Of course, as discussed in section 1.4 in the relativistic limit we can consider $\mathrm{d}t \approx \mathrm{d}\tau$, hence giving the geodesic equation (equation 1.4.2) as

$$\frac{\mathrm{d}^2 x^\lambda}{\mathrm{d}t^2} + \Gamma^\lambda{}_{\mu\nu} \frac{\mathrm{d}x^\mu}{\mathrm{d}t} \frac{\mathrm{d}x^\nu}{\mathrm{d}t} = 0. \tag{4.7.1}$$

The spacial components hence become

$$\begin{aligned} \frac{\mathrm{d}^2 x^l}{\mathrm{d}t^2} &= -\Gamma^l{}_{\mu\nu} \frac{\mathrm{d}x^\mu}{\mathrm{d}t} \frac{\mathrm{d}x^\nu}{\mathrm{d}t} \\ &= -c^2 \Gamma^m_{00} \end{aligned} \tag{4.7.2}$$

here as all other elements of Christoffel symbols approach zero as $\beta \to 0$, as discussed in the previous section. This leaves only one set of components which have significant contributions, these giving

$$-c^2 \Gamma^l{}_{00} = -\beta^l \beta^\epsilon v_{\epsilon,t} - \frac{1}{2} \beta^l \beta^\epsilon v^2_{,\epsilon} + \eta^{l\epsilon} v_{\epsilon,t} + \frac{1}{2} \eta^{l\epsilon} v^2_{,\epsilon} \tag{4.7.3}$$

which as $v \ll c$, $\beta \approx 0$, hence this becomes

$$\frac{\mathrm{d}^2 x^l}{\mathrm{d}t^2} = v^l_{,t} + \frac{1}{2} v^2_{,l} \tag{4.7.4}$$

which rewritten in vector form is

$$\boldsymbol{a} = \frac{\partial \boldsymbol{v}}{\partial t} + \nabla \left(\frac{v^2}{2} \right) \tag{4.7.5}$$

which is the non-relativistic form of the acceleration from the dynamical 3-space equation, up to vorticity effects, as in equation 2.2.9. This is of course a direct consequence of the assumptions made to create this form, namely no relativistic effects, and assuming negligible cross spacial terms. Of course, those cross terms may also be included to allow these vorticity effects.The right hand term may also be stated in the form

$$\nabla\left(\frac{v^2}{2}\right) = (\boldsymbol{v}\cdot\nabla)\,\boldsymbol{v} + (\nabla\times\boldsymbol{v})\times\boldsymbol{v}. \tag{4.7.6}$$

Which is the first contribution to the vorticity effects within D3ST. Then consider the terms from equation 4.7.2 that include these contributions, namely

$$c\Gamma^{l}{}_{i0}\frac{\mathrm{d}x^m}{\mathrm{d}t} = \left(\beta^l\beta^\epsilon - \eta^{l\epsilon}\right)v_{[\epsilon,m]}\frac{\mathrm{d}x^m}{\mathrm{d}t} \tag{4.7.7}$$

where again, these $\beta^m\beta^\epsilon$ are relativistic terms and are here negligible. This leaves the $\eta^{m\epsilon}$ contribution, which means that using the definition that $\frac{\mathrm{d}x^i}{\mathrm{d}t} = v^i_{\mathrm{O}}$ we have that

$$c\Gamma^{l}{}_{m0}\frac{\mathrm{d}x^m}{\mathrm{d}t} = -\frac{1}{2}\left(v^l_{,m}v^m_{\mathrm{O}} - v^l_m v^m_{\mathrm{O}}\right) \tag{4.7.8}$$

which is just the double cross product

$$-\frac{1}{2}(\nabla\times\boldsymbol{v})\times\boldsymbol{v}_{\mathrm{O}} \tag{4.7.9}$$

for which there are two contributions to the full equation Γ^l_{m0} and Γ^l_{0m}, both negative, and hence as $\boldsymbol{v}_{\mathrm{R}} = \boldsymbol{v} - \boldsymbol{v}_{\mathrm{O}}$, and using the definitions $\frac{\mathrm{D}\boldsymbol{v}}{\mathrm{D}t} \equiv \frac{\partial\boldsymbol{v}}{\partial t} + (\boldsymbol{v}\cdot\nabla)\,\boldsymbol{v}$ and the definition in equation 4.7.6, equation 4.7.5 becomes

$$\boldsymbol{a} = \frac{\mathrm{D}\boldsymbol{v}}{\mathrm{D}t} + (\nabla\times\boldsymbol{v})\times\boldsymbol{v}_{\mathrm{R}} \tag{4.7.10}$$

which is now the same as the non-relativistic form of the standard 3-space acceleration, including vorticity effects. Of course, we could also include these relativistic terms, but the main concern here is the non-relativistic limit comparison with D3ST. Under these requirements, this is consistent with the form and behaviour discussed and described within D3ST in section 2.6.

4.8 Maxwell Equations

As discussed in section 1.3, the Maxwell equations in a curved spacetime may be represented in terms of the electromagnetic tensor. To start with, the inclusion of the covariant derivative form of equations 1.3.17 and 1.3.18 from section 1.3, these being in the sourceless case

$$F_{[\alpha\beta;\gamma]} = 0 \tag{4.8.1}$$

$$F^{\alpha\beta}{}_{;\alpha} = 0 \tag{4.8.2}$$

where here it is worth recalling the definitions that $F^{0i} = -\frac{1}{c}E^i$ and $F^{ij} = \varepsilon^{ijk}H_k$, while $F^{\mu\nu} = -F^{\nu\mu}$. For the purposes here, consider the covariant derivative for a general four-vector Z^μ. In this instance we have that $Z^\mu{}_{;\nu}$ is defined as

$$Z^\mu{}_{;\nu} \equiv \partial_\nu Z^\mu + Z^\lambda \Gamma^\mu{}_{\lambda\nu}. \tag{4.8.3}$$

As previously discussed in section 4.5, there are considerations for changes to the four-gradient defined out the front here, while the Chirstoffel symbols have been defined in section 4.6. In the majority of cases for $v \ll c$, this second term will be of minimal effect to the overall derivative due to the presence of the c^{-1} and c^{-2} terms. There are instances where some elements of this can become significant even in non-relativistic examples, but they generally have some factor of c involved, such as in section 4.7, which discussed the behaviour of geodesics. As such this section will consider the Maxwell equations in the essentially flat form, using

$$\begin{aligned} Z^\mu{}_{;0} &= Z^\mu{}_{,0} = \frac{1}{c}\partial_t Z^\mu \\ Z^\mu{}_{;i} &= Z^\mu{}_{,i} = \partial_i Z^\mu \end{aligned} \tag{4.8.4}$$

with this definition used for the remainder of this section. Derivatives with raised

indices in this form, assuming the non-relativistic case of $v \ll c$, follow this due to the previously stated identities $\partial^0 = -\frac{1}{c}\left(\partial_t + v^i\partial_i\right)$ and $\partial^i = \partial_i$; these discussed in section 4.7. Using this, equation 4.8.1 can be expanded in the usual sense

$$F_{\alpha\beta;\gamma} + F_{\beta\gamma;\alpha} + F_{\gamma\alpha;\beta} = 0 \tag{4.8.5}$$

which produces two sets of independent equations, the first with $\alpha = 0$ and $\beta \to b$ and $\gamma \to c$ such that $b,\ c \in [1,3]$ having raised the indices

$$F^{0b,c} + F^{bc,0} + F^{c0,b} = 0 \tag{4.8.6}$$

which reduces in the standard manner to

$$cH^{a,0} = g^{ad}\sqrt{|\det g|}\varepsilon_{dbc}E^{b,c} \tag{4.8.7}$$

which in vector form becomes

$$\left(\frac{\partial}{\partial t} + \boldsymbol{v}\cdot\nabla\right)\boldsymbol{H} = -\nabla\times\boldsymbol{E}. \tag{4.8.8}$$

Keep in mind that this pullback does have a significant effect in the calculation itself, but the above relation does hold. The other equation can be found by instead taking $\alpha,\ \beta,\ \gamma \to a,\ b,\ c$, which gives

$$F_{ab,c} + F_{bc,a} + F_{ca,b} = 0 \tag{4.8.9}$$

which is equivalent to

$$\varepsilon^{cab}F_{ab,c} = 0 \tag{4.8.10}$$

and as such is

$$H^{c}{}_{,c} = 0. \tag{4.8.11}$$

which in vector form is

$$\nabla \cdot \boldsymbol{H} = 0. \tag{4.8.12}$$

Hence this recovers two of the Maxwell-Hertz equations. The other two are from equation 4.8.2 with $\beta = 0$ and $\alpha \to a$

$$F^{a0}{}_{,a} = 0 \tag{4.8.13}$$

which simplifies to

$$E^{a}{}_{,a} = 0. \tag{4.8.14}$$

which in vector form is

$$\nabla \cdot \boldsymbol{E} = 0. \tag{4.8.15}$$

The final of the four comes from repeating the above with $\beta \to b$ and switching the first and third indices

$$F^{\alpha b,\alpha} = 0 \tag{4.8.16}$$

producing the form

$$F^{0b,0} + F^{ab,a} = 0 \tag{4.8.17}$$

which reduces to

$$\frac{1}{c}E^{b,0} = -g^{ba}\sqrt{|\det g|}\varepsilon_{acd}E^{c,d}. \tag{4.8.18}$$

which hence becomes, in vector form

$$\frac{1}{c^2}\left(\frac{\partial}{\partial t}+\boldsymbol{v}\cdot\nabla\right)\boldsymbol{E}=\nabla\times\boldsymbol{H}. \tag{4.8.19}$$

These can of course all be rewritten in vector form with evaluated derivatives as below

$$\left(\frac{\partial}{\partial t}+\boldsymbol{v}\cdot\nabla\right)\boldsymbol{H}=-\nabla\times\boldsymbol{E} \tag{4.8.20}$$

$$\frac{1}{c^2}\left(\frac{\partial}{\partial t}+\boldsymbol{v}\cdot\nabla\right)\boldsymbol{E}=\nabla\times\boldsymbol{H} \tag{4.8.21}$$

$$\nabla\cdot\boldsymbol{H}=0 \tag{4.8.22}$$

$$\nabla\cdot\boldsymbol{E}=0. \tag{4.8.23}$$

Hence under the conditions here the four Maxwell-Hertz equations do come out of this formulation, as is expected. Of course, this is essentially restating the findings of section 4.5, but the main point is further use of such formulations within this theory. In any case, this produces the same forms as seen in 2.7, and hence is consistent with those elements of D3ST. This in turn shows the consistency in lensing seen in D3ST, and GR, and how they have a common cause, that is, the warping of the paths. The difference here of course is that they have been caused by a warping of space induced by the change in a velocity field.

4.9 Weak Field Approximation

Of course, the 3-space equation can be found by taking a similar weak field approximation to the one that was discussed in section 1.4. That is, the 3-space equation, at least in its α and δ free case, should be reproduced from the Field Equations. For simplicity here however, first consider the trace reverse form of the

field equation in the form

$$R_{\mu\nu} = \frac{8\pi G}{c^4}\left(T_{\mu\nu} - \frac{1}{2}T g_{\mu\nu}\right) \tag{4.9.1}$$

where T is the trace of the energy-stress tensor such that here we can find this right hand term with the simplified energy-stress tensor as $T_{00} = -c^2\rho$ and other $T_{\mu\nu} = 0$, giving in the case that $v \ll c$ for the 00 component of the field equation

$$T_{00} - \frac{1}{2}T g_{00} = -\frac{4\pi G\rho}{c^2} \tag{4.9.2}$$

this hence reducing the equation to

$$c^2 R_{00} = -4\pi G\rho. \tag{4.9.3}$$

Considering the elements of the Ricci tensor in the form

$$R_{\sigma\nu} = \Gamma^{\rho}_{\nu\sigma,\rho} - \Gamma^{\rho}_{\rho\sigma,\nu} + \Gamma^{\rho}_{\rho\lambda}\Gamma^{\lambda}_{\nu\sigma} - \Gamma^{\rho}_{\nu\lambda}\Gamma^{\lambda}_{\rho\sigma} \tag{4.9.4}$$

elements σ and ν are not equal to zero and will become negligible and dominated by relativistic and vorticity terms, and hence this leaves only

$$c^2 R_{00} = c^2\Gamma^{\rho}_{00,\rho}. \tag{4.9.5}$$

Using the previous definitions of the Christoffel symbols in section 4.6, this becomes

$$R_{00} = \frac{1}{c}\partial_t\left(\beta^{\epsilon}\left(\beta_{\epsilon,0} + \frac{1}{2}\beta^2_{,\epsilon}\right)\right) + \partial_i\left(\left(\beta^i\beta^{\epsilon} - \eta^{i\epsilon}\right)\left(\beta_{\epsilon,0} + \frac{1}{2}\beta^2_{,\epsilon}\right)\right). \tag{4.9.6}$$

Of this the first term here is negligible compared to the second as it is of the order of c^{-2} out, and the $\beta^i\beta^{\epsilon}$ term is negligible compared to the remaining term

for the same reason, hence this becomes

$$R_{00} = -\partial_i \eta^{i\epsilon} \left(\beta_{\epsilon,0} + \frac{1}{2} \beta_{,\epsilon}^2 \right) \tag{4.9.7}$$

which simply becomes

$$R_{00} = -\frac{1}{c^2} \nabla \cdot \left(\frac{\partial \boldsymbol{v}}{\partial t} + \nabla \left(\frac{v^2}{2} \right) \right). \tag{4.9.8}$$

Bringing back in the other side of the equation this produces

$$\nabla \cdot \left(\frac{\partial \boldsymbol{v}}{\partial t} + \nabla \left(\frac{v^2}{2} \right) \right) = -4\pi G \rho \tag{4.9.9}$$

which is the 3-space equation in the case of zero vorticity, and without α and δ effects. That is, in the Newtonian limit these are in effect equivalent methods of defining this. This of course also points to how D3ST may be used to generalise the Field Equations with α and δ effects, although this analysis has not been carried out in this work.

4.10 Discussion

Hence from this it is clear that the PG class of metrics does behave appropriately as a covariant formulation of D3ST, covering a number of key results within the theory in the Newtonian limit, while allowing the theory to be generalised for the relativistic case more readily. Of course, this as it currently stands neglects α and δ effects, as well as the nature of the g_0–conjecture as discussed in Chapter 3, although these may be added and defined later.

The key point out of this however is that a flow dynamic version of GR can indeed be used and compared with D3ST, showing that whilst the language usually used within the theory is distinctly focused on these flow dynamics, and the α and δ effects, there is indeed a relationship between these theories. Indeed, the key

point out of this is this relationship between the curvature of GR, and the change in velocity seen in D3ST. Of course, this is to be expected, but still an important point to make and emphasise within context. Ultimately though, the key difference between the two theories is the timekeeping.

Concluding Remarks

This chapter has, through reference to the PG coordinates of GR, demonstrated that results within D3ST are a natural consequence of these coordinates, as well as discussed methods of how this may be used to better understand these phenomena. The flowing characteristics of both the PG class of metrics and D3ST can be clearly compared through this lens, and the reasons for the comparison become clearer. It is also worth considering the nature of the transformation between PG coordinates and more commonly used coordinates within GR however. It is the change in how time is considered that leads to these effects, including notably the relativistic effects being relative to 3-space itself, as within D3ST. This in a sense can be considered the fundamental difference between D3ST and more standard GR in this regard.

Whilst this chapter has considered the comparison with GR, and how a covariant formulation of D3ST may be developed, it has not considered it more generally in reference to the α and δ effects seen within the theory as discussed in sections 2.9.1 and 2.9.2. These effects however, whilst significant in specific circumstances, are not a major contributor in many large scale phenomena, including expansion of the universe in the current epoch. It is worth noting however that it has been argued that α effects in the early expansion of the universe may be a crucial part in understanding the inflation epoch of the early universe [108]. With this in mind, there is still room for developing a full 3-space field equation. Overall however, this chapter has completed its original aim of developing a potential covariant formulation of D3ST through comparisons with GR.

Conclusion

Dynamical 3-Space Theory is a theory of gravity that attempts to model gravity in a different manner to other theories. Rather than modeling it as a force as with Newtonian gravity or as curvature of spacetime as with the General Theory of Relativity, the theory models gravity as being the result of movement against a background substratum; a quantum foam. This theory, developed to compliment work done on Process Physics, has seen a number of developments in the last decade, going from a unique generalisation of Newtonian Gravity, to developing predictive and modeling capabilities, and offering solutions to current issues within gravitational research. Most notable here being the search for the elusive dark matter and dark energy, which may be explained as being a result of an incomplete theory of gravity according to dynamical 3-space theory. Despite offering resolution to the dark energy problem without free parameters however, dark matter, whilst consistent with the theory, is still not completely explained without additional parameters.

Previous work on the g_0–hypothesis has been greatly improved to include a wider range of phenomena, though a complete answer to why this effect occurs is still unknown. This has been achieved firstly through a comparison with MOND, as well as with use of newer data and research into the behaviour of spiral galaxies at large, including comparisons between them. Notably, an effect reported by McGaugh, Lelli & Schombert [80] is included within this discussion. This all together has allowed for the development of the more complete g_0–conjecture, which is compatible with wider dynamical 3-space theory, along with an appropriate fitting function. Along

with explaining the Tully-Fisher relationship and a number of other galactic scale relationships, it has also become apparent that the Newtonian and non-Newtonian contributions to the acceleration is set by g_0 such that they are equal when gravitational acceleration is exactly g_0, although the overall significance of this is currently unknown. Overall, the research into the relationship between MOND and dynamical 3-space theory has been fruitful, and the g_0–conjecture, while incomplete, provides a good way to model the behaviour of galaxies within the theory, particularly in reference to dark matter.

The development of a covariant form of 3-space theory with comparison to the PG class of metrics within GR has provided an interesting way of both expressing the results of the theory, as well as an avenue for future development. The changes to the time coordinate of more standard coordinate systems in GR, such as Schwarzschild coordinates, and expression of these results in analogous language to dynamical 3-space theory has been shown to lead to a number of the key results seen and used within the theory, and do so in a unique manner. Key comparisons between the source of lensing between the theories, and the equivalence brought about through this formulation are important to consider within this. This work in effect opens a new way of expressing and studying new results within the theory.

Overall, this thesis, through comparisons with MOND and GR has developed D3ST in a number of key areas which may be of interest to future research. In particular, this has presented a new way to study dark matter and dark energy within the theory, and doing so in a way more congruent with the language and methods used in other research within the field itself.

Future Work

This work has presented a number of new tools for the study of dark matter and dark energy within dynamical 3-space. In regard to the g_0–conjecture, this is both in allowing greater study of galactic scale dynamics, while also leaving the larger question of the origin of these effects currently unsolved. The finding that the actual point where Newtonian and non-Newtonian parts of gravitational acceleration appear to become equal at g_0, as opposed to the previously assumed $2g_0$ also opens up an avenue for future research, and may point to a potential reason to the g_0–conjecture.

The use of covariant language within future work within this theory offers the chance to better develop elements of this theory in the future, particularly in regard to expansion and inflation epochs. Equally, the covariant language in and of itself offers newer methods of solving one of the larger unsolved problems within the theory, this being time dependent solutions to $\rho \neq 0$ cases. Incorporation of α and δ effects into the covariant forms of this theory equally may present a fruitful area for future research. The incorporation of δ effects in cases where $\rho \neq 0$ remains an issue within the theory due to the difficulty in solving such equations by current methods. Equally, further generalisation of the dynamical 3-space equation remains an area of interest.

Equally, the theory could also be compared more directly with other theories such as Entropic Gravity to further develop some elements of it, particularly due to some similarities in the way that elements of the theory are handled, that is, in

the way that information is handled and may lead to effects such as gravitation. Particularly with developments within that theory in recent years, this could be a fruitful area for further research.

Overall, it is hoped that the work presented here will be of use in future research into the theory, and potentially other theories of gravity.

Bibliography

[1] Anderson, JD, Schubert, G, Trimble, V & Feldman, MR 2015, 'Measurements of Newton's gravitational constant and the length of day', *EPL (Europhysics Letters)*, vol. 110, no. 1, p. 10,002.

[2] Angus, GW, Famaey, B & Zhao, H 2006, 'Can MOND take a bullet? Analytical comparisons of three versions of MOND beyond spherical symmetry', *Monthly Notices of the Royal Astronomical Society*, vol. 371, no. 1, pp. 138–146.

[3] Angus, GW & McGaugh, SS 2007, 'The collision velocity of the bullet cluster in conventional and modified dynamics', *Monthly Notices of the Royal Astronomical Society*, vol. 383, no. 2, pp. 417–423.

[4] Armstrong, T & Fitzgerald, M 2003, 'New measurements of G using the measurement standards laboratory torsion balance', *Physical review letters*, vol. 91, no. 20, p. 201,101.

[5] Baer, W, Reiter, E & Jabs, H 2017, 'Null Result for Cahill's 3-Space Gravitational Wave Experiment with Zener Diode Detectors', *Progress in Physics*, vol. 13, pp. 118–122.

[6] Bagley, CH & Luther, GG 1997, 'Preliminary results of a determination of the Newtonian constant of gravitation: a test of the Kuroda hypothesis', *Physical Review Letters*, vol. 78, no. 16, p. 3047.

[7] Bekenstein, JD 2004, 'Relativistic gravitation theory for the modified Newtonian dynamics paradigm', *Physical Review D*, vol. 70, no. 8, p. 083,509.

[8] — 2006, 'The modified Newtonian dynamics–MOND and its implications for new physics', *Contemporary Physics*, vol. 47, no. 6, pp. 387–403.

[9] — 2009, 'Relativistic MOND as an alternative to the dark matter paradigm', *Nuclear Physics A*, vol. 827, no. 1-4, pp. 555c–560c.

[10] Bekenstein, JD & Milgrom, M 1984, 'Does the missing mass problem signal the breakdown of Newtonian gravity?', *Astrophysical Journal*, vol. 286, pp. 7–14.

[11] Bennett, C, Hill, R, Hinshaw, G, Nolta, M, Odegard, N, Page, L, Spergel, D, Weiland, J, Wright, E & Halpern, M 2003, 'First Year Wilkinson Microwave

Anisotropy Probe (WMAP) Observations: Foreground Emission', *Astrophysical Journal Supplement*, vol. 170, pp. 288–334.

[12] Bertone, G & Hooper, D 2016, 'A History of Dark Matter', *arXiv preprint arXiv:1605.04909*.

[13] Bolton, AS, Burles, S, Koopmans, LV, Treu, T, Gavazzi, R, Moustakas, LA, Wayth, R & Schlegel, DJ 2008, 'The Sloan Lens ACS Survey. V. The Full ACS Strong-Lens Sample', *The Astrophysical Journal*, vol. 682, no. 2, p. 964, URL http://stacks.iop.org/0004-637X/682/i=2/a=964.

[14] Cahill, R & Kerrigan, D 2011, 'Supermassive Galactic Black Holes and Cosmic Filaments', *Progress in Physics*, vol. 4, pp. 79–82.

[15] Cahill, RT 2002, 'Process physics: inertia, gravity and the quantum', *General Relativity and Gravitation*, vol. 34, no. 10, pp. 1637–1656.

[16] — 2003, 'Quantum-Foam In-Flow Theory of Gravity and the Global Positioning System (GPS)', *arXiv preprint physics/0309016*.

[17] — 2004, 'Review of gravitational wave detections: dynamical space', *Physics International*, vol. 5, pp. 49–86.

[18] — 2005, '3-Space in-flow theory of gravity: Boreholes, blackholes and the fine structure constant', *Progress in Physics*, vol. 2, pp. 9–16.

[19] — 2005, 'Black holes in elliptical and spiral galaxies and in globular clusters', *Progress in Physics*, vol. 3, pp. 51–56.

[20] — 2005, 'The Michelson and Morley 1887 experiment and the discovery of absolute motion', *Progress in Physics*, vol. 3, pp. 25–29.

[21] — 2005, 'Novel Gravity Probe B frame-dragging effect', *Progress in Physics*, vol. 3, pp. 30–33.

[22] — 2005, *Process physics: from information theory to quantum space and matter*, Nova Science Publishers.

[23] — 2006, 'Black holes and quantum theory: the fine structure constant connection', *Progress in Physics*, vol. 4, pp. 44–50.

[24] — 2006, 'Dynamical Fractal 3-Space and the Generalised Schrodinger Equation: Equivalence Principal and Voricity Effects', *Progress in Physics*, vol. 1, pp. 27–34.

[25] — 2006, 'A new light-speed anisotropy experiment: absolute motion and gravitational waves detected', *Progress in Physics*, vol. 4, pp. 73–92.

[26] — 2006, 'The Roland De Witte 1991 experiment (to the memory of Roland De Witte)', *Progress in Physics*, vol. 3, p. 60.

[27] — 2008, 'Unravelling Lorentz covariance and the spacetime formalism', *Progress in Physics*, vol. 4, pp. 19–24.

[28] — 2009, 'Combining NASA/JPL One-Way Optical-Fiber Light -Speed Data with Spacecraft Earth-Flyby Doppler-Shift Data to Characterise 3 space Flow', *Progress in Physics*, vol. 4, pp. 50–64.

[29] — 2009, 'Dynamical 3-Space: A Review in Ether Space-time and Cosmology: New Insights into a Key Physical Medium', *Apeiron*, pp. 135–200.

[30] — 2009, 'Unravelling the Dark Matter - Dark Energy Paradigm', *Aperion*, vol. 16, pp. 323–375.

[31] — 2011, 'Dynamical 3-space: Cosmic filaments, sheets and voids', *Progress in Physics*, vol. 2, pp. 44–51.

[32] — 2013, 'Nanotechnology quantum detectors for gravitational waves: Adelaide to London correlations observed', *Progress in Physics*, vol. 4, pp. 57–62.

[33] — 2015, 'Quantum gravity experiments', *Progress in Physics*, vol. 11, pp. 317–320.

[34] Capria, MM 2005, *Physics before and after Einstein*, IOS Press.

[35] Chaitin, G 1990, *Information, randomness & incompleteness: papers on algorithmic information theory, second edition*, World Scientific.

[36] Clowe, D, Bradač, M, Gonzalez, AH, Markevitch, M, Randall, SW, Jones, C & Zaritsky, D 2006, 'A direct empirical proof of the existence of dark matter', *The Astrophysical Journal Letters*, vol. 648, no. 2, p. L109.

[37] Cohen, IB & Whitman, A 1999, *Philosophiae Naturalis Principia Mathematica (Newton, Isaac, 1687; 1713; 1726)*, University of California Press.

[38] De Blok, W, Walter, F, Brinks, E, Trachternach, C, Oh, S & Kennicutt Jr, R 2008, 'High-resolution rotation curves and galaxy mass models from THINGS', *The Astronomical Journal*, vol. 136, no. 6, p. 2648.

[39] Drake, S 1978, *Galileo at work: his scientific biography*, Courier Corporation.

[40] Einstein, A 1916, 'Die Grundlage der allgemeinen Relativitätstheorie', *Annalen der Physik*, vol. 354, pp. 769–822.

[41] Eisenhauer, F, Genzel, R, Alexander, T, Abuter, R, Paumard, T, Ott, T, Gilbert, A, Gillessen, S, Horrobin, M, Trippe, S et al. 2005, 'SINFONI in the Galactic center: young stars and infrared flares in the Central Light-Month', *The Astrophysical Journal*, vol. 628, no. 1, p. 246.

[42] Ferrarese, L & Merritt, D 2000, 'A fundamental relation between supermassive black holes and their host galaxies', *The Astrophysical Journal Letters*, vol. 539, no. 1, p. L9.

[43] Fitzgerald, M & Armstrong, T 1995, 'Newton's gravitational constant with uncertainty less than 100 ppm', *IEEE transactions on instrumentation and measurement*, vol. 44, no. 2, pp. 494–497.

[44] Fresnel, A 1818, 'Lettre d'Augustin Fresnel á François Arago sur l'influence du mouvement terrestre dans quelques phénoménes d'optique', in 'Annales de chimie et de physique', vol. 9, pp. 57–66.

[45] Gamow, G 1970, 'My world line: An informal autobiography.', *My world line: An informal autobiography., by Gamow, G.. New York, NY (USA): Viking Press, 178 p.*, vol. 1.

[46] Gebhardt, K, Bender, R, Bower, G, Dressler, A, Faber, S, Filippenko, AV, Green, R, Grillmair, C, Ho, LC, Kormendy, J et al. 2000, 'A relationship between nuclear black hole mass and galaxy velocity dispersion', *The Astrophysical Journal Letters*, vol. 539, no. 1, pp. L13–L16.

[47] Gentile, G, Famaey, B & de Blok, W 2011, 'THINGS about MOND', *Astronomy & Astrophysics*, vol. 527, p. A76.

[48] Ghez, A, Salim, S, Weinberg, N, Lu, J, Do, T, Dunn, J, Matthews, K, Morris, M, Yelda, S & Becklin, E 2008, 'Measuring Distance and Properties of the Milky Way's Central Supermassive Black Hole with Stellar Orbits', *The Astrophysical Journal*, vol. 689, no. 2, p. 1044, URL http://stacks.iop.org/0004-637X/689/i=2/a=1044.

[49] Grant, E 1996, *The Foundations of Modern Science in the Middle Ages*, Cambridge University Press.

[50] Greene, JE, Peng, CY, Kim, M, Kuo, CY, Braatz, JA, Impellizzeri, CV, Condon, JJ, Lo, K, Henkel, C & Reid, MJ 2010, 'Precise black hole masses from megamaser disks: black hole-bulge relations at low mass', *The Astrophysical Journal*, vol. 721, no. 1, p. 26.

[51] Gullstrand, A 1922, *Allgemeine lösung des statischen einkörperproblems in der Einsteinschen gravitationstheorie*, Almqvist & Wiksell.

[52] Gültekin, K, Richstone, DO, Gebhardt, K, Lauer, TR, Tremaine, S, Aller, MC, Bender, R, Dressler, A, Faber, S, Filippenko, AV et al. 2009, 'The M-σ and ML relations in galactic bulges, and determinations of their intrinsic scatter', *The Astrophysical Journal*, vol. 698, no. 1, p. 198.

[53] Gundlach, JH & Merkowitz, SM 2000, 'Measurement of Newton's constant using a torsion balance with angular acceleration feedback', *Physical Review Letters*, vol. 85, no. 14, p. 2869.

[54] Guth, AH 1981, 'Inflationary universe: A possible solution to the horizon and flatness problems', *Physical Review D*, vol. 23, no. 2, p. 347.

[55] Häring, N & Rix, HW 2004, 'On the black hole mass-bulge mass relation', *The Astrophysical Journal Letters*, vol. 604, no. 2, p. L89.

[56] Hubble, E 1929, 'A relation between distance and radial velocity among extra-galactic nebulae', *Proceedings of the National Academy of Sciences*, vol. 15, no. 3, pp. 168–173.

[57] Jeans, J 1915, 'On the theory of star-streaming and the structure of the universe', *Monthly Notices of the Royal Astronomical Society*, vol. 76, pp. 70–84.

[58] Kafle, PR, Sharma, S, Lewis, GF & Bland-Hawthorn, J 2014, 'On the shoulders of giants: properties of the stellar halo and the milky way mass distribution', *The Astrophysical Journal*, vol. 794, no. 1, p. 59.

[59] Kaiser, N & Squires, G 1993, 'Mapping the dark matter with weak gravitational lensing', *The Astrophysical Journal*, vol. 404, pp. 441–450.

[60] Kapteyn, JC 1922, 'First Attempt at a Theory of the Arrangement and Motion of the Sidereal System', *The Astrophysical Journal*, vol. 55, p. 302.

[61] Karagioz, O & Izmailov, V 1996, 'Measurement of the gravitational constant with a torsion balance', *Measurement Techniques*, vol. 39, no. 10, pp. 979–987.

[62] Kerrigan, D 2011, *Dynamical 3-Space Theory and Black Holes*, Master's thesis, Flinders University.

[63] Kleinevoß, U, Meyer, H, Schumacher, A & Hartmann, S 1999, 'Absolute measurement of the Newtonian force and a determination of G', *Measurement Science and Technology*, vol. 10, no. 6, p. 492.

[64] Le Verrier, U 1859, 'Lettre de M, Le Verrier á M: Faye sur la théorie de Mercure et sur le mouvement du périhélie de cette planéte', *Comptes rendus hebdomadaires des séances de l'Académie des sciences*, vol. 49, pp. 379–383.

[65] Lee, J & Komatsu, E 2010, 'Bullet cluster: a challenge to ΛCDM cosmology', *The Astrophysical Journal*, vol. 718, no. 1, p. 60.

[66] Lemaître, AG 1931, 'Contributions to a British Association Discussion on the Evolution of the Universe', *Nature*, vol. 128, no. 24, pp. 704–706.

[67] Lemaître, G 1933, 'L'univers en expansion', in 'Annales de la Société Scientifique de Bruxelles', vol. 53.

[68] Lerch, FJ, Klosko, SM, Laubscher, RE & Wagner, CA 1979, 'Gravity model improvement using Geos 3 (GEM 9 and 10)', *Journal of Geophysical Research: Solid Earth*, vol. 84, no. B8, pp. 3897–3916.

[69] Li, Y 2016, 'A Possible Exact Solution for the Newtonian Constant of Gravity', *British Journal of Mathematics & Computer Science*, vol. 19.

[70] Lorentz, H 1892, 'The electromagnetic theory of Maxwell and its application to moving bodies', *EJ Brill, Leiden*.

[71] Luo, J, Hu, ZK, Fu, XH, Fan, SH & Tang, MX 1998, 'Determination of the Newtonian gravitational constant G with a nonlinear fitting method', *Physical Review D*, vol. 59, no. 4, p. 042,001.

[72] Magorrian, J, Tremaine, S, Richstone, D, Bender, R, Bower, G, Dressler, A, Faber, S, Gebhardt, K, Green, R, Grillmair, C et al. 1998, 'The Demography of massive dark objects in galaxy centers', *The Astronomical Journal*, vol. 115, no. 6, p. 2285.

[73] Martel, K & Poisson, E 2001, 'Regular coordinate systems for Schwarzschild and other spherical spacetimes', *American Journal of Physics*, vol. 69, no. 4, pp. 476–480.

[74] Maxwell, JC 1881, *A treatise on electricity and magnetism*, vol. 1, Clarendon press.

[75] May, RD & Cahill, RT 2011, 'Dynamical 3-space gravity theory: effects on polytropic solar models', *Progress in Physics*, vol. 1, pp. 49–55.

[76] McConnell, NJ & Ma, CP 2013, 'Revisiting the scaling relations of black hole masses and host galaxy properties', *The Astrophysical Journal*, vol. 764, no. 2, p. 184.

[77] McGaugh, SS 2005, 'The Baryonic Tully-Fisher relation of galaxies with extended rotation curves and the stellar mass of rotating galaxies', *The Astrophysical Journal*, vol. 632, no. 2, p. 859.

[78] — 2012, 'The baryonic Tully-Fisher relation of gas-rich galaxies as a test of ΛCDM and MOND', *The Astronomical Journal*, vol. 143, no. 2, p. 40.

[79] — 2014, 'A tale of two paradigms: the mutual incommensurability of ΛCDM and MOND 1', *Canadian Journal of Physics*, vol. 93, no. 2, pp. 250–259.

[80] McGaugh, SS, Lelli, F & Schombert, JM 2016, 'Radial Acceleration Relation in Rotationally Supported Galaxies', *Physical Review Letters*, vol. 117, no. 20, p. 201,101.

[81] Michelson, AA & Morley, EW 1887, 'On the Relative Motion of the Earth and of the Luminiferous Ether', *Sidereal Messenger, vol. 6, pp. 306-310*, vol. 6, pp. 306–310.

[82] Milgrom, M 1986, 'Solutions for the modified Newtonian dynamics field equation', *The Astrophysical Journal*, vol. 302, pp. 617–625.

[83] — 2001, 'MOND–a pedagogical review', *arXiv preprint astro-ph/0112069*.

[84] Miller, DC 1933, 'The ether-drift experiment and the determination of the absolute motion of the earth', *Reviews of modern physics*, vol. 5, no. 3, p. 203.

[85] Misner, CW, Thorne, KS & Wheeler, JA 1973, *Gravitation*, Macmillan.

[86] Moffat, JW 2006, 'Scalar–tensor–vector gravity theory', *Journal of Cosmology and Astroparticle Physics*, vol. 2006, no. 03, p. 004.

[87] Mohr, PJ, Newell, DB & Taylor, BN 2016, 'CODATA recommended values of the fundamental physical constants: 2014', *Journal of Physical and Chemical Reference Data*, vol. 45, no. 4, p. 043,102.

[88] Mohr, PJ, Taylor, BN & Newell, DB 2008, 'CODATA recommended values of the fundamental physical constants: 2006 a', *Journal of Physical and Chemical Reference Data*, vol. 80, no. 3, pp. 633–1284.

[89] NASA n.d., 'Planetary Fact Sheets', URL https://nssdc.gsfc.nasa.gov/planetary/planetfact.html.

[90] Newman, R, Bantel, M, Berg, E & Cross, W 2014, 'A measurement of G with a cryogenic torsion pendulum', *Phil. Trans. R. Soc. A*, vol. 372, no. 2026, p. 20140,025.

[91] Newton, I 1687, *Philosophiæ naturalis principia mathematica*, London.

[92] — 1979, *Opticks, or, a treatise of the reflections, refractions, inflections & colours of light*, Courier Corporation.

[93] Oort, JH 1932, 'The force exerted by the stellar system in the direction perpendicular to the galactic plane and some related problems', *Bulletin of the Astronomical Institutes of the Netherlands*, vol. 6, p. 249.

[94] Ott, T, Schoedel, R, Genzel, R, Eckart, A, Lacombe, F, Rouan, D, Hofmann, R, Lehnert, M, Alexander, T, Sternberg, A & et al. 2003, 'Inward Bound: Studying the Galactic Centre with NAOS/CONICA', *The Messenger*, vol. 111, p. 19, URL http://arxiv.org/abs/astro-ph/0303408.

[95] Painlevé, P 1921, 'La mécanique classique et la théorie de la relativité', *Comptes Rendus Academie des Sciences (serie non specifiee)*, vol. 173, pp. 677–680.

[96] Pardo, K 2017, 'Testing Emergent Gravity with Isolated Dwarf Galaxies', *arXiv preprint arXiv:1706.00785*.

[97] Parks, HV & Faller, JE 2010, 'Simple pendulum determination of the gravitational constant', *Physical Review Letters*, vol. 105, no. 11, p. 110,801.

[98] Perlmutter, S, Gabi, S, Goldhaber, G, Goobar, A, Groom, D, Hook, I, Kim, A, Kim, M, Lee, J, Pain, R et al. 1997, 'Measurements* of the Cosmological Parameters Ω and Λ from the First Seven Supernovae at z$\geq$ 0.35', *The astrophysical journal*, vol. 483, no. 2, p. 565.

[99] Perlmutter, S, Schmidt, BP & Riess, AG 2011, 'The Nobel Prize in Physics 2011', .

[100] Persic, M, Salucci, P & Stel, F 1999, 'The universal rotation curve of spiral galaxies - I. The dark matter connection', *Monthly Notices of the Royal Astronomical Society*, vol. 281, pp. 27–47.

[101] Poincare, H 1906, 'The Milky Way and the Theory of Gases', *Popular Astronomy*, vol. 14, pp. 475–488.

[102] Quinn, T 2016, 'Gravity on the balance', *Nature Physics*, vol. 12, no. 2, pp. 196–196.

[103] Quinn, T, Speake, C, Parks, H & Davis, R 2014, 'The BIPM measurements of the Newtonian constant of gravitation, G', *Phil. Trans. R. Soc. A*, vol. 372, no. 2026, p. 20140,032.

[104] Quinn, T, Speake, C, Richman, S, Davis, R & Picard, A 2001, 'A new determination of G using two methods', *Physical Review Letters*, vol. 87, no. 11, p. 111,101.

[105] Reid, M, Menten, K, Zheng, X, Brunthaler, A, Moscadelli, L, Xu, Y, Zhang, B, Sato, M, Honma, M & Hirota, T 2009, 'Trigonometric Parallaxes of Massive Star-Forming Regions. VI. Galactic Structure, Fundamental Parameters, and Noncircular Motions', *The Astrophysical Journal*, vol. 700, no. 1, p. 137, URL http://stacks.iop.org/0004-637X/700/i=1/a=137.

[106] Riess, AG, Filippenko, AV, Challis, P, Clocchiatti, A, Diercks, A, Garnavich, PM, Gilliland, RL, Hogan, CJ, Jha, S, Kirshner, RP et al. 1998, 'Observational evidence from supernovae for an accelerating universe and a cosmological constant', *The Astronomical Journal*, vol. 116, no. 3, p. 1009.

[107] Rosi, G, Sorrentino, F, Cacciapuoti, L, Prevedelli, M & Tino, G 2014, 'Precision measurement of the Newtonian gravitational constant using cold atoms', *Nature*, vol. 510, no. 7506, pp. 518–521.

[108] Rothall, D 2016, *Towards Understanding Reality using Dynamical 3-Space Theory*, Ph.D. thesis, Flinders University.

[109] Rothall, DP & Cahill, RT 2014, 'Dynamical 3-Space: Observing Gravitational Wave Fluctuations and the Schnoll Effect using Zener Diode Quantum Detector', *Progress in Physics*, vol. 10, pp. 16–18.

[110] Rovelli, C 2015, 'Aristotle's Physics: A Physicist's Look', *Journal of the American Philosophical Association*, vol. 1, no. 1, pp. 23–40.

[111] Rubin, VC & Ford Jr, WK 1970, 'Rotation of the andromeda nebula from a spectroscopic survey of emission regions', *The Astrophysical Journal*, vol. 159, p. 379.

[112] Rubin, VC, Ford Jr, WK & Thonnard, N 1980, 'Rotational properties of 21 SC galaxies with a large range of luminosities and radii, from NGC 4605/R= 4kpc/to UGC 2885/R= 122 kpc', *The Astrophysical Journal*, vol. 238, pp. 471–487.

[113] Sanders, R 2005, 'A tensor–vector–scalar framework for modified dynamics and cosmic dark matter', *Monthly Notices of the Royal Astronomical Society*, vol. 363, no. 2, pp. 459–468.

[114] Schlamminger, S, Gundlach, JH & Newman, RD 2015, 'Recent measurements of the gravitational constant as a function of time', *Physical Review D*, vol. 91, no. 12, p. 121,101.

[115] Schlamminger, S, Holzschuh, E, Kündig, W, Nolting, F, Pixley, RE, Schurr, J & Straumann, U 2006, 'Measurement of Newton's gravitational constant', *Phys. Rev. D*, vol. 74, p. 082,001.

[116] Schwarzschild, K 1999, 'On the gravitational field of a mass point according to Einstein's theory', *arXiv preprint physics/9905030*.

[117] Seaver, JR 2016, 'Attempt to replicate Cahill's quantum gravity experiment to measure absolute velocity', *Progress in Physics*, vol. 12, no. 4, pp. 362–365.

[118] Stark, DV, McGaugh, SS & Swaters, RA 2009, 'A First Attempt to Calibrate the Baryonic Tully-Fisher Relation with Gas-Dominated Galaxies', *The Astronomical Journal*, vol. 138, no. 2, p. 392.

[119] Tapley, B, Ries, J, Bettadpur, S, Chambers, D, Cheng, M, Condi, F, Gunter, B, Kang, Z, Nagel, P, Pastor, R et al. 2005, 'GGM02–An improved Earth gravity field model from GRACE', *Journal of Geodesy*, vol. 79, no. 8, pp. 467–478.

[120] Tapley, BD, Bettadpur, S, Watkins, M & Reigber, C 2004, 'The gravity recovery and climate experiment: Mission overview and early results', *Geophysical Research Letters*, vol. 31, no. 9.

[121] Tolish, A n.d., 'General Relativity and the Newtonian Limit', Available from url: <http://www.math.uchicago.edu/ may/VIGRE/VIGRE2010/REUPapers/Tolish.pdf>.

[122] Torr, D & Kolen, P 1984, 'Precision Measurements and Fundamental Constants, ed. by Taylor BN and Phillips WD Nat', *Bur. Stand.(US), Spec. Pub*, vol. 617, p. 675.

[123] Tremaine, S, Gebhardt, K, Bender, R, Bower, G, Dressler, A, Faber, SM, Filippenko, AV, Green, R, Grillmair, C, Ho, LC et al. 2002, 'The slope of the black hole mass versus velocity dispersion correlation', *The Astrophysical Journal*, vol. 574, no. 2, p. 740.

[124] Tu, LC, Li, Q, Wang, QL, Shao, CG, Yang, SQ, Liu, LX, Liu, Q & Luo, J 2010, 'New determination of the gravitational constant G with time-of-swing method', *Physical Review D*, vol. 82, no. 2, p. 022,001.

[125] Tully, RB & Fisher, JR 1977, 'A new method of determining distances to galaxies', *Astronomy and Astrophysics*, vol. 54, pp. 661–673.

[126] Verlinde, E 2011, 'On the Origin of Gravity and the Laws of Newton', *Journal of High Energy Physics*, vol. 2011, no. 4, pp. 1–27.

[127] Verlinde, EP 2016, 'Emergent gravity and the dark universe', *arXiv preprint arXiv:1611.02269*.

[128] Visser, M 2011, 'Conservative entropic forces', *Journal of High Energy Physics*, vol. 2011, no. 10, pp. 1–22.

[129] Von Eötvös, R 1890, 'Über die Anziehung der Erde auf verschiedene Substanzen', *Math. Naturwissenschaft. Ber. Ungarn*, vol. 8, pp. S65–S68.

[130] Wittman, DM, Tyson, JA, Kirkman, D, Dell'Antonio, I & Bernstein, G 2000, 'Detection of weak gravitational lensing distortions of distant galaxies by cosmic dark matter at large scales', *Nature*, vol. 405, no. 6783, pp. 143–148.

[131] Zhao, H & Famaey, B 2006, 'Refining the MOND interpolating function and TeVeS Lagrangian', *The Astrophysical Journal Letters*, vol. 638, no. 1, p. L9.

[132] Zwicky, F 1937, 'On the Masses of Nebulae and of Clusters of Nebulae', *The Astrophysical Journal*, vol. 86, p. 217.

Appendix A

Values of Big G

Table A.1: Table of values used to produce figure 1.3

Type	Year	Value ($m^3\ kg^{-1}\ s^{-2}$)	Uncert.	Ref.
CODATA	2014	6.67408×10^{-11}	47 ppm	[87]
Pendulum	2014	$6.67433\,(11) \times 10^{-11}$	19 ppm	[90]
Cold Atoms	2014	$6.67191\,(99) \times 10^{-11}$	150 ppm	[107]
Torque Balance	2014	$6.67554\,(16) \times 10^{-11}$	25 ppm	[103]
Two Pendulum	2010	6.67234×10^{-11}	21 ppm	[97]
Torsion Swing	2010	6.67349×10^{-11}	26 ppm	[124]
CODATA	2008	6.67428×10^{-11}	100 ppm	[88]
Beam Balance	2006	$6.674252\,(109) \times 10^{-11}$	18 ppm	[115]
Torque Balance	2003	6.67387×10^{-11}	95 ppm	[4]
Torsion Balance	2001	$6.67559\,(27) \times 10^{-11}$	41 ppm	[104]
Torsion Balance	2001	6.674215×10^{-11}	14 ppm	[53]
Resonator	1999	6.6735×10^{-11}	432 ppm	[63]
Torsion Balance	1998	6.6699×10^{-11}	105 ppm	[71]
Torsion Balance	1997	6.6740×10^{-11}	105 ppm	[6]
Torsion Balance	1996	6.6729×10^{-11}	75 ppm	[61]
Torque Balance	1995	$6.6656\,(6) \times 10^{-11}$	40 ppm	[43]